MULTIWALLED CARBON NANOTUBE- POLY(2-HYDROXYETHYL METHACRYLATE) COMPOSITE CONDUIT FOR PERIPHERAL NERVE REPAIR

A THESIS SUBMITTED TO
THE GRADUATE SCHOOL OF NATURAL AND APPLIED SCIENCES
OF
MIDDLE EAST TECHNICAL UNIVERSITY

BY

DAMLA ARSLANTUNALI

IN PARTIAL FULFILLMENT OF THE REQUIREMENTS
FOR
THE DEGREE OF MASTER OF SCIENCE
IN
BIOTECHNOLOGY

FEBRUARY 2012

Approval of the thesis**:**

MULTIWALLED CARBON NANOTUBE- POLY (2-HYDROXYETHYL METHACRYLATE) COMPOSITE CONDUIT FOR PERIPHERAL NERVE REPAIR

submitted by **DAMLA ARSLANTUNALI** in partial fulfillment of the requirements for the degree of **Master of Science in Biotechnology Department, Middle East Technical University** by,

Prof. Dr. Canan Özgen _____
Dean, Graduate School of **Natural and Applied Sciences**

Prof. Dr. Nesrin Hasırcı _____
Head of Department; **Biotechnology**

Prof. Dr. Vasıf Hasırcı _____
Supervisor, **Biotechnology Dept., METU**

Assoc. Prof. Dr. Gürer Budak, MD _____
Co-Supervisor, **Vocational High School of Health Services, Gazi University**

Examining Committee Members:

Prof. Dr. Levent Toppare _____
Chemistry Dept., METU

Prof. Dr. Vasıf Hasırcı _____
Biotechnology Dept., METU

Prof. Dr. Tülin Güray _____
Biotechnology Dept., METU

Prof. Dr. Emir Baki Denkbaş _____
Chemistry Dept., Hacettepe University

Assist. Prof. Dr. Can Özen _____
Biotechnology Dept., METU

Date: 10.02.2012

I hereby declare that all information in this document has been obtained and presented in accordance with academic rules and ethical conduct. I also declare that, as required by these rules and conduct, I have fully cited and referenced all material and results that are not original to this work.

Name, Last name : Damla Arslantunalı

Signature :

ABSTRACT

MULTIWALLED CARBON NANOTUBE- POLY (2-HYDROXYETHYL METHACRYLATE) COMPOSITE CONDUIT FOR PERIPHERAL NERVE REPAIR

Arslantunalı, Damla

M. Sc., Department of Biotechnology
Supervisor: Prof. Dr. Vasıf Hasırcı
Co-Supervisor: Assoc. Prof. Dr. Gürer Budak, MD

February 2012, 94 pages

There are different methods used in the surgical treatment of peripheral nerve injury. In this respect, end-to-end surgical reconnection of the damaged nerve ends or autologous nerve grafts are applied as soon as possible after the injury. When autologous tissue transplant is considered, there are some medical devices available generally for relatively short nerve defects. As a solution for this problem, different tissue engineered nerve conduits have been developed.

In the current study, a pHEMA hydrogel membranes were designed to mimic the tubular conduits and they were loaded with 1-6% (w/w) multiwalled carbon nanotubes (mwCNTs) to obtain electrical conductivity. The most important reason for the use of CNTs in peripheral nerve injury is their electrical conductivity. Within the context of the study, the degree of swelling, contact angles, electrical conductivity and mechanical properties of the membranes were analyzed. As the amount of

mwCNTs were increased, the contact angles, indicating higher hydrophobicity and the electrical conductivity increased. The tensile test of the mwCNT-pHEMA composite membranes showed that the membranes have viscoelastic structure similar to the structure of the soft tissues. The structure of the mwCNT containing pHEMA composite membranes were analyzed with different microscopical techniques such as SEM, CSLM and microCT. MwCNTs on the hydrogels were morphologically similar to the original. SEM micrographs also showed that the mwCNTs were grouped in clumps on hydrogel surfaces. No mwCNT leaching was observed because the mwCNTs were embedded in the hydrogel, therefore, no cytotoxic effect was observed. The pHEMA hydrogels were porous which is suitable for transportation of materials, electrolytes and gas needed for cell nutrition and growth.

In the *in vitro* studies, SHSY5Y neuroblastoma cells were seeded on the membranes to determine the sustainability and effects of the membranes on the cell growth. Electrical potential of 1 and 2 V were used to stimulate the cells. Microscopical examination with SEM and CSLM, and MTT viability assay were used. The SHSY5Y neuroblastoma cells were attached and proliferated on both the composite and the hydrogel membranes. The cells on pHEMA membranes without mwCNTs, however, were not able to survive after application of electrical potential.

As a conclusion, use of composite membranes in the treatment of peripheral nerve injury as a nerve conduit is appropriate. Electrical stimulation, however, did not induce the cells to align in contrast to the expected results, indicating potential and current application regime needs to be optimized to obtain the desired results.

Keywords: Peripheral Nerve Injury, Nerve Tissue Engineering, Nerve Conduit, pHEMA, Multiwalled Carbon Nanotube

ÖZ

PERİFERAL SİNİR YARALANMALARININ TAMİRİ İÇİN ÇOK DUVARLI KARBON NANOTÜP YÜKLÜ POLİ(2-HİDROKSİETİL METAKRİLAT) KANAL TASARIMI

Arslantunalı, Damla

Yüksek Lisans, Biyoteknoloji Bölümü
Tez Yöneticisi: Prof. Dr. Vasıf Hasırcı
Ortak Tez Yöneticisi: Doç. Dr. Gürer Budak

Şubat 2012, 94 sayfa

Periferik sinir yaralanmalarının cerrahi tedavisinde değişik yöntemler uygulanmaktadır. Bu kapsamda, mümkün olan en erken dönemde zarar görmüş olan sinirin iki ucu cerrahi olarak uç uca birleştirme yöntemiyle dikilmekte ya da otolog sinir nakli yöntemi ile onarılmaya çalışılmaktadır. Otolog doku nakli konusunda genelde kısa ya da küçük sinir yaralanmalarında kullanılan medikal malzemeler bulunmaktadır. Bu sorunun çözümü amacıyla doku mühendisliği kapsamında değişik tipte sinir kanalları geliştirilmektedir.

Bu çalışmada tübüler kanalları temsil etmek üzere pHEMA hidrojel membranlar geliştirilmiş ve elektriksel iletkenliği sağlayabilmek için kanal yüzeyine % 1-6 (w/w) oranlarında çok duvarlı karbon nanotüpler (KNT) yerleştirilmiştir. KNT'lerin bu tip periferik sinir tedavisi çalışmalarında tercih edilmesinin en önemli nedeni iletken olmalarıdır. Çalışma kapsamında, membranların şişme dereceleri, temas açıları,

elektrik iletkenlikleri ve mekanik özellikleri incelenmiştir. KNT miktarı arttıkça yüksek hidrofobikliği gösteren temas açıları ve elektrik iletkenlikler artmaktadır. KNT-pHEMA kompozit zarlar üzerine uygulanan çekme-gerilme deneyi, bu kompozit zarların yumuşak dokularda görülen viskoelastik yapıya benzer olduğunu göstermiştir. KNT içeren pHEMA kompozit zarların yapısı SEM, CSLM ve mikroCT gibi farklı mikroskopik tekniklerle incelenmiştir. Hidrojel üzerindeki KNT'ler morfolojik açıdan kullanım öncesi hallerine çok benzemektedirler. SEM fotoğrafları aynı zamanda karbon nanotüplerin hidrojel yüzeyinde kümelendiklerini göstermiştir. Bu KNT'ler kanal yüzeyine gömülü oldukları için ortama KNT kaçışı ve buna bağlı bir sitotoksik etki gözlenmemiştir. PHEMA hidrojelleri hücre beslenme ve büyümesi için gerekli olan madde, elektrolit ve gaz elişverişine olanak sağlayan gözenekli bir yapıya sahiptir.

Çalışmanın *in vitro* kısmında, membranlara sürdürülebilirlik ve hücre büyümesi üzerine etkilerinin araştırılması için, SHSY5Y nöroblastom hücreleri ekilmiştir. Hücreleri elektriksel olarak uyarmak amacıyla zarlar üzerine 1 ve 2 V elektrik potansiyeli uygulanmıştır. Mikroskopik değerlendirme için SEM ve CSLM yöntemleri, canlılık testi için ise MTT yöntemi kullanılmıştır. SHSY5Y nöroblastom hücrelerinin hem hidrojel hem de kompozit zar yüzeylerine tutundukları ve çoğaldıkları görülmüştür. Ancak elektrik potansiyel uygulandığında KNT içermeyen pHEMA zarların yüzeyine tutunmuş nöroblastomların canlılıklarını sürdüremedikleri gözlenmiştir.

Sonuç olarak, geliştirilen kompozit zarlar, periferik sinir yaralanmalarının tedavisinde, sinir kanalı olarak kullanıma uygun gözükmektedir. Ancak deneyler sırasında uygulanan elektriksel potansiyeli beklenenin aksine, hücrelerin yönlenmesine yardımcı olmamıştır. Bu da göstermektedir ki potansiyel ve akım ugygulama metodunun istenen sonuçları elde etmek için optimize edilmesine ihtiyaç vardır.

Anahtar Kelimeler: Periferal Sinir Yaralanması, Sinir Doku Mühendisliği, Sinir Kanalı, pHEMA, Çok Duvarlı Karbon Nanotüp

To my parents

ACKNOWLEDGEMENTS

The special thank goes to my helpful supervisor, Prof. Dr. Vasıf Hasırcı. The supervision and support that he gave truly helped the progression and smoothness of the master program. The co-operation is much indeed appreciated. I also thank to my co-supervisor Assoc. Prof. Dr. Gürer Budak for his contribution and support.

Great deals appreciated go to the contribution of METU Central Lab and Department of Materials and Metallurgy workers for their contributions to my study. I also thank to Prof. Dr. Levent Toppare and Prof. Dr. Muammer Ermiş and his students for their sincere helps.

Though only my name appears on the cover, a great many people have contributed to its production. I owe my gratitude to all those people who have made this possible and because of whom my graduate experience has been one that I will cherish forever.

I would like to thank all of the members of METU-BIOMAT group and my lab mates Dr. Türker Baran, Dr. Deniz Yücel, Dr. Albana Ndreu, Senem Heper, Bilgenur Kandemir, Tuğba Dursun, Gökhan Bahçecioğlu, Selcen Alagöz, Cemile Kılıç, Sepren Öncü, Aylin Acun, Ezgi Antmen and our technician Zeynel Akın for their support.

I also thank Dr. Tolga Çamlı, Dr. Aysel Kızıltay and Hayriye Özçelik for their friendly help and for contributions to my study. I am also grateful to my lab partners and special friends Gözde Eke and Birsen Demirbağ for their support, friendship and sharings.

My special thanks go to Arda Büyüksungur for his endless help, patience, and encouragement and especially for all greetings mixed with advice.

I owe special thanks to the special man who came at the right time to wake me up to study hard and left at the right time to wake me up to be aware of the importance of my own life.

I also owe special thanks to my long distance brothers and sisters; Selcen Öztürk, Elif Yaprak, Koray Kırlı, Ahmet Kerim Uysal, Sinem Saka and Kemal Aşık. Their magic touches to my life made me more aware of both the working principle and importance of friendship. I am certain that they will be always there for me even if we cannot see each other for a very long time.

My grateful thanks go to Menekşe Ermiş and Aysu Küçükturhan, my lab mates and best friends. A big contribution and hard worked from both of them are very great indeed. All projects during the study would be nothing without the enthusiasm and imagination from both of them. In addition to the contributions to my academic life I want to thank them for their sense of humor about life, patiently listening and support to my personal life. Their presence has always made my life easier.

I would like to express my special thanks to my best friends Deniz Sezlev, Çiğdem Yılmaz, Mustafa Çiçek and Canan Kurşungöz for their amazing friendship and support to my personal life. I specifically thank them for their incredible patient and support in the face of my complicated life. I have always felt lucky to have them.

Most importantly, none of this would have been possible without the love and patience of my family. My family, to whom this thesis is dedicated to, has been a constant source of love, concern, support and strength all these years. I would like to express my heart-felt gratitude to my family and I want to thank them just for being there for me.

"Insanity is doing the same thing, over and over again,
but expecting different results."
Albert Einstein

TABLE OF CONTENTS

LIST OF TABLES

TABLES

LIST OF FIGURES

FIGURES

LIST OF ABBREVIATIONS

2D	Two Dimensional
3D	Three Dimensional
A	Area
ANS	Autonomic Nervous System
APS	Ammonium Persulfate
BSA	Bovine Serum Albumin
cm	centimeter
CNS	Central Nervous System
CNT	Carbon Nanotube
CO_2	Carbon Dioxide
CSLM	Confocal Laser Scanning Microscopy
d	days
DAPI	4', 6-Diamidino-2-phenylindole
DMEM	Dulbecco's Modified Eagle Medium
DMEM/F12	Dulbecco's Modified Eagle Medium/Ham's F12 Nutrient Mixture
DMSO	Dimethyl Sulfoxide
DS	Degree of Swelling
E	Elastic Modulus
ECM	Extracellular Matrix
EDTA	Ethylenediamine tetraacetic acid
EGDMA	Ethyleneglycol dimethacrylate
ESC	Embryonic Stem Cells
F	Force
FBS	Fetal Bovine Serum

FDA	Food and Drug Administration
FITC	Fluorescein Isothiocyanate
g	gram
h	hour
HEMA	2-Hydroxyethyl methacrylate
kPa	Kilo pascal
kΩ	Kilo ohm
L	Length
L_i	Initial Length
L_f	Final Length
MicroCT	Micro Computed Tomography
min	minute
mm	millimeter
MSC	Mesenchymal Stem Cells
mV	milliVolt
MTT	Thiazolyl blue tetrazolium bromide
mwCNT	Multi-walled Cabon Nanotube
PBS	Phosphate Buffer Saline
PEG	Polyethylene Glycol
Pen/Strep	Penicillin/Streptomycin
pHEMA	Poly(2-hydroxyethyl methacrylate)
PNS	Peripheral Nervous system
SEM	Scanning Electron Microscopy
SIS	Small Intestinal Submucosa
SNS	Somatic Nervous System
TCPS	Tissue Culture Polystyrene
TEMED	N,N,N',N'-tetramethylethylene diamine
UTS	Ultimate Tensile Strength
v	volume

V	Volt
w	weight
w_d	dry weight of pHEMA
w_s	swollen weight of pHEMA
$\in_f$	Strain at break
µL	Micro Liter
ρ	Resistivity
Ω	ohm
σ	Electrical conductivity

CHAPTER 1

INTRODUCTION

1.1. An Overview of the Nervous System

The nervous system is the most complex system in the body. Its processes and action controls are unique. In a minute, millions of information go through different sensory nerves and generate response from the body. The most important role of the nervous system is to process information and thus to control the activities of the body. The muscles and the glands in the nervous system are called effectors due to the control of the nervous system on them (Guyton and Hall, 2006). Figure 1 shows the structural and functional hierarchy of the nervous system.

1.1.1. The Anatomy of the Nervous System

The nervous system is structurally divided into two: central nervous system (CNS) and peripheral nervous system (PNS) (Hall, 1998). The CNS includes the brain, spinal cord, optic, olfactory and auditory systems while the PNS consists of the cranial nerves, sensory nerve bundles and the spinal nerves, first two arise from the brain and the last one arises from the spinal cord. In addition to the structural systems of the nervous system, structural units of the nervous system called nerves allow a person to sense and feel in response to the stimuli of the external environment. They also control movement. The brain is at the center of this system, receiving and sending the signals (Schmidt and Leach, 2003).

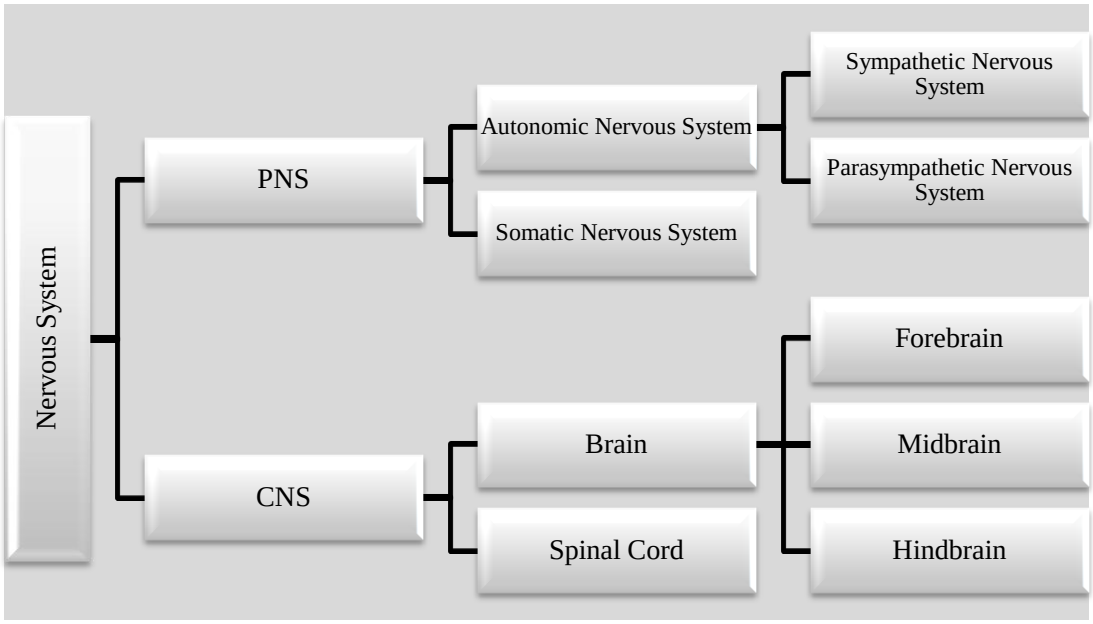

Figure 1. Structural and functional organization of the nervous system.

1.1.1.1. Central Nervous System

The CNS has three major functional capabilities arising from the stages of human evolutionary development: 1) the spinal cord level, 2) the lower brain or subcortical level, 3) the higher brain or cortical level. At the level of spinal cord signals are sent to the control centers of the cord rather than the periphery of the body. At the second level, the lower brain or subcortical level, equilibrium is controlled by mid- and hindbrains in a combined manner. Lastly, at the higher brain level, the cerebral cortex, which cannot function by itself, is mainly a memory storehouse. In other words, it is the thinking machinery of the brain (Guyton and Hall, 2006).

1.1.1.2. Peripheral Nervous System

The peripheral nervous system (PNS) is the second structural unit of the nervous system. It connects the CNS to the real world. The PNS cannot elaborate the projection of the central nervous system and it is not responsible of all the processes

performed by the CNS (Hall, 1998). But it has a crucial role in the body. Peripheral nerves are called “spinal” because they carry information to and from the spinal cord (Heimer, 1983). There are also 12 cranial nerves that conduct information to and from the brain more directly; that is, this does not involve the spinal cord. The PNS is made up of the somatic nervous system that oversees voluntary activities, and the autonomic nervous system that controls involuntary activities (Figure 1).

1.1.1.3. Nervous System Cells

Neural system contains two major cell types: neurons and glial cells. Neurons can be distinguished from other cells in a number of ways, but their most fundamental property is that they communicate with other cells via synapses, which are membrane-to-membrane junctions containing molecular machinery that allows rapid transmission of electrical or chemical signals (Kandel et al., 2000). Glial cells provide support and nutrition, maintain homeostasis, form myelin, and participate in signal transmission in the nervous system (Allen and Barres, 2009).

1.1.1.3.1. Neurons

Electrical-chemical conductance of impulses constitutes the major activity in the nervous system. The basic element, neuron has the ability of generating signals. Each neuron is an independent cell with some specialties. It receives all signals from environment, integrates and processes them and makes a decision to send the message to other neurons. All the neurons work on the same basic principle; however, they are different in size, shape, number of projections, number of receptive fibers (dendrites), and chemical messengers (neurotransmitters) (Kandel et al., 2000).

Ganlia refers to the groups of cell body in the peripheral system while the axons are known as nerves. Peripheral nerves are generally made up of sensory neurons and motor neurons. Sensory neurons receive information from somatosensory system. The motor neurons, however, send signals to the effector organs like glands, muscles

and internal organs. Mixed nerves are the nerves that are responsible for dual purpose (Kandel et al., 2000).

The Structure and Classification of Neurons

Neurons generally have four morphological regions: 1) The cell body (also called the soma or perikaryon), 2) Dendrites, 3) Axon, and 4) The terminal end button (Figure 2). The branching of the neurons specializes in electrical communication. This branching is mainly composed of projections of dendrites arising from the cell body. Dendrites have a high content of ribosomes and specific cytoskeletal proteins and serve in receiving and integrating messages from the environment or the other neurons. This function makes the dendrites the primary target for synaptic input. Some of the neurons lack dendrites while some other have dendritic projections that rival the complexity of a mature tree. The presence of a dendrite and dendrite projections determine the ability of the neuron to receive incoming messages. The messages received are integrated at the origin of the axon which is an extension from the neuronal cell and specialized for signal conduction. The axon has the ability to travel a few hundred micrometers depending on the type of a neuron and the size of the body. Another property of the axon is that it has a unique cytoskeleton whose elements are central for its functional integrity. In CNS, some of the neurons in human brain may have axons of a few millimeters length while some have no axons at all (Augistin et al., 2004). In the peripheral nerve system, nerve structure is different than in the CNS in that the peripheral nerve system contains bundle of nerve fibers. Those fibers are surrounded by connective tissue Figure 3. Epineurium layer is found at the out site and it is very dense. Those fascicles, each bundle of nerve fibers, are wrapped in perineurium, less dense tissue. Endoneurium is the connective tissue surrounding nerve fibers. Epineurium and perineurium contain the blood vessels. The vessels are found in the form of capillaries. (Schmidt, 2003).

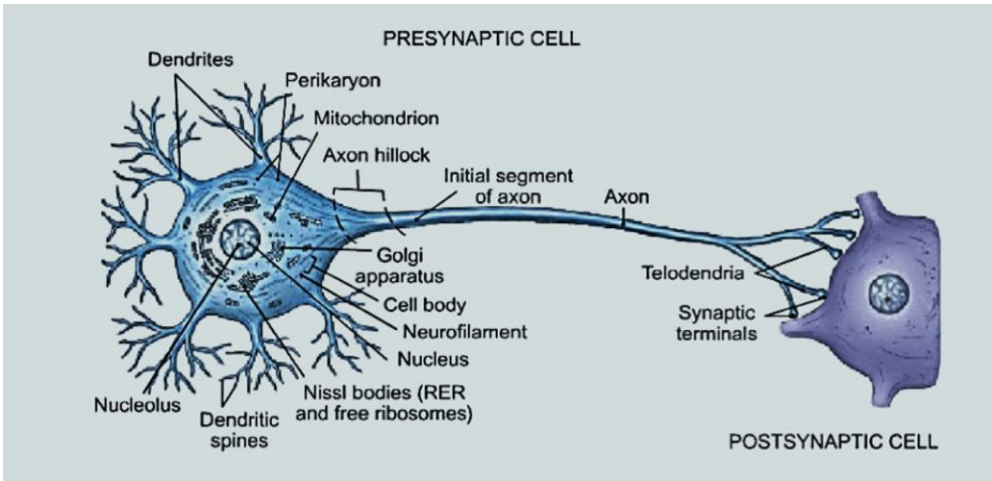

Figure 2. A structure of a neuron (Single nerve cell). Adapted from Martini, 2006.

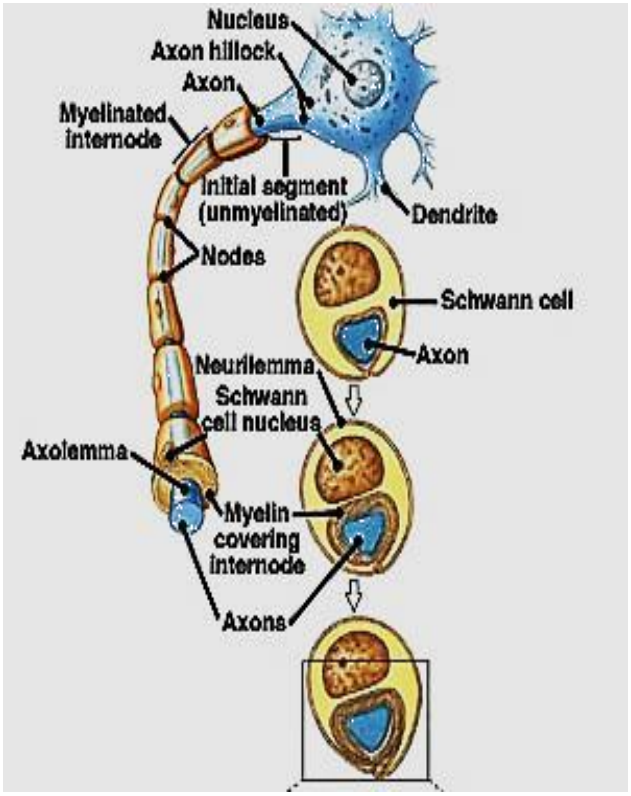

Figure 3. Peripheral nerve structure. Adapted from Martini, 2006.

The peripheral nervous system and central nervous system process the neural impulses conducted by the axons. Many of these axons are individually wrapped with a covering called myelin which serves as insulation around each nerve is the myelin. The spinal nerves emerge from both sides of the spinal cord in a very specific manner. They emerge from the dorsal and ventral horns (Schmidt, 2003).

The neurons are classified functionally in three groups: 1) sensory neurons, 2) motor neurons, and 3) interneuron. Sensory neurons are also called afferent neurons and they deliver messages from sensory receptors to the central nervous system (Kincaid, 2009). The back of the spinal cord is dorsal part and the belly of the structure is knows as ventral portion. The purpose of the ventral region is to send signals to muscles and glands making the process efferent function. Efferent means the information going away from the central nervous system. The function of the ventral region is "motor". It is responsible from the skeletal muscle movement. The dorsal region is responsible from carrying information toward the CNS making the function "afferent". The sensory information is provided by the afferent region and the sending information to internal organs, glands and muscles is achieved by the afferent portion. The schematic representation of this is shown in Figure 4. Some spinal nerves are known as mixed due to the presence of sensory and motor fibers together. As shown in Figure 4b, spinal nerve has two parts. Those parts are the dorsal and the ventral roots. Sensory dorsal root and motor ventral root are known as the Bell-Magendie law. In Figure 4a, an enlargement of the sensory nerve is shown. It is the dorsal root ganglion. A cell body is the main part of the neurons. It is a life support of the axon and it is also known as perikaryon. The axoplasm is found in the cell body and it is an internal constituent. The axon lives, in other words it maintains its existence with the help of the axoplasm. The dorsal root ganglion is a gathering together of the cell bodies associated with each sensory fiber in the spinal nerve. Myelin is not found around the cell bodies. Because of this reason cell bodies are seen gray. Efferent fibers do not have ganglion. The cell bodies of the efferent fibers are found in the

spinal cord. In addition, the axon often has additional projections that permit a single axon to send impulses to and communicate with many other cells. At the distal end of the neural element, there is often a specialized modification; a receptor (Augistin, 2004).

Neurons structurally classified as anaxonic, bipolar, unipolar or multipolar. The relationship of dendrites with the cell body determines the structural classification (Figure 5). In anaxonic neurons, dendrites are similar to axons. In other words all the cell processes are similar to each other (Figure 5a). They are mostly found in brain as well as in special sense organs. Bipolar neurons (Figure 5b) are characterized by 2 different processes. The first one is dendritic and the other one is axon. The cell body is found in between. They are generally smaller than the others and found in special sense organs rarely. The dendrites and axon are fused in a unipolar neuron and the cell body is at one side of the cell (Figure 5c). Most sensory neurons in the PNS are unipolar. The dimension of the axon may be meter or more, ending at synapses in the CNS. Lastly, the multipolar neurons with two or more dendrites and an axon are the most common type of the neurons (Figure 5d). All the motor neurons with axons as long as axons of unipolar neurons generally control skeletal muscles (Martini, 2006).

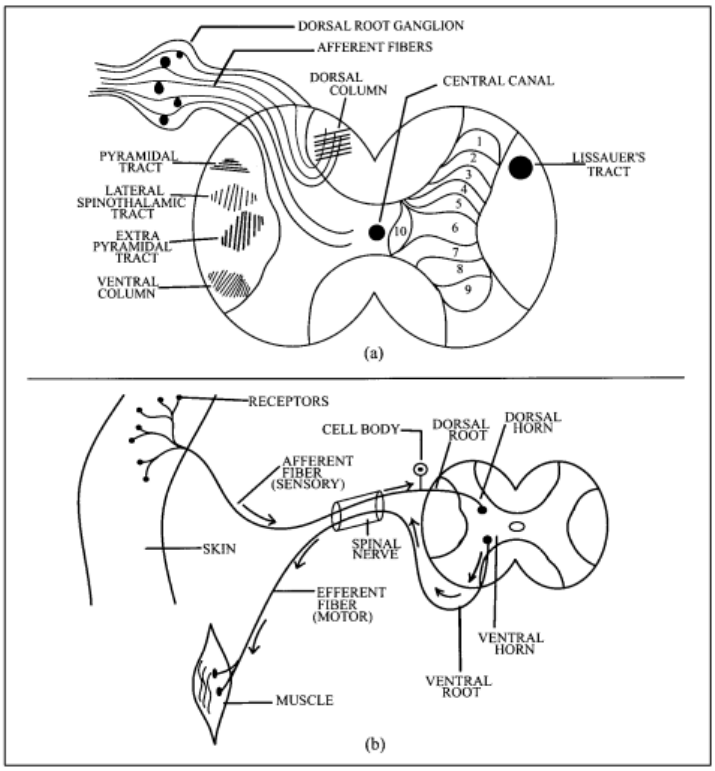

Figure 4. The spinal cord and neuronal pathways: a) the dorsal root ganglion as an enlargement of the sensory nerve, b) the dorsal and ventral roots. Adapted from Hall, 1998.

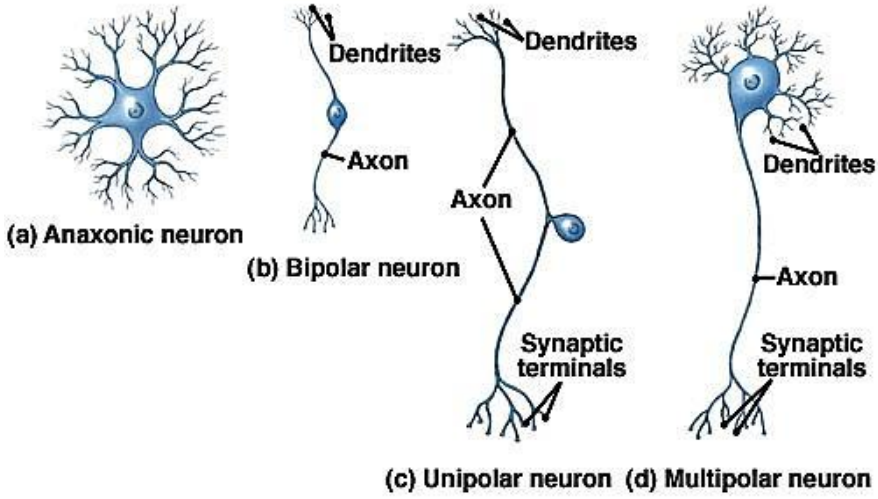

Figure 5. A Structural classification of neurons. Adapted from Martini, 2006.

The Synapse

A synapse is a site specialized for the communication of two neurons: 1) the message is sent by the presynaptic cell, and 2) the message is received by the post synaptic cell (Figure 2). The communication is performed by the release of neurotransmitters affecting the activity of the postsynaptic cell by the synaptic terminal. The presynaptic cell is usually a neuron while the post synaptic cell can be another cell type as well as a neuron. When two neurons communicate, the synapse may occur on a dendrite, on the cell body or on the axon of the post synaptic cell. The post synaptic cell can be muscle or secretory cells, making the junction a neuromuscular or neuroglandular junction, respectively. The synaptic terminal may have different structures according to the type of postsynaptic cell. When a neuron is the post synaptic cell, a simple, round synaptic knob is found (Martini, 2006).

1.1.1.3.2. Glial Cells

Glial cells are quite different than nerve cells. The major difference is in their roles; they do not participate in synaptic interactions or electrical signaling, but they help synaptic contacts and signaling abilities of neurons. The glial cells support the nerve cells in many functions: they maintain the ionic environment for the nerve cells, modulate the propagation of the signal and synaptic action via control of neurotransmitters uptake, and provide synaptic cleft and an environment for neural development. Three types of glial cells are found in the mature central nervous system: star like astrocytes (maintain a chemical environment for neuronal signaling), oligodendrocytes (under a laminated, lipid rich wrapping myelin) and microglial cells (remove cellular debris from the sites of injury or control cell turnover). In the peripheral nervous system, myelin sheath has important effects on the speed of the transmission of electrical signals. In the CNS, it is not the microglial cells but macrophages that remove the cell debris from the sites of injury. In this respect, the

microglial cells are considered to be a type of macrophages by some neurobiologists (Augistin et al., 2004).

1.1.1.4. Neurotransmitters and Neuromodulators

The neurons of the central nervous system and the peripheral nervous system are regulated by the neurotransmitters in neuromodulation. In the direct synaptic transmission a postsynaptic cell is directly affected by the presynaptic cell. However, some neurons secrete neuromodulatory transmitters and those molecules diffuse through the nervous system. They may have an effect on multiple cells. (Delcomyn, 1997).

1.1.2. The Function of the Nervous System

Basically, the function of the nervous system is to interpret the messages coming from the environment and to create mental and motor responses accordingly. When the sensory information is received, it excites the relevant pathways and the desired responses are given by proper integrative and motor regions of the brain (Guyton and Hall, 2006).

The nervous system is functionally classified into two systems: 1) somatic nervous system (SNS) which operates under conscious control, and 2) autonomic nervous system (ANS) which is operated under unconscious control (Figure 6). The ANS uses two neuron pathways and there is a significant difference between the synapses at autonomic effectors and muscle cells. Basically, the SNS controls the skeletal muscles, and therefore the output is voluntary control (Kinjaid, 2009).

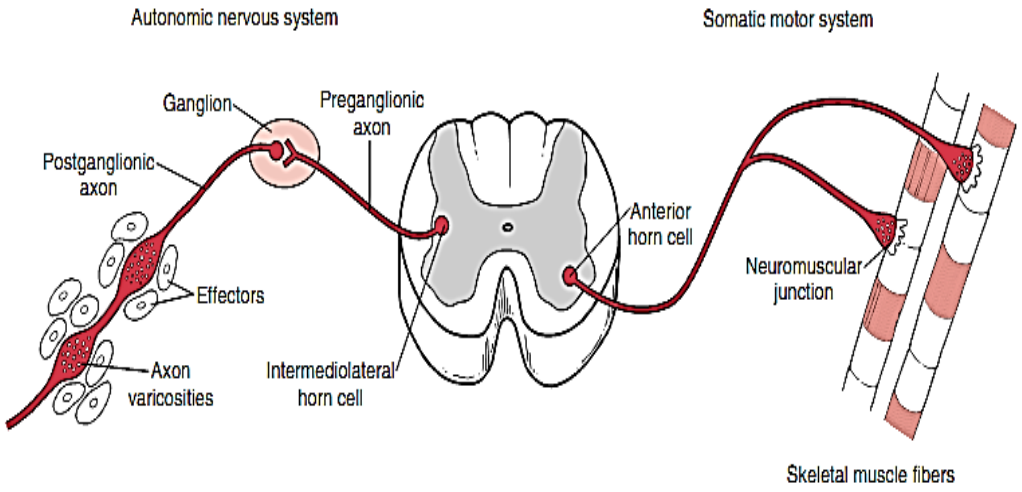

Figure 6. The efferent path of the ANS as contrasted with the somatic motor system. Adapted from Kinjaid, 2009.

1.1.2.1. Somatic Nervous System

The somatic nervous system (SNS) including peripheral nerve fibers has a role in sending sensory information to CNS motor nerve fibers. There are three somatic senses: 1) mechanoreceptive; including tactile and position sensations, 2) thermoreceptive; detecting cold and heat and 3) pain activated; by factors damaging the tissues (Guyton and Hall, 2006). Somatic motor neurons and pathways are also called as motor neurons and motor control, respectively. Pathways involve at least two motor neurons: 1) a lower motor neuron, and 2) an upper motor neuron. The synapse between those two neurons makes a single motor unit in a skeletal muscle. Only part of this motor unit that extends the outside the CNS is the axon of the lower motor neuron. Any injury to this axon extension inhibits the voluntary and reflex control over the motor unit (Martini, 2006).

1.1.2.2. Autonomic Nervous System

There are three functions of autonomic nervous system (ANS): 1) to maintain homeostatic conditions of the body, 2) to coordinate the body's response to exercise and stress, and 3) to assist the endocrine system in the regulation of reproduction. In other words, the ANS has roles in the functions of the involuntary organs, heart, blood vessels, exocrine glands and visceral organs. Considering anatomic, functional and neurochemical differences, there are three divisions of the ANS: 1) enteric nervous system regulating gastrointestinal function, 2) sympathetic nervous system functioning in the response of "fight or flight" response, and 3) the parasympathetic responsible for relaxation and restoration (Kinjaid, 2009). Sympathetic and parasympathetic divisions work synergistically in some organs (Forehand, 2009).

1.1.2.3. Signal Transduction

For a neuron to receive and transmit a message to another, electrical and chemical signaling are necessary. Neurons like the other cells are triggered by the chemical signals via their receptors. When chemical signals, neurotransmitters, hormones or other factors bind to the receptors on the cell membrane or in the cell, the intracellular events start. Overall signaling pathway in the neurons coordinates electrical and chemical activity by controlling the function of individual neurons precisely (Augistin et al., 2004). In physiological processes (like neural differentiation, learning and memory), coordination between an individual nerve and glial cells are maintained by chemical signaling. There are diverse and complex chemical signaling pathways: synaptic, paracrine and endocrine (Augistin et al., 2004). The neuronal cell membrane contains passive and active channels. Passive channels are always open while the active channels are regulated.

A neuron can be in three different states (Figure 7). When there is no stimulus, the cell will be in the resting form (resting potential). After a stimulus comes, a

temporary localized change occurs. The effect decreases with the distance from the stimulus and is a graded potential. If this graded potential is high enough, an action potential will be produced, triggering synaptic activity (Augistin et al., 2004).

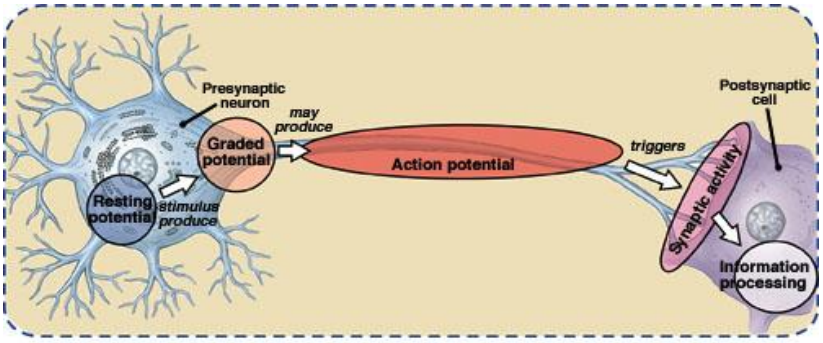

Figure 7. An overview of neural activities. Adapted from Martini, 2006.

1.1.2.3.1. Graded Potential

Graded potentials are produced locally in the vicinity of the stimulation. A stimulus opening the gated channels will responsible for the production graded potential while the leak channels (always open channels) are not involved in the production of graded potentials. Potential is produced by entering of sodium ions inside the cells that attracts the negative charges. So, the resting potential (-70 mV) goes towards zero mV. This means decrease in potential from –70 (–65 mV, –45 mV, –10 mV) as well as increase in membrane potentials above 0 mV (+10 mV, +30 mV). The diameter of the local current area depends on the size of the stimulus. More stimulus results in the greater degree of depolarization (Martini, 2006).

1.1.2.3.2. Action Potential

An action potential is produced when the neuronal membrane depolarized. In most of the neurons voltage gated ion channels that trigger the action potential are found on the axons, no action potential is produced on cell bodies or dendrites. The action potential propagates to the axon and it causes the release of neurotransmitters

(acetylcholine, epinephrin, dopamine, etc.). If the depolarization does not reach a threshold, the regenerative process is not initiated. The initiation of an action potential is, therefore, an "all-or-none" event. (Meiss, 2009).

The conduction velocity of the action potential depends on several factors. A myelin sheath is responsible for an insulation of axon. It is a layer of lipid membrane formed by Schwann cells in the PNS and oligodendrocytes in the CNS. Generally axons larger than 1 micrometer length have the myelin membrane. The nodes of Ranvier are located between segments of the axon myelinated. These nodes are the places where action potentials are generated. The thickness of the myelin increases with increase in axon diameter. The fact that the smallest myelinated axon is bigger than the largest unmyelinated axon makes the conduction velocity faster for myelinated axons. Action potentials are successively generated at neighboring nodes of Ranvier (Figure 8) (Meiss, 2009).

1.1.2.3.3. Synaptic Activity

In the nervous system, the messages are transmitted from one location to another in the form of action potentials. At a synapse, the activity of the postsynaptic cell is affected by the transmembrane potential of the presynaptic cell (Martini, 2006).

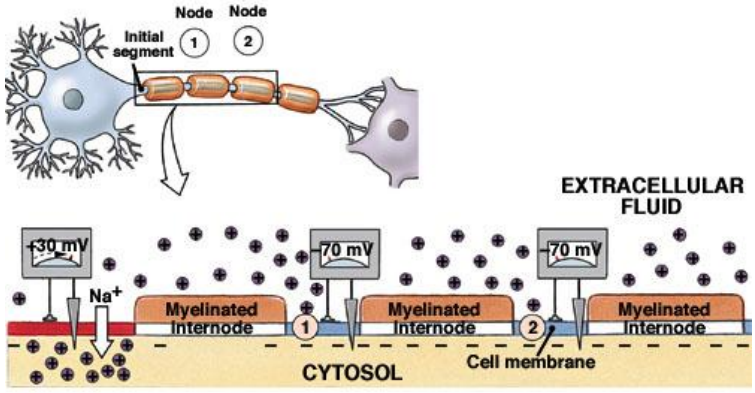

Figure 8. Saltatory propagation along the myelinated axon. Adapted from Meiss, 2009.

1.1.2.3.3.1. Electrical and Chemical Synapses

A synapse can be either electrical with direct physical contact or chemical with a neurotransmitter. In the CNS and the PNS, there are electrical synapses, but the number is extremely low. They are mostly found in the brain, in the eye and in the at least one pair of PNS ganglia. Gap junctions are found between the presynaptic and postsynaptic membranes at an electrical synapse, producing quick and efficient propagation of action potential via an electrical synapse from one cell to the next. The number of the chemical synapses is higher than the electrical synapses and this kind of synapse only occurs in only one direction. In the chemical synapse, action potential of the presynaptic cell results in the release of a neurotransmitter. If the amount of the neurotransmitter is enough for the production of an action potential in the post synaptic cell, the message goes through (Forehand, 2009).

1.2. Neuronal Injury

Neurons are kind of cells that can be easily affected by external and internal environment such as mechanical effects, anoxia, hypoglycemia, viral infections. Any traumatic injury to nerves may result in the loss of neuronal functions. The nerve may repair itself by regeneration of injured axons through complex reactions. The response of the PNS to a traumatic injury is termed as Wallerian degeneration (Waller, 1850).

1.2.1. The types of injury

A traumatic nerve injury can be a penetrating injury, crush, traction, or ischemia and they could be a result of thermal and electrical shock, radiation exposure, percussion and vibration (Robinson, 2000 and 2004). The most common injuries are stretch related injuries. Most injuries (30%) are caused by lacerations. Compression leasing to ischemia is another common injury (Stanec et al., 1997). The degree of the injury may change including: 1) reversible functional injury, 2) death of an axon but without

discontinuity in the endoneurial tube, 3) axonal death along with damage to endoneurial tube, 4) destruction of the whole nerve fiber, and 5) interruption of nerve cord (Bernadic, 1997).

1.2.2. Neuronal Response to Injuries

The individual myelinated axons are surrounded by the endoneurium oriented longitudinally as discussed earlier. Axons are collected to form fascicles and they are surrounded by perineurium oriented circumferential (Sunderland, 1990). The permeability of the epineurial vessels is increased by a trauma. Those vessels are more susceptible to compression trauma than are the endoneurial vessels. The endoneurial vessels may also be injured by pressure at higher levels. This results in intrafascicular edema, eventually leading to secondary injury to the nerve (Rydevik and Lundborg, 1977). In the literature, injuries are divided into 3 groups: neurapraxia, axonotmesis and neurotmesis (Seddon, 1943).

1.2.2.1. Neuropraxia

Neurapraxia which is the mildest form of nerve injury is a result of segmental demyelination. In this case, although axons maintain the intact structure, they are not functional. The impulses can not be transmitted by the nerve. There for there is both sensory and motor loss. The motor fibers are mostly effected by the neurapraxia usually affects motor fibers. Clinically, muscle atrophy does not develop, except for mild atrophy due to disuse. Electrophysiologically, the nerve conducts normally distally but there is impaired conduction across the lesion. Until the remyelination function is lost. Recovery can last hours or a few months. If there is no more compression, the function will be back in 12 weeks. Although motor paralysis can persist for 6 months, most lesions are recovered in 3 months (Dumitru et al., 2001). Reversible physiological conduction blocks are also known as neurapraxia. They persist only for minutes. The foot falls asleep; there is no loss of myelin sheath because it is mainly because of the local ischemia. (Wilbourn, 2002).

1.2.2.2. Axonotmesis

In axonotmesis, completely severed nerve occurs or it is internally disrupted. So the spontaneous regeneration does not occur to reproduce the function. Axon discontinuity occurs. The surrounding stroma however is still partially intact. Generally in stretch and crush injuries axonotmesis is expected. Internal disorganization degree determines the reinnervation (Wilbourn, 2002).

1.2.2.3. Neurotmesis

As a result of massive trauma, a sharp injury and/or severe traction the neurotmesis is seen. The result is nerve rupture. The continuity of nerve trunk is lost because of total disruption of supporting elements. Reinnervention is not possible for this case. The recovery needs a surgery, without it is extremely poor. (Sunderland, 1978).

1.2.2.4. Wallerian Degeneration

Traumatic injury to PNS nerves produces abrupt tissue damage, and the nerve stumps distal to the lesion site undergo cellular changes characterstic of Wallerian degeneration even though they did not encounter the physical trauma directly (Figure 9). Among the other damages, axons breakdown, Schwann cells reject the myelin portions, and bone-marrow derived macrophages are recruited and activated along with resident Schwann cells to remove degenerated axons and myelin (Figures 9 C, D and E) (Rothshenker, 2011).

1.2.2.5. Regeneration

Regeneration and repair processes go on at multiple levels following nerve injury, including the nerve cell body, proximal stump, and the distal stump (Burnett and Zager, 2004; Seckel, 1990). The repair process may be disrupted at one or more of these sites. With mild injuries, regeneration and repair begin almost immediately.

With more severe injuries, there is an initial shock phase, after which regeneration and repair phases continue for many months (Pollock, 1995; Thomas, 1989).

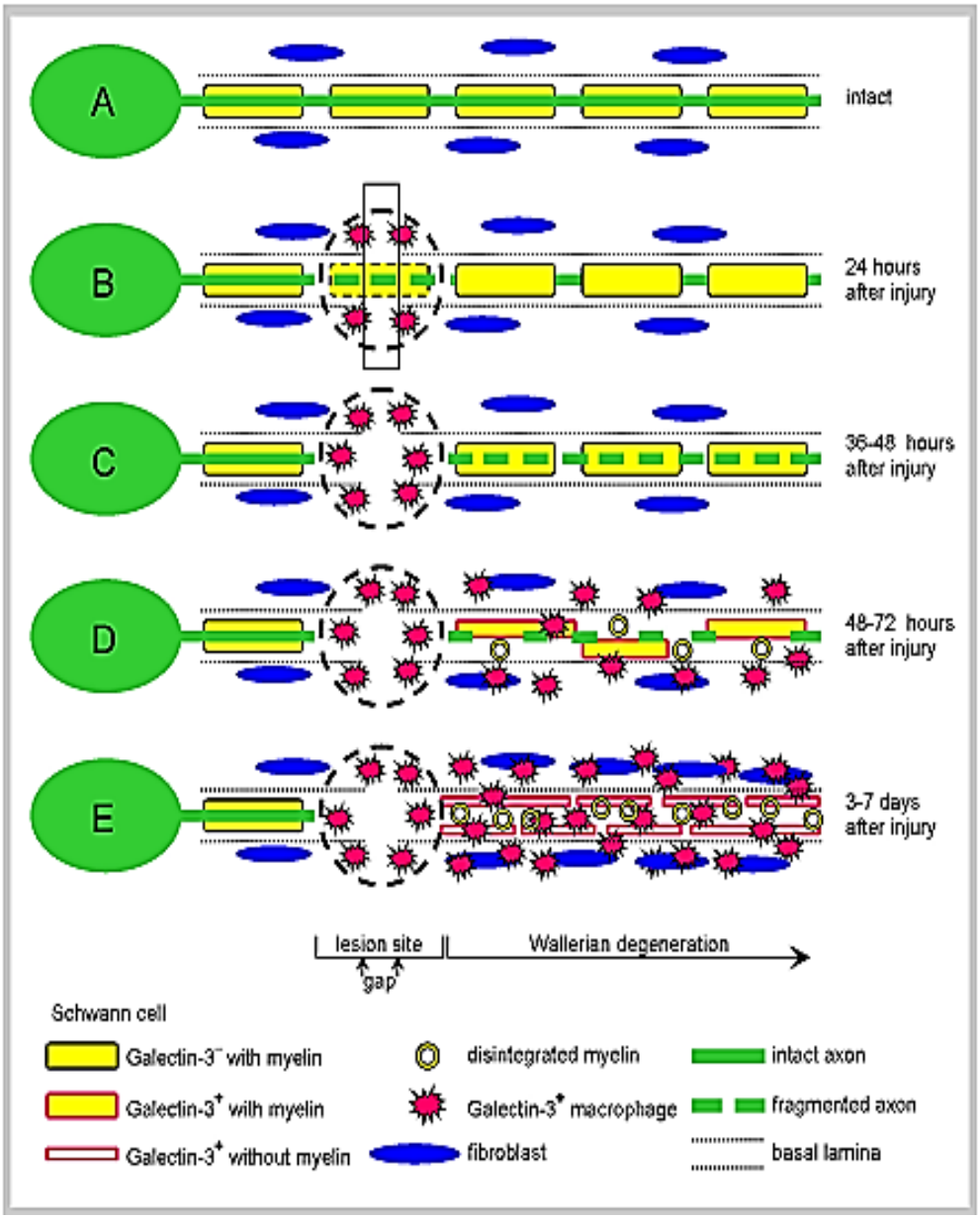

Figure 9. Intact and injured PNS nerves undergoing Wallerian degeneration. Adapted from Rothshenker, 2011.

A cascade of events involving cell signaling molecules and neurotrophic factors occur after nerve injury (Liuzzi and Tedeschi, 1991). The blood–nerve barrier plays an important role (Maricevic and Erceg, 1997). Schwann cells also play an indispensable role in promoting regeneration which they do by increasing their synthesis of cell surface adhesion molecules, and by forming basement membrane containing extra cellular matrix proteins, such as laminin and fibronectin (Fu and Gordon, 1997). Schwann cells produce neurotrophic factors (neurothrophin) that bind to tyrosine kinase receptors and are responsible for a signal that leads to gene activation (Funakoshi et al., 1993). Intracellular processes for repair and regeneration are activated within 30 min (Dahlin, 2006).

Schwann cells begin to divide and create a pool of dedifferentiated daughter cells. Without axon contact, Schwann cells down-regulate the production of normal proteins and convert to the phenotype of a premyelination (Hall, 2005). These dedifferentiated Schwann cells up-regulate expression of nerve growth factor (NGF), other neurotrophic factors, cytokines that lead to differentiation of the Schwann cell and proliferation in anticipation of the arrival of a regenerating sprout. After injury, macrophages migrate into the distal stump and may be involved in the initiation of Schwann cell proliferation. Macrophages up-regulate IL-1, which induces an increase in NGF transcription and NGF receptor density, and also secrete mitogens that trigger Schwann cell proliferation (Davis and Stroobant, 1990). Inflammatory cells and their products also contribute to neuronal survival and axonal regeneration after injury. Macrophages that accumulated after nerve injury provide neurotrophic support to nerve cell bodies, and enhance axonal regeneration (Richardson and Lu, 1994).

1.3. Current Clinical Approaches to Neuronal Injury

Many methods have been studied for the repair of neuronal injury including surgical approaches, grafting, and nerve guidance (Schmidt and Leach, 2003). In the PNS, I is important to obtain an alternative methods to the autologous nerve grafts. It is a

challenging issue. By the help of the alternative methods, it is possible to eliminate a required second surgeries and any damages to the donor site. Besides, clinical functional recovery rates are around 80% for nerve injuries treated using autologous nerve grafts (Chiu, 1995). Thus, bioengineering strategies for the larger defects in the PNS have focused on developing alternative treatments. The other purpose is to improve recovery rates and the outcome in functionality.

1.3.1. End to End Surgical Reconnection

Surgery is performed in cases of a peripheral nerve cut. This is called peripheral nerve reconstruction. The small gaps or defects can be repaired by the procedure including suturing the ends of the two nerve ends together (Lundborg, 2000) (Figure 10).

In this suturing method, there is a possibility of introduction of tension to the nerve cable. It may result in the nerve activity inhibition. So for longer nerve gaps, suturing approach is not useful and not desired. Once completed, the nerve repair site must be covered by healthy tissue, which can be as simple as closing the skin or it can require moving skin or muscle to provide a healthy padded coverage over the nerve (Millesi et al., 1967).

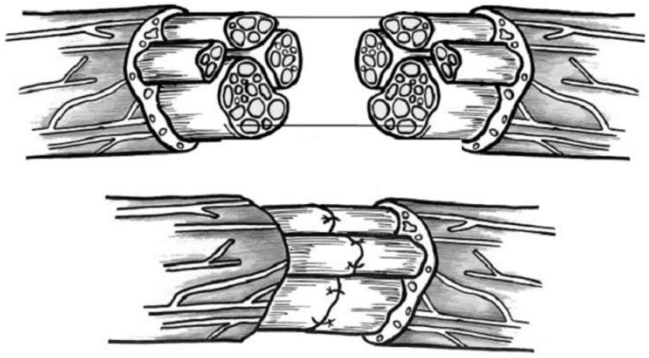

Figure 10. Surgical reconnection. Adapted from Lundborg, 2000.

1.3.2. Tissue Grafting

For the larger nerve defect, an autologous graft that is harvested from another site in the patient's own body is used to fill the gap at the injury site. Disadvantages of this technique include loss of function at the donor site and necessity for multiple surgeries (Lundborg, 1988). When appropriate, a nearby donor may be used to supply innervation to damaged nerves. Trauma can be minimized by utilizing "end-to-side" repair. In this procedure, an epineurial window is created in the donor nerve and the proximal stump of the lesioned nerve is sutured over the window. Regenerating axons are redirected into the stump. Effectiveness of this technique is partially dependent upon the extend of partial neurectomy; increasing degrees of neurectomy gives rise to higher axon regeneration within the lesioned nerve, but with the consequence of increased deficit to the donor (Kalantarian et al., 1998).

Variations on the nerve autograft include the allograft and the xenograft. Allografts and xenografts have the same disadvantages as autografts, though the damage to the donor site is not a concern for the patient, and additionally, the possibility of tissue rejection due to immune responses has to be taken into account. Often, immunosuppression is required with these grafts. Disease transmission is another factor to be considered when the donor is another person or an animal. Overall,

allografts and xenografts cannot match the performance of the autografts, but they are extremely valuable when autologous nerve grafts cannot be used (Comet and Revillard, 1978).

1.3.3. Nerve Guidance

It is commonly accepted that physical guidance of axons is a vital component of nerve repair. Many materials have been used in an attempt to physically guide the regenerating damaged peripheral nerves, using bone, metal tubes, and fat sheaths (Schmidt and Leach, 2003). Similar techniques are also being explored for the repair of transected nerves of the spinal cord. These serve to direct axons sprouting from the proximal nerve end, provide a conduit for the diffusion of growth factors secreted by the injured nerve ends, and prevent or reduce the infiltration of scar tissue. Natural tissues are also explored for nerve repair applications; these include small intestinal submucosa (SIS) and amniotic tissue. SIS is an acellular matrix derived from small intestines porcine origin. SIS is prepared from the mucosa and muscle layers of the small intestine. These are treated with a hypotonic solution to lyse and remove the cells. The resultant material is composed of collagen, fibronectin, growth factors, glycosaminoglycans, proteoglycans, and glycoproteins (Voytik-Harbin et al., 1997). SIS was used with encouraging results as a substrate in the repair of a number of tissues including vascular grafts, urinary tract, and tendon. Recently, SIS derived from rats was used in conjunction with Schwann cells to create nerve grafts that promote regeneration almost as well as the nerve autograft (Schmidt and Leach, 2003).

Amnion of human placental tissues was also used in a similar context in nerve regeneration applications. The amnion is a natural biodegradable tissue that does not exhibit immunogenicity and stimulates vascularization (Gray et al., 1987). The acellular connective tissue matrix can be processed to form thin membranes and converted into conduits. These amnion tubes were shown to promote regeneration

comparable to that obtained with nerve autografts across 1 cm defects in the treatment of siatic nerves of rats, where the tubes completely degrade in 4 months (Mohammad et al., 2000).

1.4. Regenerative Medicine and Tissue Engineering

Regenerative medicine can be defined as "process of replacing or regenerating tissues or organs to restore or establish normal function". This is planned to be achieved by replacing damaged tissue and/or by stimulating the body's own repair mechanisms. It is a group of approaches that involve the use of cells preferable stem cells. Examples include the injection of stem cells or progenitor cells (cell therapies); the induction of regeneration by biologically active molecules administered alone or as a secretion by infused cells; and transplantation of in vitro grown organs and tissues (Riazzi et al., 2009). This field is used to understand how and why various kinds of stem cells are able to develop into specialized cells. Researchers also aim to develop tissue replacement therapies that could restore lost function in damaged organs, or perhaps even grow new, fully functioning organs for transplant (Kamp and Svendsen, 2008).

Tissue engineering is similar to regenerative medicine in the sense that it uses stem cells but in addition it has cell carriers called scaffolds. Tissue engineering can be defined as the process of creating living 3D tissues and organs by using engineering and materials methods, and specific combinations of cells and cell signals (Yucel et al., 2012). The 3D structure created by tissue engineering is different than basic biomaterials in that a new tissue is produced by combining living components with cell carriers or scaffolds (Yucel et al., 2012). To repair a damaged tissue there are 3 approaches (Langer et al., 1993). The first approach is to inject tissue specific viable cells to damaged site, while the second one is to deliver tissue-inducing substances. The last one is the tissue engineering (Kamp and Svendsen, 2008). When the injury is small, the first two approaches are considered as a repair process. More severe injuries require 3D engineered scaffolds so the tissue engineering of which the aim is

to seed a porous, biodegradable 3D, cell carrier scaffolds (Yucel et al., 2012). After the implantation of the scaffold, the cells of the body are also expected to attach and grow inside the scaffolds. In our body all the tissues are surrounded by extracellular matrix composed of parenchymal cells, masenchymal cells and structural materials. In tissue engineering, tissue formation on this extracellular matrix is mimicked.

1.4.1. Nerve Tissue Engineering

When a PNS nerve is injured, the result is a permanent functional disability. Neural tissue engineering is considered as an alternative to grafting in the repair of injured nerve trunks (Yucel et al., 2012). Nerve conduits from different biomaterials and with the use of additional factors like cells, cell signaling molecules like growth factors are being intensely studied. In the neurite extension studies, an additional factor, electrical stimulation, is also being used. It was shown that by electrical stimulation, the rate of neurite extension was enhanced when the cells seeded on a conductive polypyrole sheath and a core with electrospun nanofibers of PCL was used (Schmidt et al., 1997).

1.4.1.1. Nerve Tissue Engineering Scaffolds

A scaffold is an essential component of tissue engineering and provides 3D supports or creates a 3D microenvironment for the cells. Scaffolds with a porous structure provide a site for cell attachment and proliferation that allows and transport of nutrients and metabolites. The first requirements for a scaffold are biocompatibility and biodegradability. They should provide a large enough surface area for cell attachment and reorganization. Its mechanical strength must be appropriate for the target tissue. The products of biodegradation should also be biocompatible. The scaffold’s surface topography and chemistry should encourage cell attachment and growth. And finaly a scaffold must be easily handled, shaped and sutured (if necessary) (Yucel et al., 2012).

1.4.2. Materials Used in Tissue Engineering

A biomaterial scaffold presents a 3D environment for cells to form a tissue or an organ in a highly controlled way (Takezawa, 2003). The principal function of the scaffold is to direct cell behavior, such as migration, proliferation, differentiation, maintenance of phenotype, and apoptosis, by facilitating sensing and responding to the environment via cell–matrix communications and cell–cell communications (Zu et al., 2004). In addition, the scaffold has to provide physical signals to modulate the organization of the cells as well as that of the extracellular matrix derived from them (Lanza et al., 2000). Biologically active molecules, such as cell adhesion molecules and soluble factors, introduce to the biomaterial surfaces adhesion opportunities that are inductive of the attachment of particular cell types. Biologically active molecules interact with cell surface receptors, or activate intracellular cell signaling pathways, trigger the expression or repression of genes, and alter the protein products that regulate cell behavior. Selective incorporation of such biologically active molecules into the tissue engineering constructs makes the fine tuning of cell behavior possible (Wang, 1996). For nerve tissue engineering, synthetic or biological polymers are generally used to form structure of the conduit.

1.4.2.1. Polymers

Various bioengineered nerve grafts have been developed from polymeric materials that have properties and dimensions that meet the requirements for peripheral nerve regeneration. Generally, an ideal nerve guide should be non-cytotoxic, highly permeable to low molecular weight compounds, and sufficiently flexible and to provide guidance for regenerative (Ruiter et al., 2009).

Natural Polymers

Natural polymers are generally hydrophilic and biodegradable, and sometimes carry functional groups suitable for scaffold construction. Natural polymers utilized for

fabricating nerve conduits include chitosan (Wang et al., 2008), collagen (Pfister et al., 2007), gelatin (Gamez., 2004), hyaluronic acid (Sakai et al., 2007), and silk fibroin (Yang et al., 2007). These natural polymers do not invoke serious immune response, provide appropriate signaling to cells without the need of growth factors and some can be degraded by enzymes naturally occurring in the body. However, natural polymers generally suffer from variation between batches or sources. Besides, they need extensive purification and characterization. Furthermore, most lack mechanical strength and degrade relatively fast under *in vivo* conditions (Wang and Cai, 2010).

Synthetic Polymers

Compared with their naturally derived counterparts, synthetic polymers have advantages such as more controlled and tailorable properties. The ease of copolymerization facilitates the regulation and optimization of material characteristics such as degradation, mechanical, thermal, and chemical properties. These polymers are generally classified into two categories based on degradability. Non-biodegradable polymers may also be used in fabricating scaffolds but then have the disadvantage of the need to be removed after completion of their role (Yucel et al., 2010; Wang and Cai, 2010). Such nerve conduits include silicone rubber or polydimethyl siloxane (PDMS) (Jeng et al., 1985), polyethylene (PE) (Seckel et al., 1985), polysulfone (PSU) (Dodla et al., 2008), poly(acrylonitrile-co-vinyl chloride) (PAN-PVC) (Wen et al., 2006), poly(2-hydroxyethyl methacrylate (pHEMA) (Midha et al., 2003), poly(2-hydroxyethyl methacrylate- co-methyl methacrylate) (PHEMA-MMA) (Dalton et al., 2002), and polypyrrole (PPy) (George et al., 2009). Biodegradable polymers used in fabricating nerve conduits include poly(ε-caprolactone) (PCL) (Kokai et al., 2010), PCL acrylate (PCLA) (Cai et al., 2010), PCL fumarate (PCLF) (Wang et al., 2008), polydioxanone (PDO) (verreck et al., 2005), PCL-co-PDO (PCD) (Verreck et al., 2005), polyglycolic acid (PGA) (Yoshitani et al., 2007), poly(glycerol sebacate) (PGS) (Sundback et al., 2005),

poly(l-lactic acid) (PLLA) (Widmer et al., 1998), poly(d,l-lactide-co-caprolactone) (PDLLC) (Radulescu et al., 2007), poly(l-lactide-co-caprolactone) (PLC) (Verreck et al., 2005), poly(glycolide-co-caprolactone) (PGC) (Verreck et al., 2005), poly(lactide- co-glycolide-co-caprolactone) (PLGC) (Nakayama et al., 2007), poly(3-hydroxybutyrate) (PHB) (Kalbermatten et al., 2008), poly(3- hydroxybutyrate-co-3-hydroxyhexanoate) (PHBHHx) (Bian et al., 2009), poly(3-hydroxybutyrate-co-3-hydroxyvalerate)/ poly(l-lac-tide-co-d,l-lactide)/PLGA (PHBV/P(l-d,l)LA/PLGA) blend (Yucel et al., 2010), poly phosphoester (PPE) (Wang et al., 2001), polytrimethylene carbonate-ε-caprolactone (PTMC-CL) (Lietz et al., 2006), and polyurethane (PU) (Cui et al., 2009).

Hydrogels are polymer based networks swollen in water, and have viscoelastic behavior similar to that of soft biological tissues. With these properties they are quite suitable to serve as scaffolds or guides. It was observed that neurite extension on 2D surface was generally better than when the cells are embedded in 3D substrates. To improve their properties a 3-D scaffold structure should have interconnected, micro/macro pores that provide the required surface and also permeability for cell penetration and fluid transport. Anisotropic distribution of pores in a hydrogel scaffold can influence the progress of nerve regeneration (Studenovska et al., 2008). Poly(2-hydroxyethyl methacrylate) (PHEMA) is a hydrophilic, and inert polymer. Polymers based on HEMA are used extensively in a wide range of industrial and biomedical applications. Because of their excellent biocompatibility, hydrogels based on pHEMA have been shown to be potential carriers in drug delivery, dental, ophthalmic, and neural tissue engineering applications (Kumar et al., 2008).

Synthetic and natural polymers can also be turned into composites for improved properties. Composite materials combine at least two separate phases to produce a new material with properties superior to those of the individual components

(Macdonald et al., 2008). For example, carbon nanotubes may be added to obtain electrically conductive material.

Designing an Ideal Nerve Conduit

For the nerve guidance, the desired properties were reviewed by Hudson et al. (1999) (Figure 11). There are several general properties that all nerve guides are expected to possess: They must be easy to handle and suture, readily formed into a conduit with desired dimensions, tear resistant, and sterilizable. Additionally, guidance channels resist collapse during implantation and during regeneration.

The nerve guides need not have to be empty. A larger surface are for the cells to attach inner luminal fillers can be used. Bioactive substances can be incorporated into those fillers. As a result the performance of the conduit is improved by those laminar fillers. For tubes and the fillers have some required properties determined by the intrinsic characteristics. Those characteristics can be, molecular weight, chemical composition and the fabrication method. (Chiono et al., 2009).

Electrical charges have been considered as a potential application in use. They have a role in the cellular differentiation of different cell types via stimulation. The most important example is the neurite extensions. On piezoelectric materials, the cells are stimulated and the extensions are enhanced. (i.e., materials that generate a surface charge with small deformations), such as poly(vinylidene fluo-ride) (PVDF) (Schmidt and Leach, 2003). Therefore, such materials are selected to serve as the guide or the filler. Carbon nanotubes (CNTs), for example, have many qualities that make them desirable as a material for use in neurobiological applications. They are electrically conductive, small and flexible yet possess high strength. They are relatively inert but can be modified with a variety of compounds useful for biology. These properties can be exploited in the development of numerous applications for neuroscience, such as scaffolds for cell growth, biosensors and implantable electronic devices (Malarkey

and Parpura, 2007). Lovat et al. (2009) demonstrated that carbon nanotubes (CNTs) have potential to improve signal transfer between neurons. They also support dendrite elongation as well as cell adhesion. As a result they are potential devices to be used in the neurobiological applications. The results of that study strongly suggested that the growth of neuronal circuits on a CNT grid is accompanied by a significant increase in network activity.

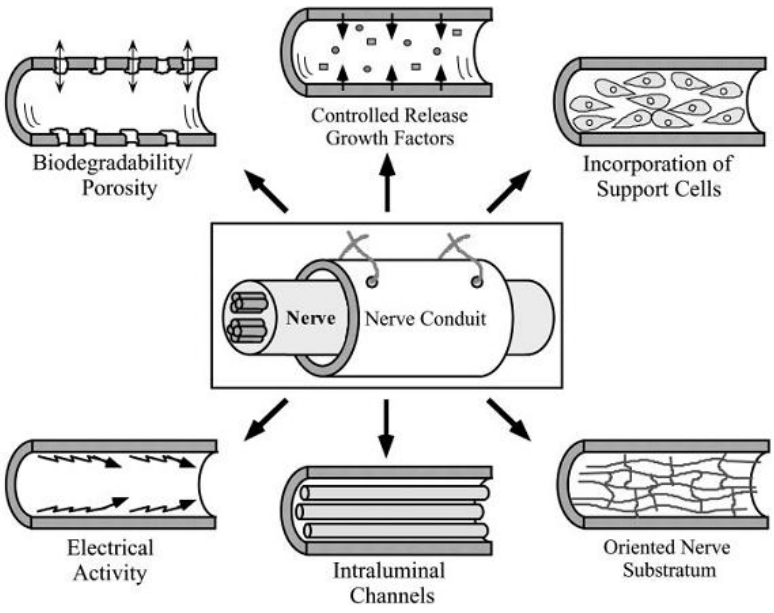

Figure 11. Properties of an ideal nerve conduit. Adapted from Hudson et al., 1999.

1.4.3. Nerve Conduits in Clinical Use

Several nondegradable synthetic materials have been used in nerve repair applications such as silicone tubing (Dahlin and Lundborg, 2001). Inert silicone tubes have been used as bridges to repair short gaps (<10 mm). They do not support regeneration of defects larger than 10 mm, possibly because they are impermeable. Repair process requires exogeneous growth factors. Decellularized muscles (Fansa et al., 1999) and veins (Wrede, 1909) were considered as a nerve conduit. Today vein nerve conduits

are used for defects not larger than 3 cm. However, the vein can collapse and block the regeneration of axons (Fansa et al., 2001).

Tubes made of fibrin glue were also suggested (Kalbermatten et al., 2009) as a After two weeks in vivo, fibrin degraded was therefore not suitable. PGA tubes were used for the repair of rat peroneal nerve (Rosen et al., 1983). After 10 weeks, there was only a minimal host response. The PGA was used with collagen for 11 mm gaps, but the problem was that axonal sprouting was not organized and dense. When tested on a rat sciatic model, collagen type I/II nerve tube did not show severe inflammatory host response (Keilhoff et al., 2003). Collagen nerve tubes were extensively used in the experimental peripheral nerve repair and currently two different collagen tubes (NeuraGen®from Integra Neuroscience, and Neuromatrix/Neuroflex® from Collagen Matrix Inc.) were approved by the FDA for clinical use.

A PGA mesh that was rolled into a tube (later Neurotube®, Synovis) and heat welded was tested clinically on 15 patients for peripheral nerve reconstruction (Mackinnon and Dellon, 1990). Only two patients showed poor recovery, whereas thirteen patients achieved good or excellent results. They concluded that PGA was equivalent to autologous nerve graft.

For clinical use a tube named Neurolac® (Polyganics Inc.) made of poly(D,L-ε-caprolactone) is available. Some complications such as incomplete degradation of the conduit leading to body reaction were reported (Meek et al., 2003). Recently, AxoGen Inc. is offering acellular human nerve allografts (AvanceTM Nerve Graft) with a length between 15 and 50 mm and a diameter between 1 and 5 mm.

1.5. The Aim of the Study

This study aimed at constructing nerve guides to support peripheral neuron regeneration and improving the electrical activity. Cylindrical nerve guides of pHEMA were prepared as hollow conduits, and they were loaded with mwCNT (multiwalled carbon nanotubes) to activate the cells. Composite membranes pHEMA and mwCNTs were characterized in terms of water absorption, mechanical strength, contact angle and electrical conductivity. They were also characterized microscopically using SEM, CSLM and MicroCT. The study involved *in vitro* stages using SHSY5Y neuroblastoma cells, and cell viability and cell alignment were tested upon electrical potential application.

1.6. Novelty of the Study

As presented above, there are some nerve conduit studies in the literature. Even though pHEMA hydrogel and its blends with some other polymers have been used in the construction of a nerve conduit and there are studies in the literature analyzing the interaction between the CNTs and neuronal network, this study is the first using the mwCNTs in a pHEMA conduit to improve an electrical conductivity of the material. Improvement of the conductivity is thought to be helpful for the regeneration of the axons.

CHAPTER 2

MATERIALS AND METHODS

2.1. Materials

2-Hydroxyethyl methacrylate (>99%), ethyleneglycol dimethacrylate (98%), ammonium persulfate (APS), N,N,N',N'-tetramethylethylene diamine (TEMED), polyethylene glycol 400 (PEG400), multiwalled carbon nanotubes (mwCNT, >99% carbon, diameter 6-13 nm, length 2.5-20 μm), thiazolyl blue tetrazolium bromide, bovine serum albumin (BSA), sodium cocodylate, gluteraldehyde (25%), 4',6-diamidino-2-phenylindole dihydrochloride (DAPI) and FITC-conjugated Phalloidin were purchased from Sigma-Aldrich (USA).

Dulbecco's Modified Eagle Medium/Ham's Nutrient Mixture F12 (DMEM:F12, 1:1) with and without Phenol Red, fetal bovine serum, Penicillin/Streptomycin and Trypsin solution (0.25% w/v, in Hanks' Balanced Salt Solution, including EDTA) were purchased from Hyclone (USA).

Dimethyl sulfoxide (DMSO) and Triton-X 100 were obtained from AppliChem (Germany).

Trypan blue (0.4 %) was purchased from Invitrogen Inc. (USA). SHSY5Y neuroblastoma cell lines were purchased from ATCC (USA)

2.2. Methods

In this study, the first step was to optimize the conditions for the preparation of hollow cylindrical pHEMA hydrogel conduits. After establishing the conditions for preparation of cylindrical pHEMA hydrogel conduit, the mwCNT-pHEMA composite membranes were prepared, characterized by water absorption, contact angle, electrical conductivity and mechanical strength, followed by microscopical examination by scanning electron microscopy (SEM) and confocal laser scanning microscopy (CSLM). *In vitro* studies were performed with mwCNT-pHEMA composites using SHSY5Y neuroblastoma cells with and without induction of cellular activity with electrical currents. The 3D structures were examined with microCT.

2.2.1. Preparation of Hollow pHEMA Conduits

PHEMA samples were prepared by solution polymerization. HEMA monomer (1 mL) was first mixed with distilled water (1:1, v/v) and then the EGDMA (crosslinker) was added to this solution (0.4%, v/v, crosslinker in monomer). Afterwards, PEG 400 was included as porogen so that its final concentration was 0.16% (v/v). The solution (about 2.5 mL) was put in a glass test tube (d=1 cm) and different amounts of the accelerator (TEMED, 2.5-40 µL) were added with 100 µL APS (1%, v/v in distilled water). Mold was made by fixing a glass rod (d= 0.5 cm) in the middle of a test tube (Figure 12). During the polymerization process, the solution was incubated at 4^0C for 2 h. Then the polymer was removed, placed into excess distilled water to swell and to leach PEG 400 out for 2 h. The polymer was then air dried and stored in that form at room temperature.

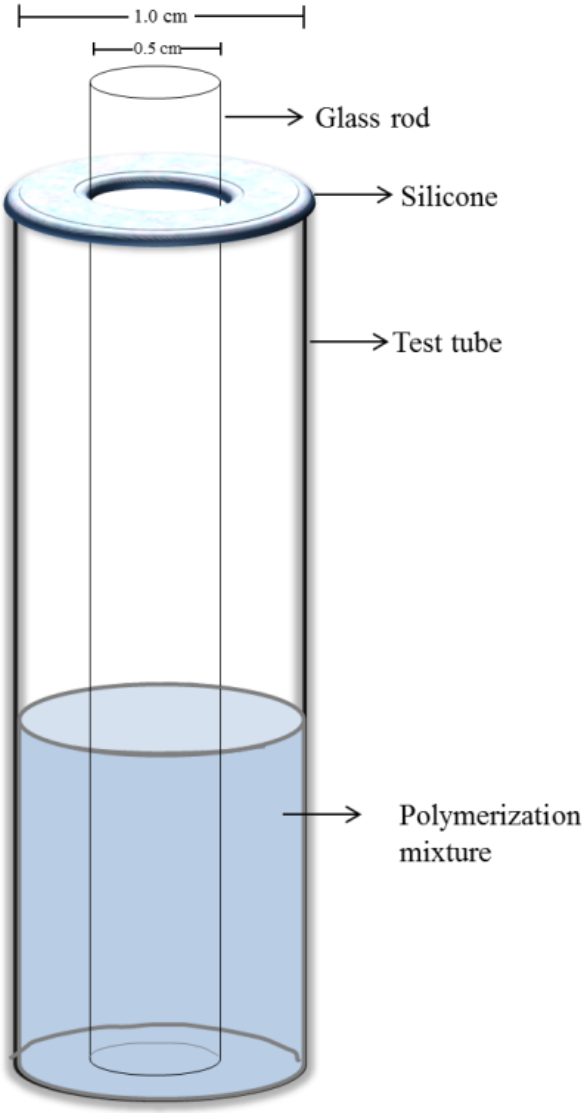

Figure 12. Polymerization mold for the preparation of pHEMA conduits.

2.2.2. Preparation of mwCNT-pHEMA Membranes

Even though the cylindrical hydrogel was to serve as the nerve guide, for convenience during characterization, the hydrogel was also prepared in the form of a membrane. MwCNT-pHEMA membranes were prepared in 6-well tissue culture plates. The polymerization mixture consisted of mwCNTs (1, 2, 3, 4, 5 and 6% w/w),

distilled water:HEMA (1:1, v/v), EGDMA (0.4%, v/v, in monomer), PEG 400 (0.16%, v/v), APS/TEMED (4% and 0.1%, v/v) was prepared. The 6-well plate containing the polymerization solution was stored at room temperature for 2 h with shaking at times to obtain a homogeneous distribution of the mwCNTs in the wells. After polymerization, distilled water was added to the wells to swell the mwCNT-pHEMA membranes which were gently removed, freeze dried, cut and stored at room temperature (Figure 13).

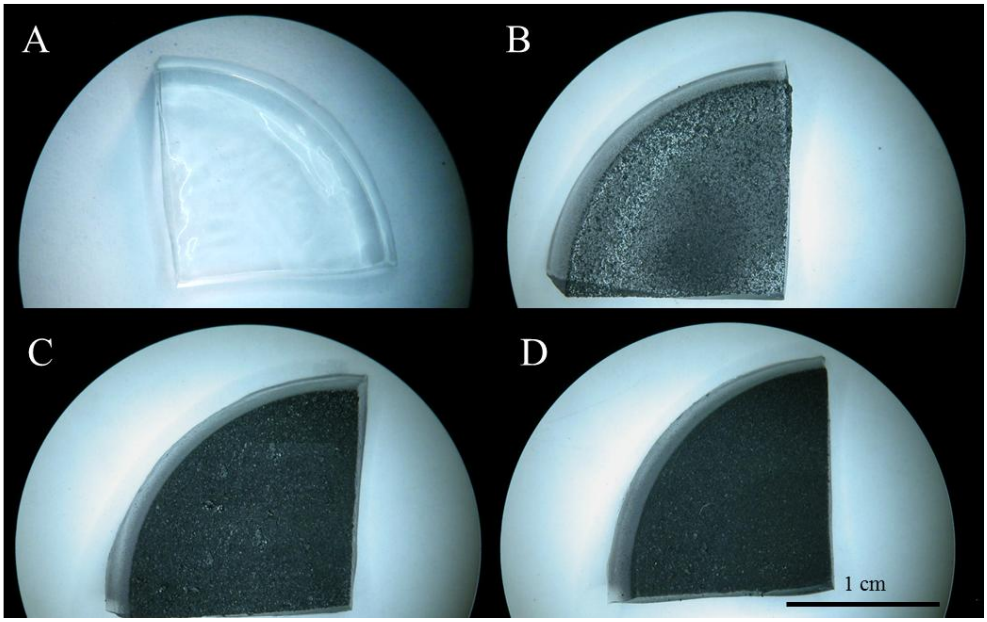

Figure 13. Stereomicroscopy images of quarter disks of mwCNT-pHEMA membranes with different mwCNT contents. A) No mwCNT, B) 1% mwCNT, C) 3% mwCNT, D) 6% mwCNT.

2.2.3. Characterization of Unseeded mwCNT-pHEMA Membranes

Characterization of the mwCNT-pHEMA membranes was conducted by determining their water absorption, contact angle, electrical conductivity and mechanical properties.

2.2.3.1. Swelling

The weights of the pHEMA conduits and composite membranes were determined. After 24 h incubation in distilled water and 24 h air dry, the weights of the swollen and dry samples were obtained. The degree of swelling was calculated according to the following equation;

$$\text{DS}\ (\%) = \frac{w_s - w_d}{w_s} \times 100 \qquad (1)$$

where

DS (%): Degree of swelling (%, w/w)

w_s: swollen weight of pHEMA (mg)

w_d: dry weight of pHEMA (mg)

2.2.3.2. Contact Angle

The mwCNT-pHEMA membranes were brought to equilibrium swelling by allowing to swell in distilled water for 24 h at room temperature, the excess water was removed and the contact angles of the mwCNT-pHEMA membranes were determined in wet state by a goniometer (KSV Instruments, CAM 200, Finland). The contact angles of dried membranes could not be determined because the dry hydrogels immediately absorbed the water droplet added for contact angle measurement.

2.2.3.3. Mechanical Testing

The mwCNT-pHEMA membranes were brought to equilibrium swelling in distilled water (24 h, room temperature) and were cut to yield rectangular test samples of 30 mm length, 10 mm width. Their thicknesses were measured with a micrometer (Erste Qualited, Germany) with a sensitivity of 10 µm. Tensile mechanical properties of the

membranes were determined in wet state at room temperature by a mechanical tester (Lloyd, LRX5K Mechanical Tester, UK) using the programWindapR. The membranes were fixed between the clamps (gauge length: 10 mm) of the instrument and their tensile properties were measured by straining at a rate of 2 mm/min.

By using the data and the plots (Appendix B) obtained during the test, the ultimate tensile strength (UTS) and elastic modulus were calculated. Ultimate tensile strength (UTS), elastic modulus (E) and strain at break (t_f, %) were calculated according to equations below;

$$\mathrm{UTS} = \frac{\mathrm{F}}{\mathrm{A}} \tag{2}$$

$$\mathrm{E} = \frac{\Delta \mathrm{F}}{\mathrm{A}} \times \frac{\mathrm{L}}{\Delta \mathrm{L}} \tag{3}$$

$$t_f\ (\%) = \frac{\mathrm{L_f} - \mathrm{L_i}}{\mathrm{L_i}}\ x\ 100 \tag{4}$$

where

F: Force (N)

A: Area (mm^2)

E: Elastic modulus (N/mm^2)

L: Length (mm)

L_i: Initial length (mm)

L_f: Final length (mm)

t_f: Strain at break

2.2.3.4. Electrical Conductivity

Electrical properties of the samples were studied by measuring their resistances in dry and wet forms using an ohm meter (Digital LCD Ohm meter, OHM 787, USA). For the wet state studies, the samples were incubated in tissue culture medium for 1 d. The length of the charge flow was 0.5 cm and the other parameters including thicknesses and lengths of the samples were measured by a micrometer with a

sensitivity of 10 µm and the cross-sectional areas were calculated from these values (Table 3.4). The conductivities were calculated according to the Equations 5 and 6. The conduits with the mwCNT concentrations of 0% and 1% were excluded from the calculations because they did not show any conductivity in the trial runs.

$$R = \frac{\rho L}{A} \quad (5)$$

$$\sigma = \frac{1}{\rho} \quad (6)$$

where

ρ: Resistivity (kΩ)

L: Length (cm)

A: Cross-sectional area (cm^2)

σ: Electrical conductivity ($\Omega^{-1}.cm^{-1}$)

2.2.3.5. Microscopical Characterization

Porosity and average pore size of the mwCNT-pHEMA membranes were determined by using different microscopical techniques, including stereomicroscopy, scanning electron microscopy (SEM) and confocal laser scanning microscopy (CLSM). SEM and CSLM results were further treated with the program Image J (NIH, USA).

2.2.3.5.1. Stereomicroscopy

The composite membranes were freeze dried and examined with a stereomicroscope (Nikon, SMZ1500, USA).

2.2.3.5.2. SEM

The membrane samples were cut to obtain 1 cm^2, freeze dried for 8 h (Labconco, FreeZone6p Plus, USA) and placed on SEM stubs with carbon tapes. The surfaces of all the membranes were coated with Au–Pd under vacuum and examined with with a scanning electron microscope (JEOL, JSM-6400, USA) equipped with NORAN System 6 X-ray Microanalysis System and with SEM (QUANTA, 400F Field Emission SEM, USA) at 5-20 kV. Micrographs were analyzed with the program ImageJ (NIH, USA) to determine porosity and average pore size of the pHEMA hydrogel. The program determined the pores according to the color intensities (the darker regions showed the pores) and the porosity of the surface was given as percent. The sizes of the pores were determined by selecting the pores with different dimensions, and calculating the average areas.

2.2.3.5.3. CLSM

The membranes were examined in wet state at room temperature with a confocal laser scanning microscope (Leica DM2500, Germany).

2.2.3.6. 3-D Characterization with MicroCT

MicroCT technique is based on the absorption dependency of X-rays on material density and atomic number. When X-rays pass through the specimen, X-ray beam intensity will be absorbed by the chemical components of the material. The beam intensity of X-rays after absorption by the components for different direction of irradiations is called projection (Neubauer and Jenning, 1996). MicroCT (SkyScan 1172, Belgium) was used to study the pHEMA conduits and membranes composed of pHEMA and mwCNT (6%, w/w). The samples were analyzed for 360 degrees unless otherwise stated. The sample was fixed on the rotatable holder and distance between x-ray source and the detector was adjusted.

After scanning, the data was reconstructed by RECON and CTan softwares (SkyScan, Belgium) was used to adjust the image threshold on gray scale. The adjustment makes it possible to analyze the pore size distribution, total pore volume, mean pore sizes, object volume among other parameters. Dataviewer software was used to calculate the distance between regions. Ctvox was used to create the 3D view of the object and Ctvol was used to create the 3D model of the object.

2.2.4. *In vitro* Studies

In vitro studies were carried out to determine the cytotoxicity of mwCNT-pHEMA composites on SHSY5Y neuroblastoma cells. In addition, the effect of electrical potential on proliferation and orientation of the cells were also studied.

2.2.4.1. SHSY5Y Neuroblastoma Cell Culture

The neuroblastoma cells were cultured in a growth medium that contains Dulbecco's Modified Eagle Medium/Ham's Nutrient Mixture F12 (DMEM/F12; 1:1), fetal bovine serum (FBS) at a final concentration of 10% and penicillin/streptomycin (final concentrations 100 units/mL: 100 µg/mL, respectively). The cells were cultured in tissue culture polystyrene (TCPS) flasks at 37 °C in a humidified 5% CO_2 incubator, and the growth medium was replaced every two days. After discarding the medium, the attached cells were washed with colorless DMEM-F12 cell culture medium containing the unattached cells and then incubated with Trypsin-EDTA (diluted to 0.05% from a 0.25% stock in PBS) at 37^0C for 5 min. Detached cells were collected with DMEM-F12 cell culture medium containing 10% serum and penicillin/streptomycin (100 units/mL/ 100 µg/mL).

2.2.4.2. Cell Seeding on the mwCNT-pHEMA Composite Membranes

The membranes were sterilized by exposing both sides to UV in a laminar flow hood for 30 min at room temperature. Following sterilization, they were transferred into 12-well tissue culture plates. Neuroblastoma cells detached from the flask (as described in the section 2.2.3.1) were seeded onto the composite membranes at a density of 100 cells/cm^2. The cell seeded membranes were incubated for 30 min at 37 °C in a humidified 5% CO_2 incubator for attachment to the composite membranes, and then DMEM:F12 growth medium with FBS (10%, v/v) and penicillin/streptomycin (final concentrations 100 units/mL/ 100 µg/mL, respectively) was added. The cells were incubated at 37°C in a humidified 5% CO_2 incubator with the medium replaced every two days.

2.2.4.3. Application of Electrical Potential

The membrane samples were 30 mm long, 10 mm wide and 0.4 mm thick. To activate the cells with electrical potential, the membranes were removed from the incubator and the electrical potentials of 1 and 2 V were applied for 10 min at every h for 12 h in a laminar flow hood after removing the excess medium (Figure 14). Gold probes were used to create the electrical potential using a power supply (Hewlett Packard, Triple Output DC Power Supply, USA) (Figure 14). After the potential application, the membranes were returned to the incubator. For the next 12 h, the cells were incubated at 37°C in a humidified 5% CO_2 incubator without further potential application. Three kinds of controls were used; a) the cells on TCPS incubated at 37°C in a humidified 5% CO_2 incubator for 24 h without any treatment, b) cells on TCPS removed from the incubator for 10 min every hour without any treatment, c) cells removed from the incubator for 10 min every hour with application of electrical potential.

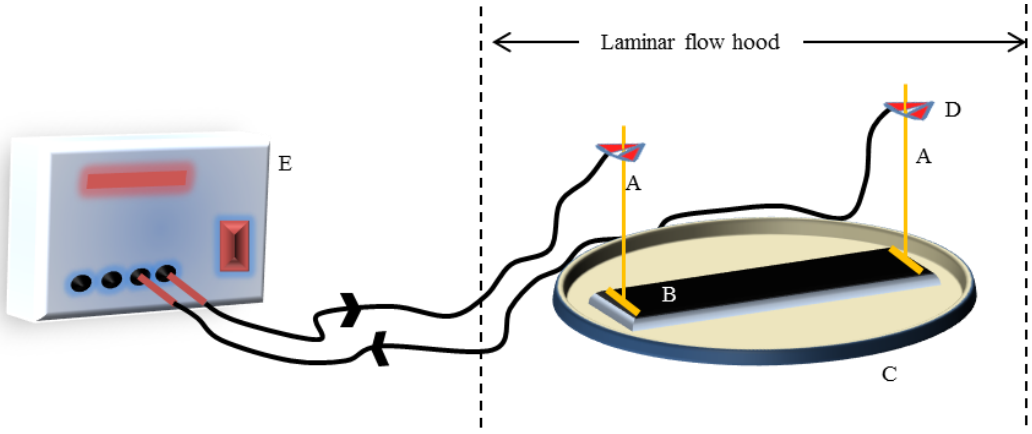

Figure 14. The set up for electrical potential application to the SHSY5Y neuroblastoma seeded mwCNT-pHEMA membranes. A) Gold probe, B) Composite membrane, C) Petri dish, D) Clamp, E) Power supply.

2.2.4.4. MTT Cell Viability Assay

MTT cell viability assay was performed using the membranes (as described in the section 2.2.3.2). Cells in TCPS wells were used as the positive control and cell-free membranes with varying mwCNTs were used as the negative control. The MTT assay was conducted 3, 12, and 24 h and on days 2 and 7 of cell culture. They were also treated after potential application at 3, 12 and 24 h. The test is based on the reduction of MTT, (3-(4,5-dimethylthiazol-2-yl)-2,5-diphenyltetrazolium bromide, a yellow tetrazole), to a purple formazan by live cells (Figure 15). At each time point, MTT solution prepared by dissolving thiazolyl blue tetrazolium bromide in colorless DMEM:F12 cell culture medium (1 mg/1 mL) was added and incubated for 3 h at 37 °C in a humidified 5% CO_2 incubator followed by addition of 4% HCl in isopropanol to dissolve the formed formazan crystals. After 1 h incubation at room temperature with regular shaking, the absorbances were measured at 550 nm using a UV-Vis spectrophotometer (Thermo Scientific, Multiscan Spectrum with Cuvette, USA). The absorbances were converted to cell numbers by using a calibration curve (Appendix

C). The average value for cell number on each membrane of different mwCNT concentrations was calculated.

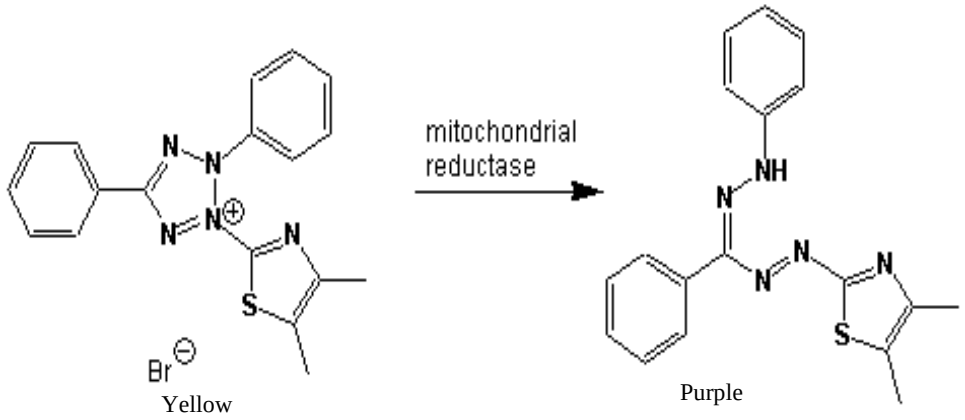

Figure 15. Scheme of MTT cell viability test of reduction of 3-(4,5-dimethylthiazol-2-yl)-2,5-diphenyltetrazolium bromide (yellow) to formazan crystals (purple).

2.2.4.5. Microscopical Characterization of SHSY5Y Neuroblastoma Cells

The behavior of the cells on membranes was studied by fluorescent microscopy, SEM and CSLM. The micrographs were further analyzed by ImageJ.

2.2.4.5.1. SEM

Cultured scaffolds were removed from media and washed twice with DMEM:F12 colorless cell culture medium, and then with cacodylate buffer (0.1 M sodium cacodylate, pH 7.4), and incubated in glutaraldehyde (2.5% v/v in cacodylate buffer) at room temperature for 2 h. After washing with cacodylate buffer, the samples were freeze dried for 2-3 h, and examined with SEM as described in section

2.2.4.5.2. CSLM

The cultured cells were fixed with 4% paraformaldehyde (v/v) for 15 min at room temperature followed by washing with colorless DMEM:F12 (1:1) cell culture medium. The fixed cells were permeabilized with 0.1% Triton X-100 (in PBS, v/v)

for 5 min, and blocked by 1% BSA (in PBS, w/v) for 30 min at 37 °C. The cells were stained with FITC-conjugated Phalloidin, prepared by dissolving in 0.1% (in PBS, w/v) BSA (1:1000, w/v) for 1 h at 37 °C and then washed with colorless DMEM:F12 (1:1) and incubated in PBS solution. They were examined by a confocal laser scanning microscope (Leica DM2500, Germany) in wet state at room temperature. CSLM micrographs were further analyzed with Image J.

2.2.4.5.3. Fluorescence Microscopy

The cultured cells were fixed and dyed as described in the section 2.2.4.5.2. Instead of the Phalloidin the fixed cells were dyed with DAPI; after blocked with 1% BSA, the cells were washed with PBS and incubated in DAPI solution (prepared by dissolving in 0.1% BSA, 1:3000, v/v) for 10 min at room temperature and then they were washed with PBS and stored in PBS solution. Fluorescence microscopy (Olympus IX70, Japan) examination was carried out in wet state at room temperature.

2.2.5. Statistical analysis

All the characterization and *in vitro* studies were performed in duplicates or triplicates. After the calculation of arithmetic means and standard deviations, significant differences between mean values in control and test groups were determined using 1-tail Student's t-test which is the standard software of Microsoft Excel. For the p values equal or smaller than 0.05, the differences were considered as statistically significant.

CHAPTER 3

RESULTS AND DISCUSSION

3.1. Preparation of pHEMA Conduits and mwCNT-pHEMA Composite Membranes

The conduits and composite membranes were prepared by solution polymerization technique as previously described by Chirila et al (1993). In this method, the monomer, the crosslinker and the porogen are all dissolved in a solvent. The solution polymerization of this monomer allow the formation of porous structures which are influenced by the type and amount of diluent used. After the polymerization, the porogen was leached out by dissolving in water and making the hydrogel porous.

3.2. Characterization of mwCNT-pHEMA Composite Conduits

Various properties of pHEMA conduits and pHEMA-mwCNT composite membranes were determined. The results are presented below.

3.2.1. Swelling

Equilibrium swelling degrees of the pHEMA conduits prepared by adding different amounts of initiators were determined. After 1 day incubation in distilled water and 1 day air dry, the weights of the samples were determined. Following the polymerization, the degree of swelling was calculated according to the Equation 1 (see section 2.2.3.1). Table 1 shows the swelling degrees of pHEMA conduits with

different TEMED amounts. TEMED accelerates the rate of formation of free radicals from the initiator persulfate and this in turn accelerates polymerization. Decreasing the concentration of the accelerator results in an increase in the average polymer chain length, in gel elasticity and in the swelling degree (Shi and Jackowski 1998). According to the Table 1, the lowest amount (2.5 µL) resulted in the highest swelling and ratio was used in the preparation of the samples used in the following studies.

Table 1. Swelling degrees of pHEMA conduits with different amounts of TEMED.

Amount of TEMED in the polymerization mixture (µL)	**Swelling Degree (%)**
40	65±5.0
20	72±3.5
10	82±4.0
5	91±2.0
2.5	102±3.0

Figure 16 shows the change in the weights of the conduits in wet and dry states. Day 1 shows the weight of the swollen samples immediately after the polymerization. The even days (2, 4 and 6) show the weights after air dry and the odd days (3 and 5) show the weights after 1 day of incubation in distilled water and thus the weights of re-swollen samples.

According to the results, when put in water (Days 3 and 5), the gel matrix actually swells to its equilibrium and upon drying expels some water from voids left after porogen. The swelling ability of the pHEMA hydrogels, thus, makes it a good candidate for the preparation of tissue engineering scaffold, because its viscoelastic nature is similar to those of soft tissues (Studenovska et al., 2008). It also shows that the gel maintains its ability to re-swell repeatedly.

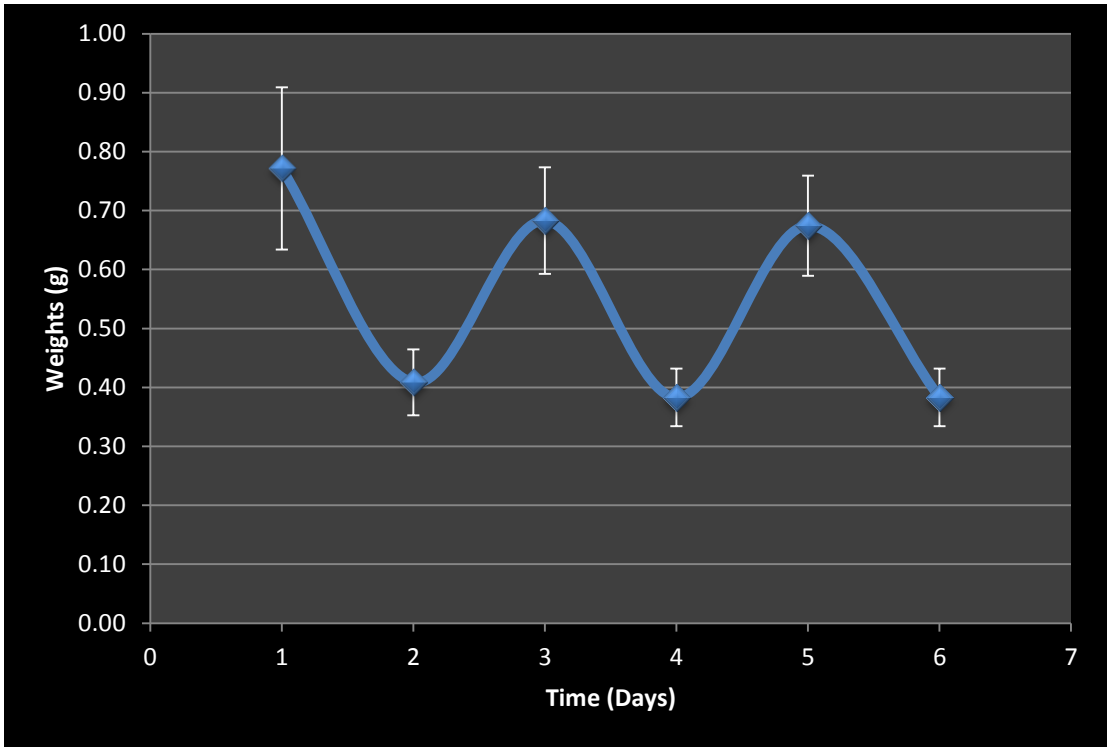

Figure 16. Swelling profile of pHEMA conduits. The gels are dry on even days and wet on odd days.

Table 2 shows the swelling ratios of mwCNT-pHEMA composite membranes. The swelling ratio of flat pHEMA membrane is smaller than the ratio of pHEMA hollow conduit. The reason may be the structural difference between the two; the conduit structure has higher surface area to absorb water. MwCNT content in the membrane structure also affects the swelling ratio; increasing amount of the mwCNT decreases the ratio, because the nanotubes cover one surface of the membranes decreasing the surface area to absorb water.

Table 2. Swelling degrees of mwCNT-pHEMA composite membranes with different mwCNT concentrations.

mwCNT content (%, w/w)	Swelling degree (%)
0	92±3.5
1	85±5.0
2	80±6.5
3	78±4.0
6	75±7.0

3.2.2. Contact Angle

Since hydrophilicity and hydrophobicity are closely related with protein adsorption and their correlations are certainly affecting subsequent cell adhesion, for any scaffold, contact angle is important for cell attachment and growth (Israelachvili, 1997). When the contact angle is above 80^0, the surface is considered as highly hydrophobic, while contact angles less than 35^0 indicate that the surface is highly hydrophilic. Researches showed that highly hydrophilic surfaces were the most suitable surfaces for cell attachment. However, on these surfaces there was less cell to cell interaction because cell to surface interaction was more favorable. Extremely high hydrophobic surfaces prevent cell attachment because they are not suitable for extracellular matrix proteins to attach (Menzies and Jones, 2010).

Contact angles of mwCNT-pHEMA composite membranes are shown in Figure 17. The results with wet samples showed that the contact angles, and therefore the hydrophobicities were higher upon increasing the concentration of the mwCNTs; the contact angle of the pHEMA membrane was $26.71^o \pm 1.66^o$ (Figure 17A), while it is $69.56^o \pm 2.26$ for mwCNT-pHEMA composite membrane containing 3% (w/w) mwCNT (Figure 17D). The difference between the contact angles of two membranes was statistically significant ($p<0.05$).

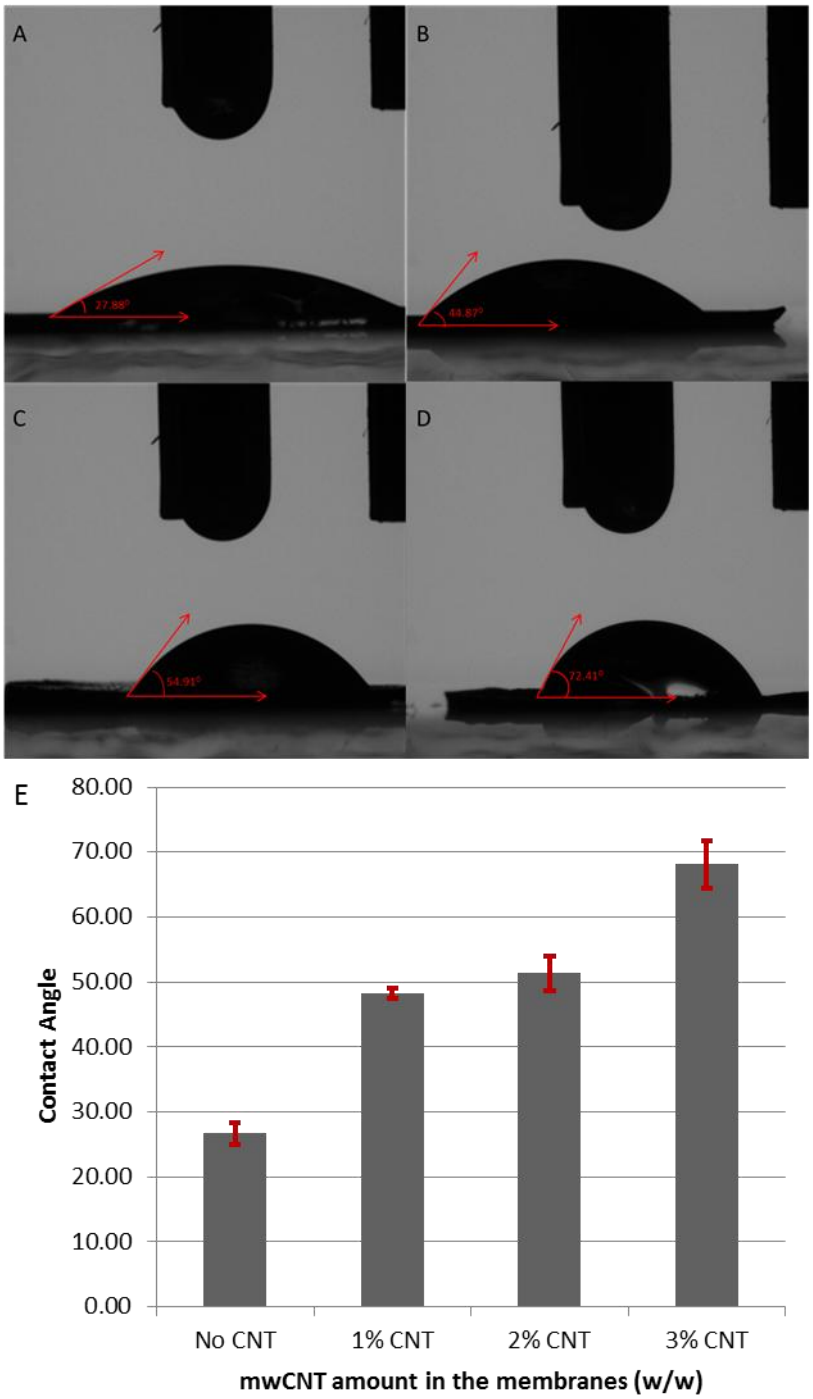

Figure 17. Contact angles of mwCNT-pHEMA composite membranes; A) 0% mwCNT, B) 1% mwCNT, C) 2% mwCNT, D) 3% mwCNT, E) Average values of membrane contact angles, n=3 for all the samples.

Hsiang et al., (2011) have produced genipin cross-linked casein (GCC) conduit with ability to swell. They used the conduit for sciatic nerve regeneration and obtained 100% nerve regeneration. The contact angle of the conduit was 59.0 ± 4.5° which was similar to the contact angle of the composite membranes. They concluded that the moderately hydrophilic structure of the GCC conduit, which was similar to that of the present study, helped the cells to attach the surface and proliferate.

3.2.3. Mechanical Testing

In addition to supporting axonal growth, it is important for a peripheral nerve conduit to have sufficient tensile strength and mechanical toughness to withstand in vivo mechanical forces (Borschel et al., 2003). Therefore, the mechanical properties of the composite membranes were of importance and thus were investigated. A stress-strain curve is given in Appendix A. The curve shows the plastic and elastic regions of a material. The slope of the elastic region gives Elastic Modulus (E) and the highest point at the stress axis is the ultimate tensile strength (UTS).

Tensile test graphs and results of the composite membranes are presented in Appendix B and in Table 3, respectively. All the membranes showed viscoelastic behavior having elastic and plastic regions. The pHEMA membranes having no mwCNTs in their structures had the lowest Elastic Modulus, while the other composite membranes had similar and higher Elastic Modulus values. With the UTS, however, the values were similar for all the membranes, except the highest UTS of composite membrane containing 3% mwCNT (Table 3). In the study conducted by Borschel et al. (2003), it was found that the UTS and elastic modulus of a nerve were 2.7 MPa and 0.57 MPa, respectively. The values were higher than the composite membranes prepared in this study. The most promising composite membrane was the one with 3% mwCNT with UTS of 2.0 MPa and elastic modulus of 0.41 MPa.

The GCC conduit was found to have UTS of 0.1657 ± 0.0249 MPa which was lower than our composite membranes with 3 and 6% of mwCNTs (Hsiang et al., 2011). They concluded that the strength of the conduit had enough mechanical strength to resist muscular contraction during sciatic nerve regeneration.

Chitosan is a biological polymer that has been used for peripheral nerve injury. Its elastic modulus, however, is extremely high (0.2-0.8 MPa) compare to the elastic modulus of the nerve tissue, making chitosan a brittle material (Cheng, 2002). Thus chitosan nerve conduits have a chance to compress regenerating nerve cells and to rupture in vivo. It can be concluded that a biomaterial with low elastic modulus, mimicking the mechanical properties of soft nerve tissue, may be favorable to use in the structure of a nerve conduit.

Table 3. Tensile test results of the mwCNT-pHEMA membranes

MwCNT concentration of the membranes (%) (n=3)	Ultimate Tensile Strength (MPa)	Elastic Modulus (MPa)
0	1.24 ±0.34	0.14±0.11
1	1.25±0.09	0.35±0.03
3	2.00±0.84	0.41±0.05
6	1.65±0.42	0.32±0.06

3.2.4. Electrical Conductivity

Sisken et al. (1989) reported that electrical stimulation has an important positive effect on axonal regeneration; therefore conductive materials were thought to be very promising substrates to seed cells on as nerve guide materials and to achieve better peripheral nerve regeneration.

Electrical properties of the membranes in dry and wet forms were calculated from their resistances. Table 4 shows the conductivities of composite membranes in dry

state calculated using Equations 5 and 6. PHEMA is nonconductive as all the non-ionic polymers (Peppas, 2004) while mwCNTs are electrically conductive materials (Jithesh et al., 2009). In this study, the results support this; while pHEMA and composite membrane with 1% CNT are not conductive, increasing mwCNT amount makes the membranes conductive. The increase in the conductivities of the membranes was found statistically significant and as a result, they are potential candidates for use in neuron regrowth. Lovat et al. (2005) showed the possibility of using mwCNTs as tools to improve neural signal transfer. It was found that the cultured neural network was in homogeneously distributed on the nanotube film, and CNT substrates increased the spontaneous synaptic activity and firing of hippocampal neurons, but there were no significant changes in the action potentials of these neuron cells.

Table 4. Electrical properties of mwCNT-pHEMA membranes with different mwCNT contents. Dry state.

mwCNT content of the composite membranes (%, w/w)	**Conductivity x10^{-2} ($\Omega^{-1}.cm^{-1}$)**
0	-
1	-
3	5.0
6	2.0

The wet samples showed a significant increase in the conductivities over those of the dry samples even for the pure pHEMA membrane and the composite membrane with 1% mwCNT (Table 5). The reason for this increase is the ionic substances contained in the cell culture medium make the medium ionically conductive.

Polypyrole is a polymer which naturally possesses electrical conductivity. It was used in the structure of a nerve conduit because of its inherent conductive properties (George et al., 2009). It was shown that regeneration and remyelination of the axon was observed 4 weeks after the implantation of the nerve conduit. In this study it was

expected that the conductive structure of the composite membranes will help improve the regeneration as in the case of polypyrole.

Table 5. Electrical properties and dimensions of mwCNT-pHEMA membranes with different mwCNT contents. Wet state.

mwCNT content of the composite membranes (%, w/w)	**Conductivity x10^{-3} ($\Omega^{-1}.cm^{-1}$)**
0	7.0
1	10.0
3	50.0
6	80.0

3.2.5. Microscopical Characterization

Microscopical characterization of the composite membranes was conducted to examine the porosity and the pore sizes by using the program NIH ImageJ and SEM and CSLM.

3.2.5.1. SEM

Commercial CNTs were 4-6 nm in diameter and 12-20 μm in length (Figure 18). CNTs appear as a scaffold composed of small fibers or tubes that have dimensions similar to those of neural processes such as dendrites. Such a similarity is expected to improve the attachment and growth of neural cells. Recent investigations have started to address the issue of the effects of CNT substrates on neural growth (Mattson et al., 2000; Hu et al., 2004). These pioneering studies on chemically modified multiwalled nanotubes (MWNTs) have already suggested the potential for these materials to support neurite outgrowth in vitro, by controlling neuron-ECM interactions.

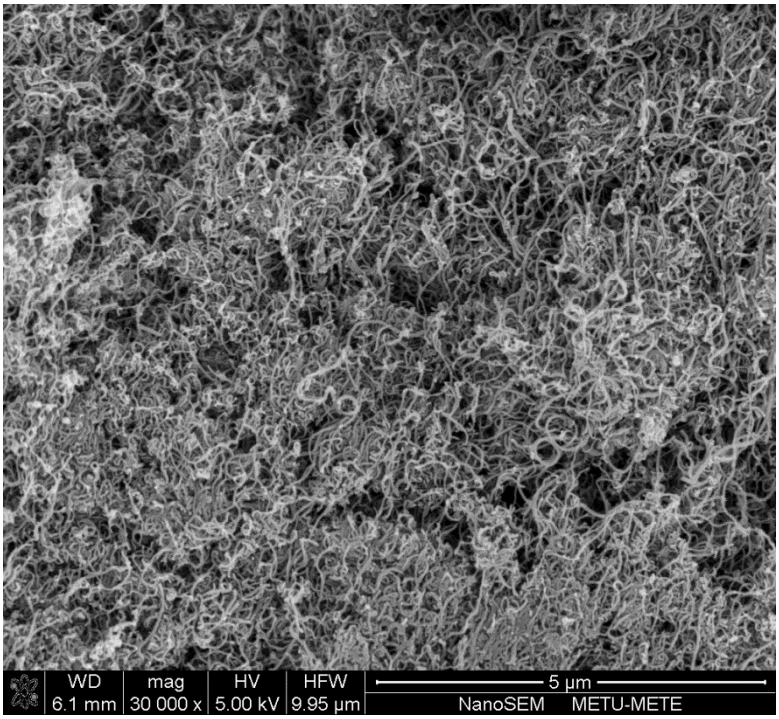

Figure 18. SEM image of the commercial CNT used in the study.

Figure 19 shows the SEM micrographs of the pHEMA and mwCNT-pHEMA composite membranes. The hydrogels were porous which is suitable for transportation of ingredients needed for cell nutrition and growth (Figure 19A). In the biomaterials and tissue engineering field, the microstructure of the scaffold material has an important effect on cell behavior, especially on their adhesion, spreading, proliferation, migration and differentiation (O'Brien et al., 2007). In addition, the scaffold porosity affects the mechanical properties in addition to on the transfer of the nutrients and metabolic wastes. As a result, it is important to study the microstructure, thus the porosity of the scaffold material. Further analysis of the pHEMA image (Figure 19A) with NIH ImageJ, the porosity and the average pore area were found as 45% and 18 μm^2, respectively.

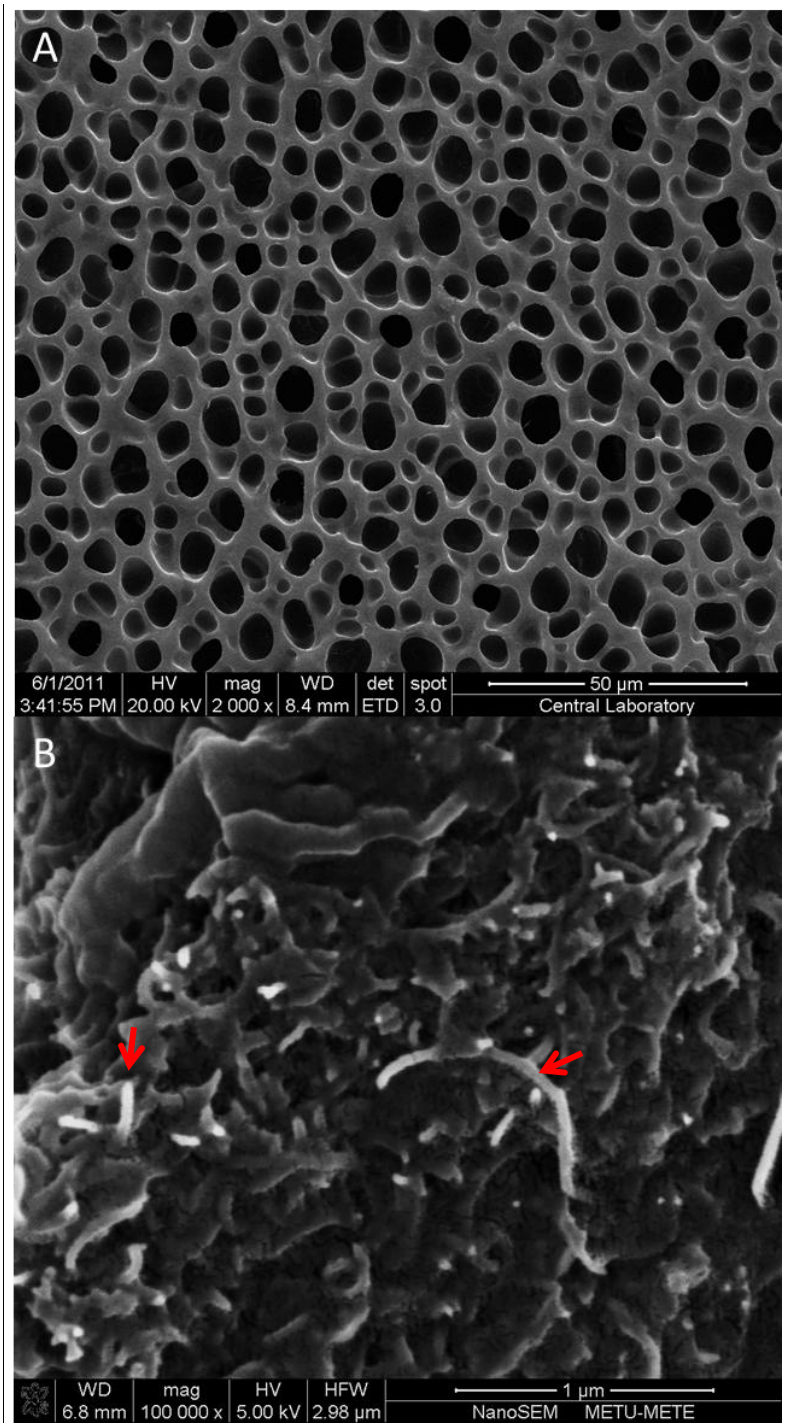

Figure 19. SEM micrographs of the PHEMA based biomaterials. A) pHEMA, and B) mwCNT-PHEMA composite sheet. Arrows show typical mwCNTs.

MwCNTs on the hydrogels were similar in appearance with the original, as received form; spaghetti-like, even though they were embedded in the hydrogel structure (Figure 19B). Due to this physical interaction between pHEMA and mwCNT no leaching after implantation is expected. This is essential because any released entities (fibers, particulates) could lead to cytotoxic effects in the body, and mwCNTs might have additional adverse effects due to their physical and chemical properties. The distribution of mwCNTs on the hydrogel surface was random, some of the nanotubes formed clumps and some were dispersed on the surface (Figure 20).

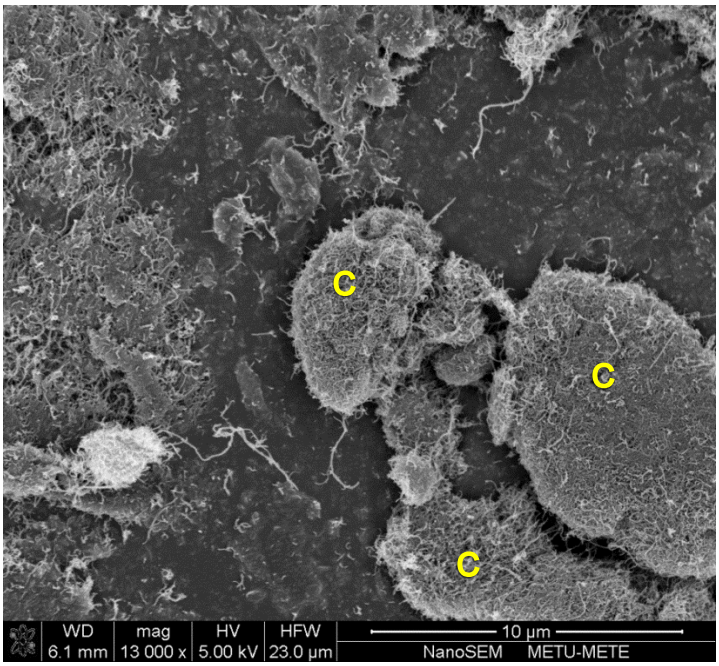

Figure 20. Distribution of 3% (w/w) mwCNTs on the pHEMA hydrogel surface. "C"s show the mwCNT clumps.

Yu et al., (2011) studied collagen/PCL composite fibrous materials produced by electrospinning. The electrospun fibers provided a large area for the cell attachment. In the present study, the carbon nanotubes, similar to those electrospun fibers, make the surface area larger and this is suitable for the attachment of more cells.

3.2.5.2. CLSM

The confocal laser scanning microscopy images of the composite membranes are presented in Figure 21. The pores on the pHEMA membrane surface are clearly seen (Figure 21A). In Figure 21B, only the mwCNT clumps are seen due to the big difference in the contrast between the mwCNT clumps and the mwCNT fibers distributed on the surface. The dark areas are where the black clumps are located.

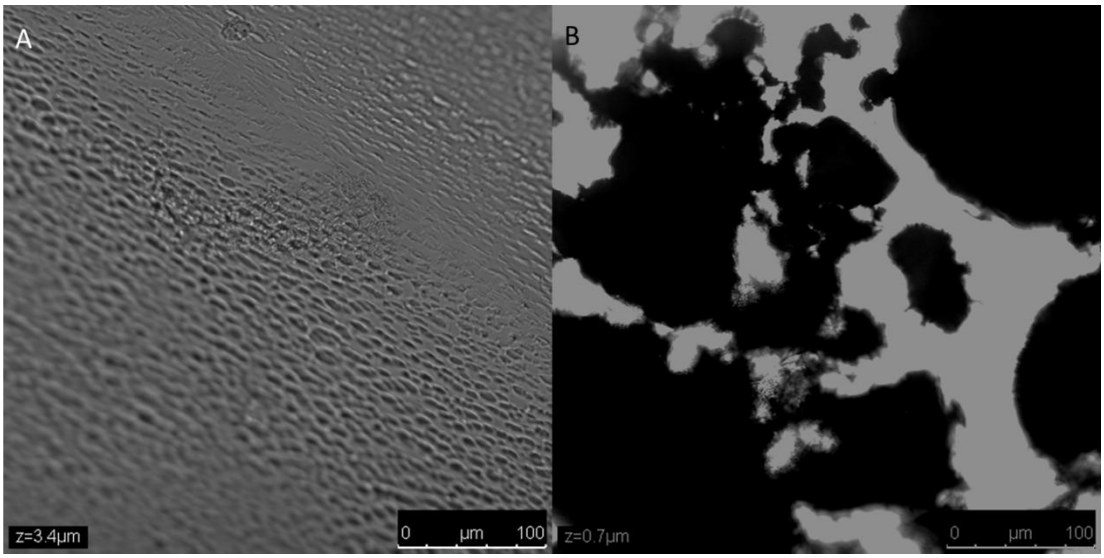

Figure 21. CSLM images of the membranes. A) pHEMA membrane, B) mwCNT-pHEMA composite membrane.

3.2.6. MicroCT

Figure 22 shows the microCT image of the tubular pHEMA conduit. The cross-section of the cylindrical structure is seen in the Figure 22A and the magnified half is presented in Figure 22B. The dimensions were measured as 4.2 and 9.1 mm for the diameter of the hollow part and the total tube, respectively (Figure 22C). In Figure 22D, the x-ray absorption pattern of the conduit is presented. The high absorption regions indicate the x-ray absorption by pHEMA while the empty middle section of

the tube did not absorb. Thus microCT showed its usefulness in the determination of dimensions.

When the conduit was further analyzed using CTan software, the total porosity of the pHEMA was found as 17.2%, about 2% of which was defined as “closed”. The total volume was 7.6 x 10^9 μm^3 and the volume of connective pore regions was found as 10^{-6} μm^3. When the conduit was analyzed by studying the outer and the inner sections separately, the porosities were 19.02% and 0.14%, respectively. These results show that the porosity is not uniform throughout the conduit; while the surface was porous, where the porosity decreased towards inside.

Figure 23 shows the microCT image of the composite membrane. The images (Figure 23A and B) show the two components of the membrane; pHEMA and mwCNT with thicknesses of about 2.85 mm and 0.84 mm, respectively (Figure 23C). The absorption pattern of the membrane is shown in the Figure 23D. Since mwCNTs absorb x-rays more than the pHEMA, the high absorption regions are due to mwCNTs. The fluctuations in the absorption pattern show the presence of mwCNT clumps on the surface. As seen in the Figure 23B, pHEMA has a porous structure below the mwCNTs phase. When analyzed with CTan software, overall porosity was found as 43.91%. It was 37.79% for mwCNT region and 55.01% for pHEMA region.

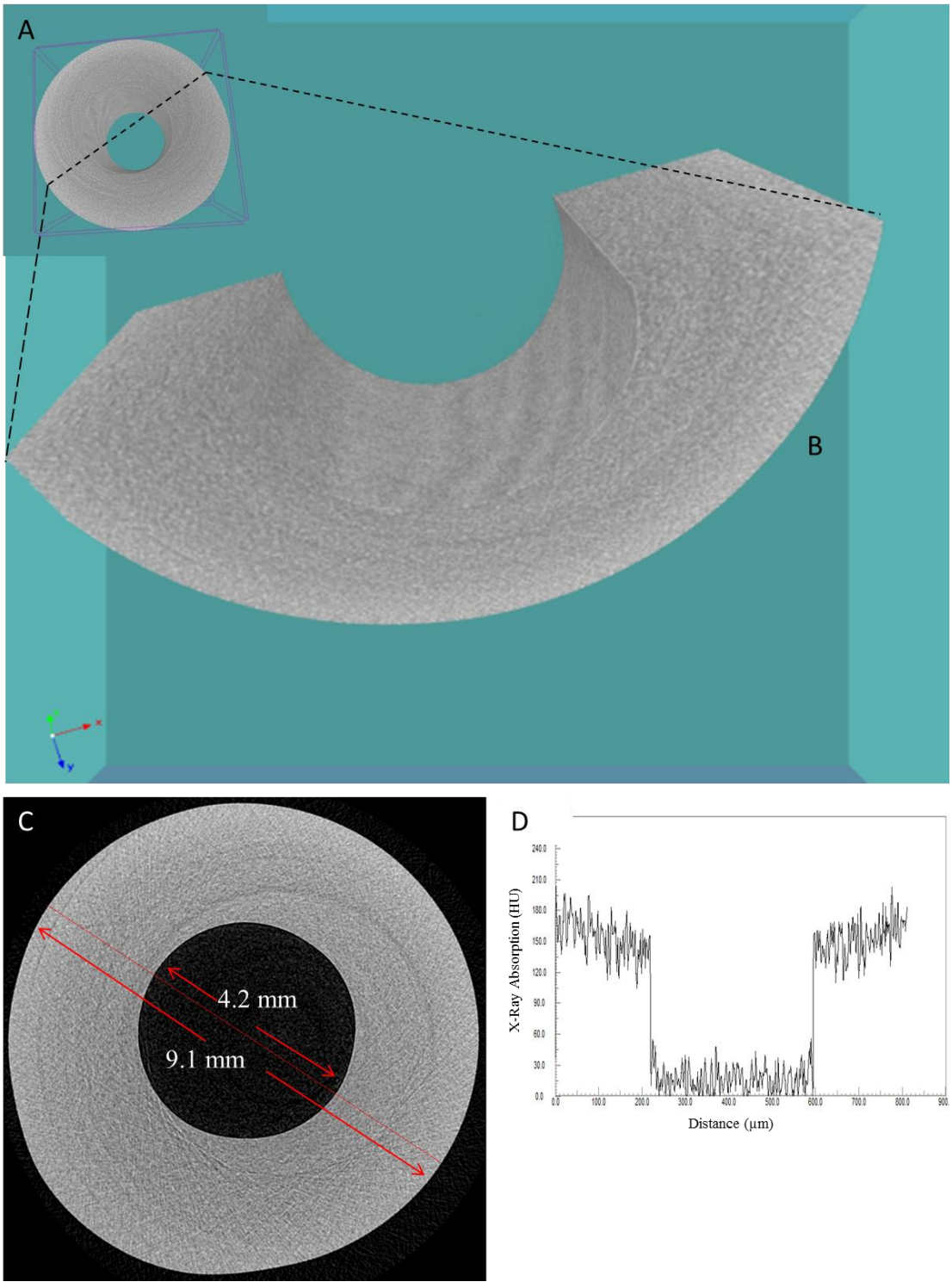

Figure 22. MicroCT image of the tubular pHEMA conduit. A) 3D structure, B) Half section of A, C) Dimensions of the conduit cross section, D) x-ray absorption pattern of the conduit cross section.

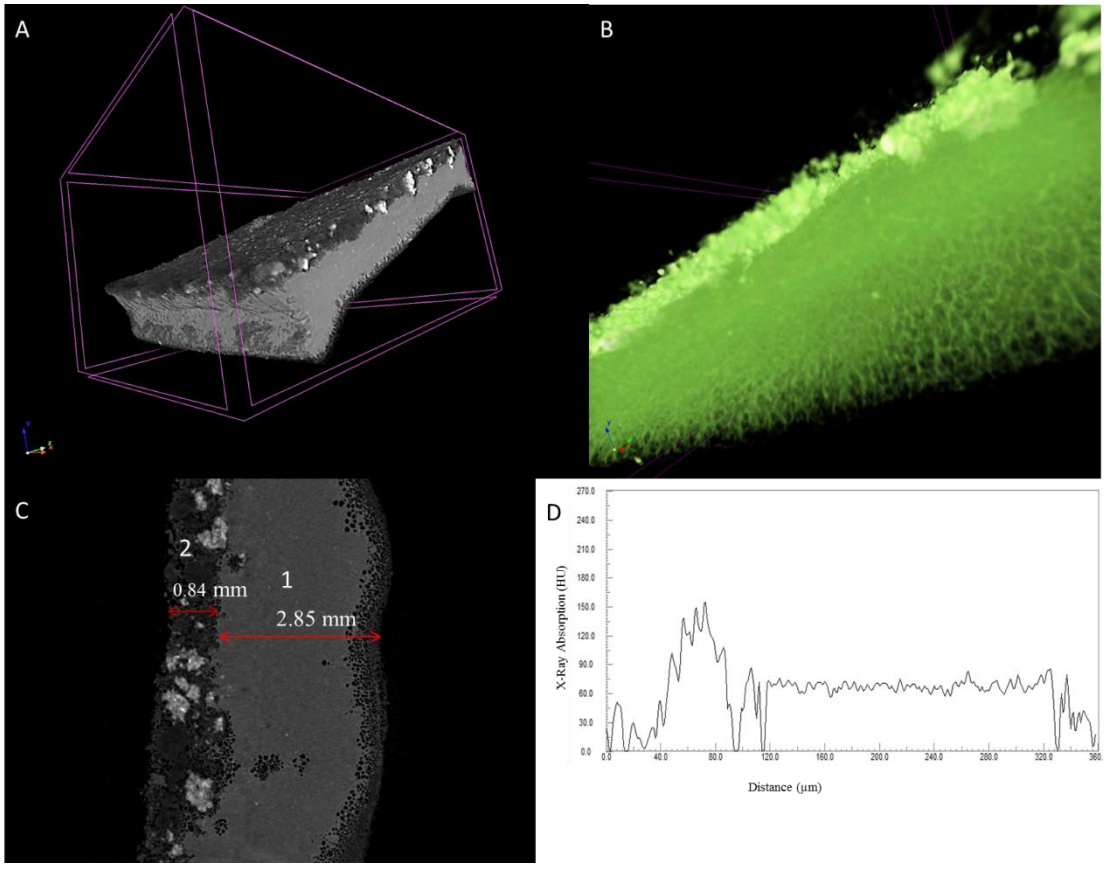

Figure 23. MicroCT image of the composite membrane containing 6% mwCNT. A) 3D structure of the membrane, B) Magnified A showing the pores on the exterior of the tube, C) Dimensions of the membrane, components 1. pHEMA 2. mwCNT, D) x-ray absorption pattern of the membrane.

3.3. *In vitro* Studies

SHSY5Y neuroblastoma cells possess certain key properties in common with primary neurons and were used in the *in vitro* studies to examine cell attachment and proliferation. The axon structure of the neuroblastoma cell lines are highly elaborated making them desirable for studying axonal alignment if it could be induced (Thiele, 1998).

3.3.1. Characterization of SHSY5Y Cells on Composite Membranes

Cells on the membranes were visualized by SEM and CSLM. The MTT cell viability assay was used to study their attachment and proliferation on the membranes.

3.3.1.1. SEM

Figure 24 shows the SEM micrograph of the neuroblastoma cells on the pHEMA membranes. The cells are seen to interact with each other after attachment and proliferation. Normally hydrophilic surfaces of pHEMA hydrogel are not considered to be suitable for the cell-to-cell interactions since the ECM proteins prefer to interact with the hydrophilic surfaces rather than with ECM proteins of neighboring cells (Menzies and Jones, 2010). The porous structure, however, may decrease the surface area of the pHEMA allowing the cells to interact with each other to grow in the monolayer. Here it is seen that the cells are overlapping, which is a characteristic of the neuroblastoma cells, while attaching the surface.

Figure 25 shows neuroblastoma cells on composite membranes having 1, 3, and 6% mwCNTs (w/w). On the 21st day of the cultured cells, the cells are seen to form a fibrous structure on the 1% (w/w) mwCNT containing membranes (Figure 25A). The fibrous structure was probably made by the axon like extensions of neuroblastoma cells. This shows the communication between the cells is strong and they can get highly organized in 3D, unlike those in the monolayer structure on pHEMA membrane (Figure 24). Figures 25B and C show that the cells produce clumps and give rise to projections that stretch from one clump to the others. In Figure 25D (higher magnification), it is clearly seen that the cells have attached and proliferated on the mwCNT structures, showing that the mwCNTs in this form do not have any cytotoxic effects on the neuroblastoma cells.

In a typical nerve guide application, when a nerve conduit is implanted into the body, first all the tube is filled with fibrin matrix, and then Schwann cells and endothelial cells arrive and attach to the surface (Stang et al, 2009). It is, therefore, important for the surface to be appropriate for the formation of fibrin matrix and attachment of Schwann and endothelial cells. The composite membranes in the present study seem to be very appropriate in this respect.

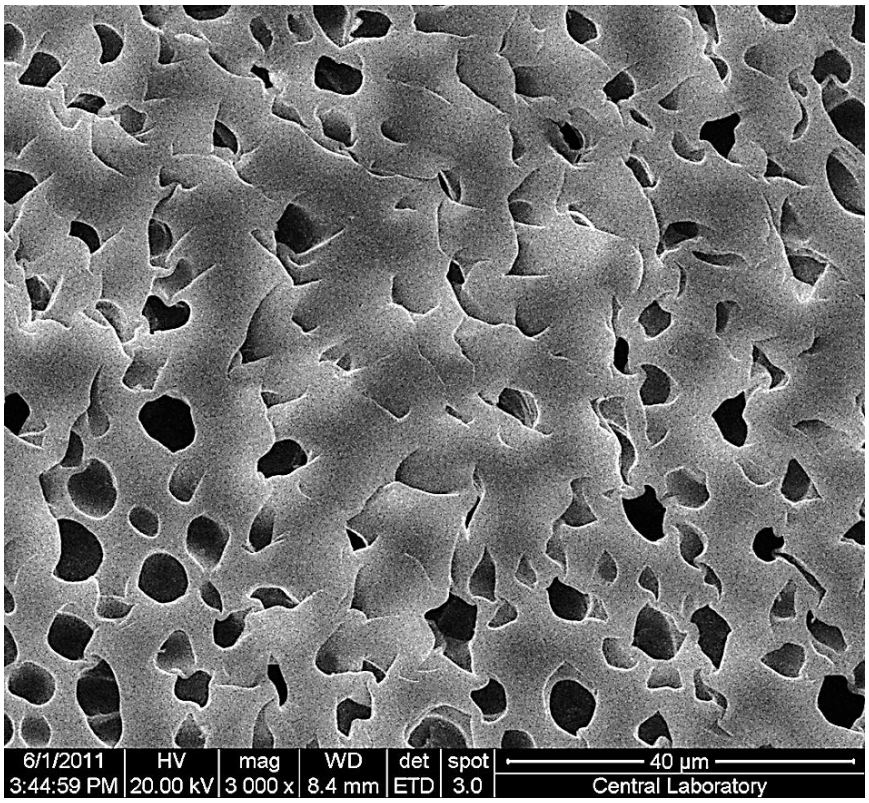

Figure 24. SEM of the SHSY5Y neuroblastoma cells on the pHEMA membrane. 21st day of the culture.

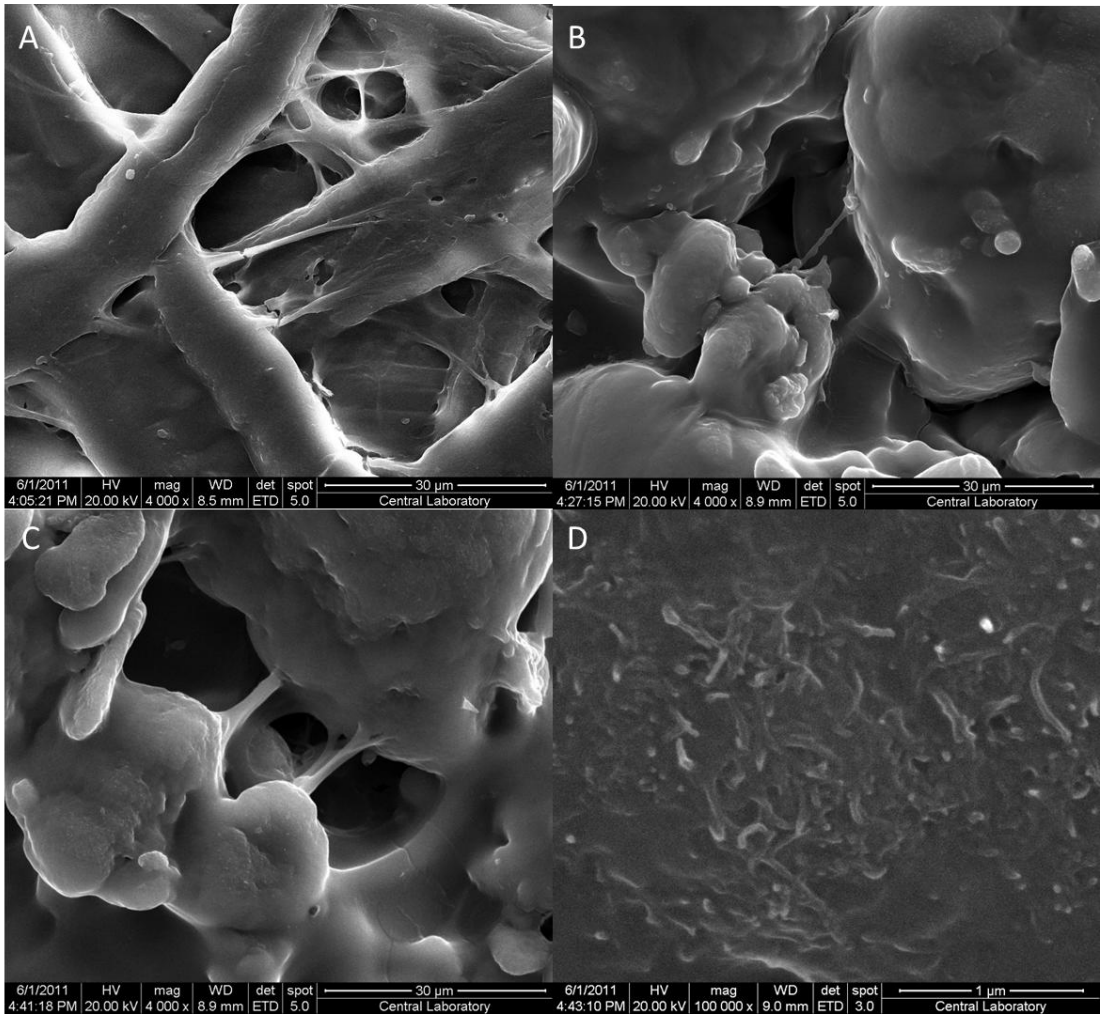

Figure 25. SEM of SHSY5Y neuroblastoma cells on mwCNT-pHEMA composite membranes; A) 1% mwCNT, B) 3% mwCNT, C) 6% mwCNT, D) 6% mwCNT with higher magnification. 21st day of the cell culture.

3.3.1.2. CLSM

The CLSM micrographs of the neuroblastoma cells on the pHEMA and composite membranes (Figure 26) show that the cells are attached and grow on both the pHEMA (Figure 26A) and the composite membranes (Figure 26B). The monolayer structure is seen on the pHEMA surface (Figure 26A).

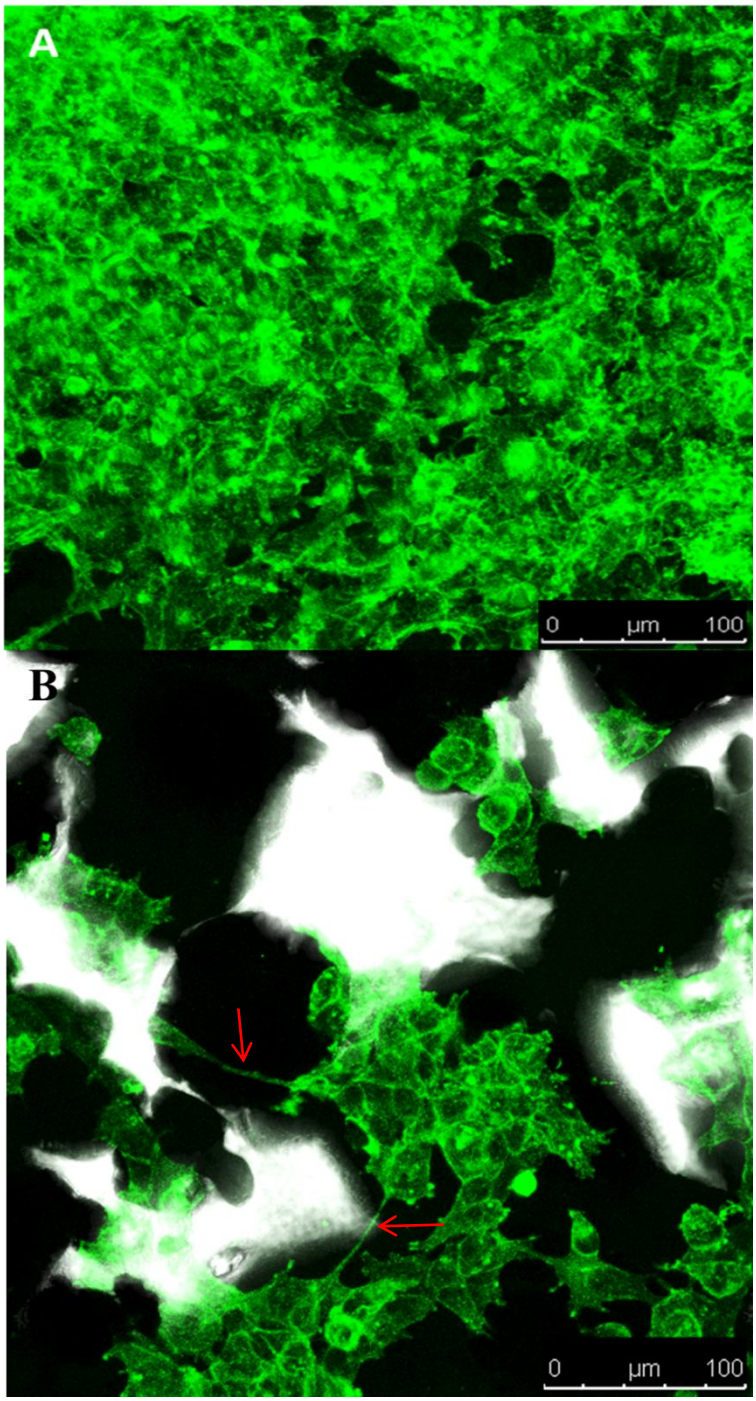

Figure 26. CSLM micrographs of the mwCNT-pHEMA composite membranes seeded with SHSY5Y neuroblastoma cells. A) pHEMA membrane, B) 1% mwCNT-pHEMA, Day 21. FITC-Phalloidin (green): cytoskeleton. The arrows show the cell projections through the mwCNT clumps.

The monolayer structure is similar to the CSLM analysis of SHSY5Y neuroblastoma cells conducted by Li et al. (2007). When the cells were cultured on 2D Matrigel, extensions were longer than seen on collagen matrix and the TCPS. The more fibrillar and porous structure of collagen I did not allow the formation of long extensions when compared to the denser structure of Matrigel. It was concluded that the dimensions of the extensions varied with the type of the material. In the present study, while the monolayer characteristics were dominant on the pHEMA surface, the extensions of the neuroblastoma cells are seen on the mwCNT clumps. Z-stack image of the membrane shows the cells on both the mwCNT clump and the surface covered by mwCNTs (Figures 27A and B).

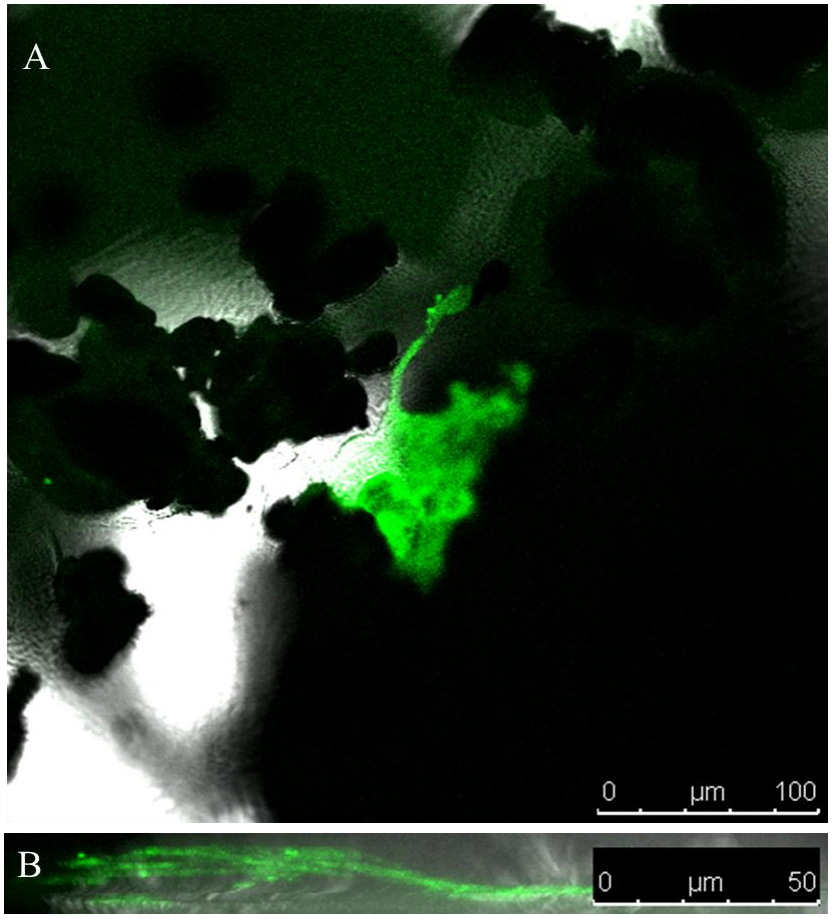

Figure 27. CSLM images of the 3% (w/w) mwCNT containing membrane seeded with SHSY5Y neuroblastoma cells. A) Cells on the composite clump, B) z-stack of the cells in A. FITC-Phalloidin (green): cytoskeleton.

3.3.1.3. MTT Viability Assay

After preparation and characterization of the membranes with different mwCNT contents, they were tested using SHSY5Y neuroblastoma cells in the purpose of assessing their suitability for use in nerve regeneration. The MTT test was used to quantitatively determine the changes in cell adhesion and proliferation upon surface modification using mwCNT (Figure 28) (Calibration curve in Appendix C). The cells were seeded on TCPS and composite membranes. Separate experimental and control groups were used for each time point.

After 3 h of cell seeding the cells were counted to determine the attachment. Almost 75% of the 2×10^5 cells seeded were attached on TCPS and on the membranes containing 0 and 3% mwCNTs. The membranes with 1 and 6% mwCNTs, however, were seen to prevent almost half of the cells from attachment ($1.01 \times 10^5 \pm 4.1 \times 10^3$ and $6.6 \times 10^4 \pm 2.3 \times 10^3$ cells were attached, respectively.

After 12 h, more cells were found on TCPS and the membranes except for 6% mwCNT. The increases for the membranes were not statistically significant, but the decrease in the cell number on 6% mwCNT containing membrane was statistically significant. At 24 h, however, the number of cells on all the surfaces was almost equal to the number of cells on TCPS. Only the increase seen for the membrane including 6% mwCNT during 12 h - 24 h period was statistically significant. On day 2, the cells on all the surfaces were doubled and the numbers on the composite membranes were similar to each other, and they were smaller than those on TCPS. The difference after duplication was statistically significant for all the membranes. On day 7, it was observed that, the membranes with 0, 1 and 3% mwCNTs showed statistically significant increases in cell numbers indicating that the surfaces were not toxic and did not hinder cell proliferation, except for the membrane with 6% mwCNT, which was cytotoxic.

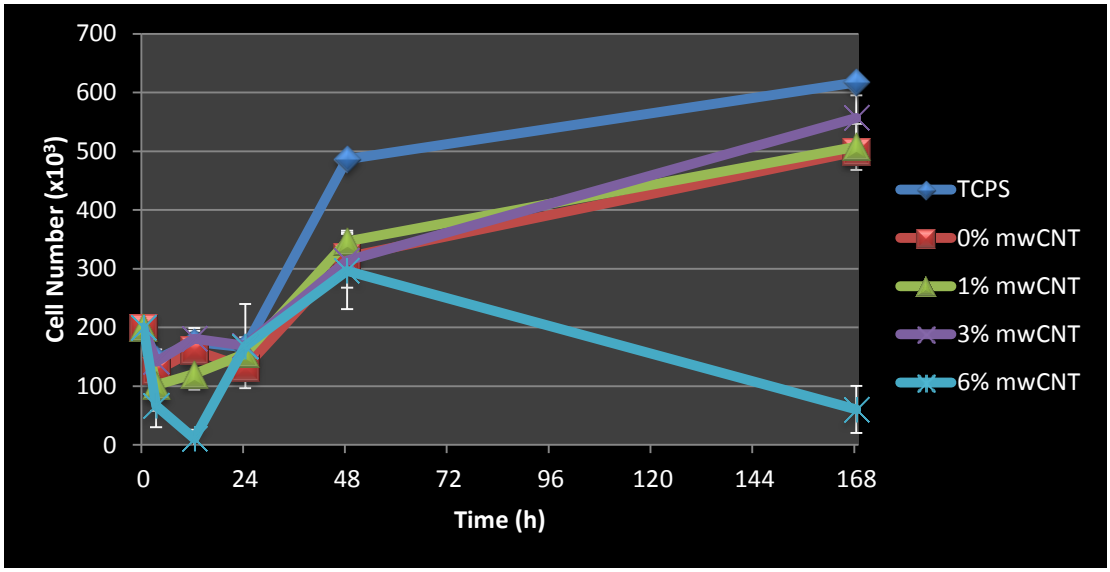

Figure 28. MTT viability assay of SHSY5Y cells on composite membranes (10^4 cells/cm^2, n=3).

3.3.2. Effect of Electrical Potential

In order to assess the effect of application of electrical potential on neuroblastoma cells, 1 and 2 V were applied to the cells seeded pHEMA and 3% mwCNT containing membranes chosen after the characterization studies. The morphologies of the cell layers were examined with SEM, and attachment and viability of the cells were determined by fluorescent microscopy and MTT viability assay.

3.3.2.1. SEM

For the analysis of the effect of electrical potential, SEM micrographs of the membranes were obtained in 3 groups. The first group consisted of the ones that were removed from the incubator for 10 min at every hour without application of potential (control). The other 2 groups were exposed to 1 and 2V.

Figure 29 shows the control samples. Cells on the pHEMA membranes showed some kind of alignment (Figure 29A). The alignment seems to be the result of cell-to-cell communication rather than the external forces like the structure of the surface or potential application. With higher magnification (Figure 29B), cell extensions across the pores could be seen. The cells on the mwCNT clumps (Figures 29B and C) were seen as attached and in interaction with each other. The extensions from one clump to the other again show the strong communication between the cells. As a result, it can be stated that periodic removal from the incubator did not affect the cells in terms of attachment and communication.

Figure 30 presents cells exposed to 1 V potential. The cells on pHEMA membrane were attached after 3 h (Figure 30A); the cells are seen producing a communication pathway. After 12 h, however, the cells were not healthy and not communicating well (Figure 30C). Their responses recovered by the 24 h (Figure 30F). The cells on the composite membrane were expected to produce a response like alignment upon potential application, but none could be detected (Figures 30B, D and G).

Upon application of 2 V, the cells on the pHEMA membranes lost their viability (Figures 31A and C). The cells on the mwCNTs, however, were not affected by the applied potential (Figures 31B, D and F). They produced a cell layer and extensions on the mwCNTs. After 24 h (12 h with periodic electrical potential application and 12 h incubation without potential) the live cells remaining on the pHEMA membrane recovered and produced extensions and started communicating (Figure 31E). In Figure 32, SEM micrographs of the cells on composite membranes with higher magnification after application of 2 V potential are presented. The cells were not affected by the application of electrical potential and had extensions between the clumps. The absence of the cell alignment shows that for the cells to align it is either necessary to have aligned mwCNTs as the seeding surface or to apply a higher potential.

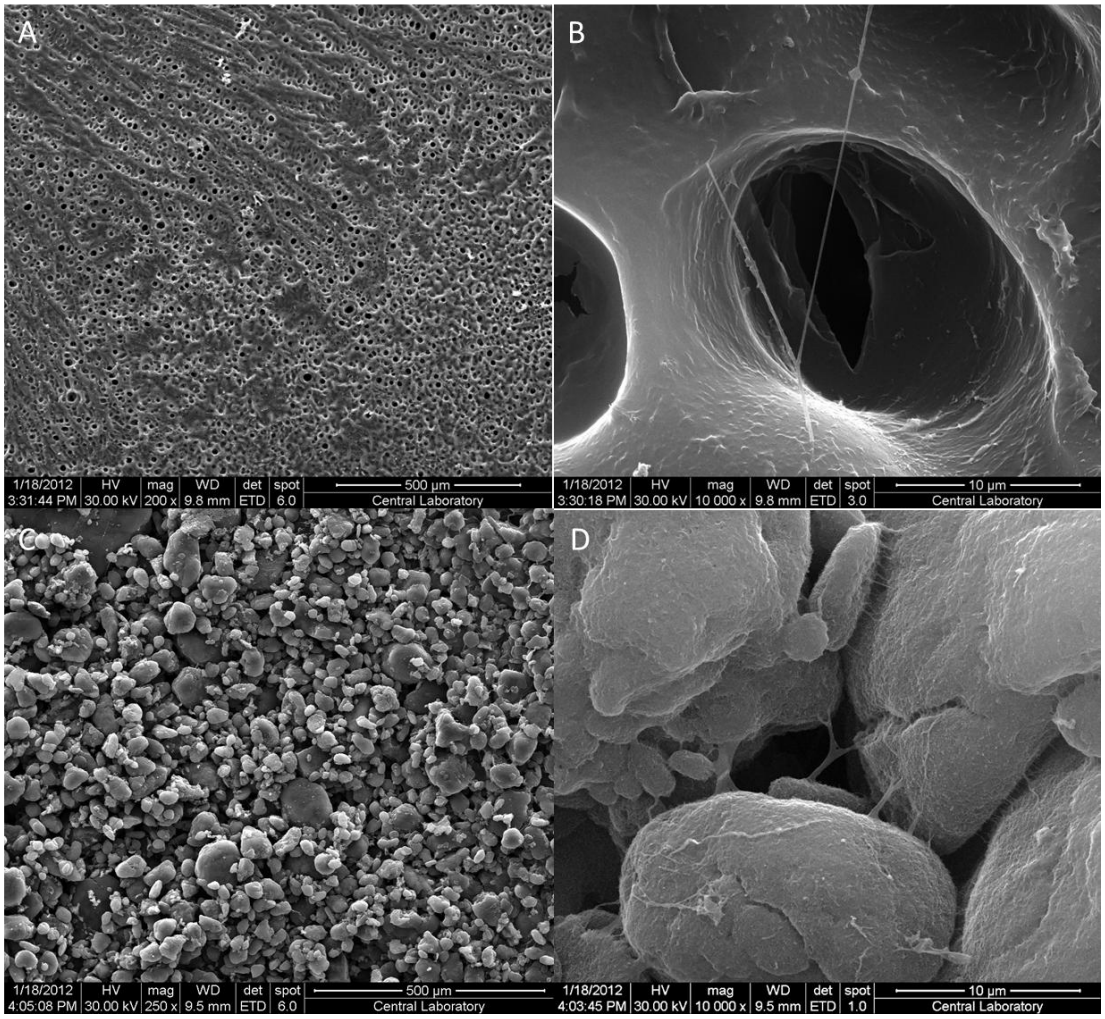

Figure 29. SEM micrographs of neuroblastoma cells on pHEMA and 3% mwCNT- pHEMA membranes (control). A) Cells on pHEMA membrane, B) Higher magnification of A, C) Cells on 3% mwCNT-pHEMA membrane, D) Higher magnification of C. The membranes were removed from the incubator for 10 min at every hour but re-incubated without electrical potential application.

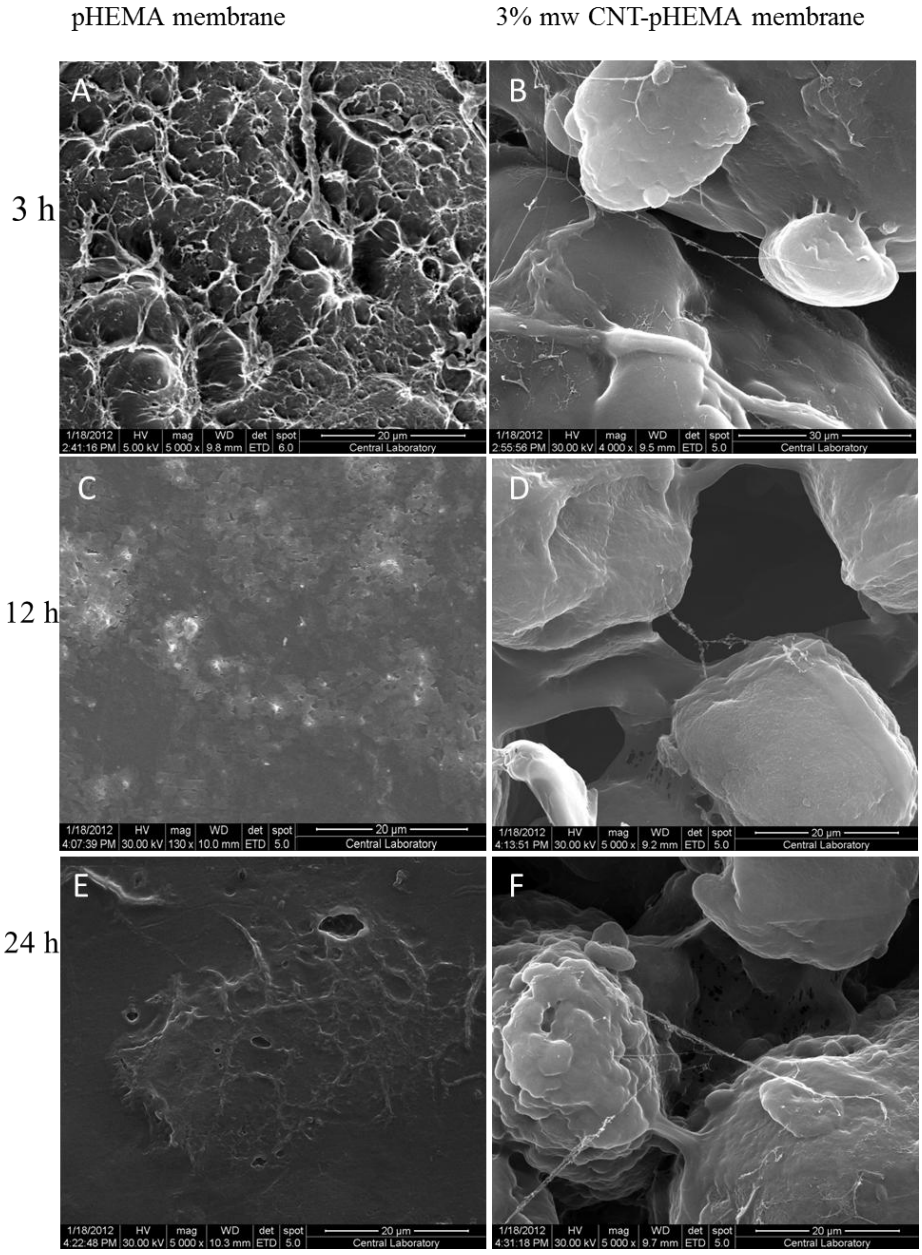

Figure 30. SEM micrographs of culture of neuroblastoma cells on pHEMA and 3% mwCNT- pHEMA membranes with 1 V potential application. A) pHEMA membrane after 3 h, B) mwCNT-pHEMA membrane after 3 h, C) pHEMA membrane after 12 h, D) mwCNT-pHEMA membrane after 12 h, E) pHEMA membrane after 24 h, F) mwCNT-pHEMA membrane after 24 h. The membranes were removed from the incubator for 10 min at every hour and 1 V of electrical potential was applied.

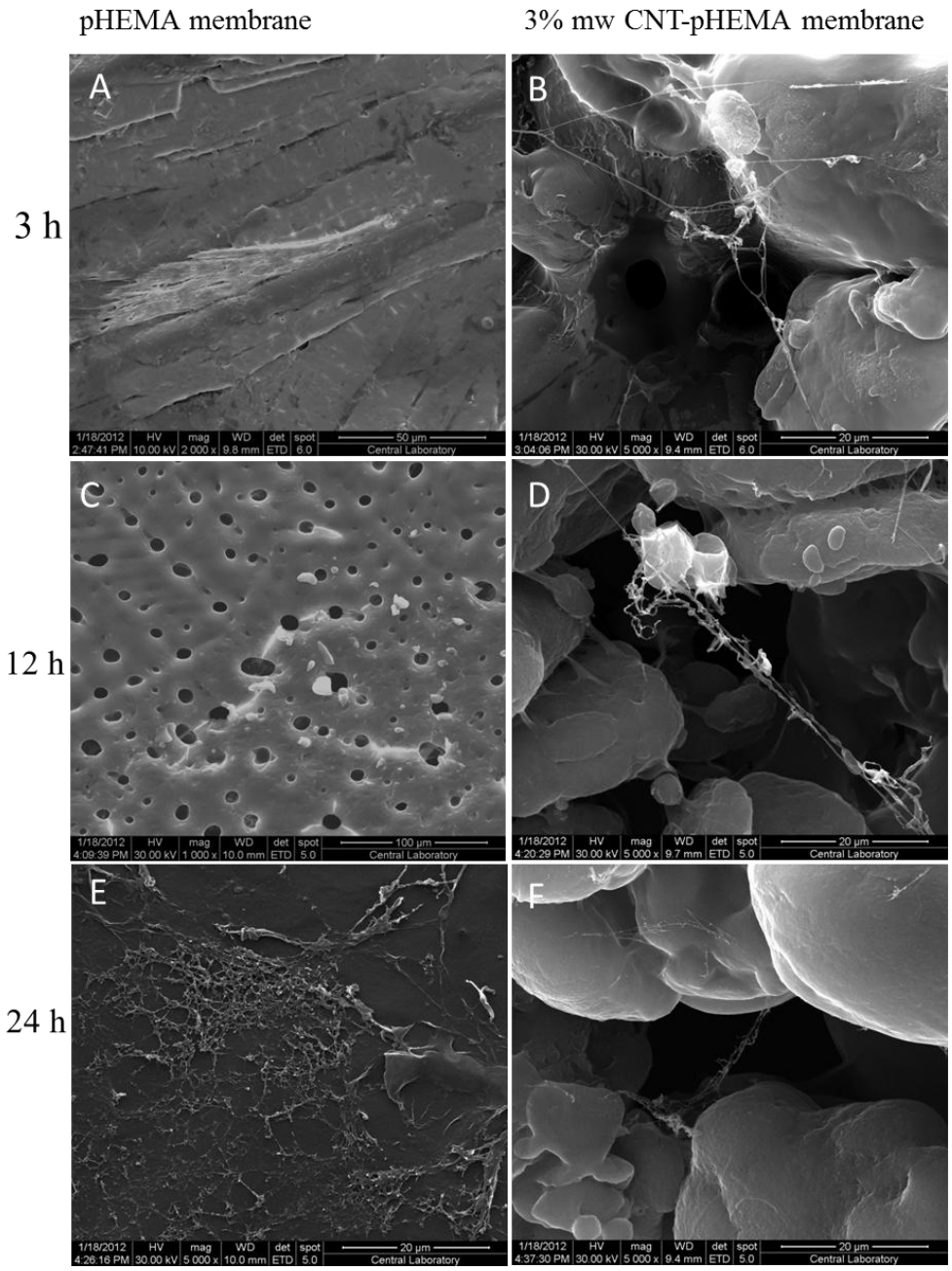

Figure 31. SEM micrographs of culture of neuroblastoma cells on pHEMA and 3% mwCNT- pHEMA membranes with 2 V potential application. A) pHEMA membrane after 3 h, B) mwCNT-pHEMA membrane after 3 h, C) pHEMA membrane after 12 h, D) mwCNT-pHEMA membrane after 12 h, E) pHEMA membrane after 24 h, F) mwCNT-pHEMA membrane after 24 h. The membranes were removed from the incubator for 10 min at every hour and 2 V of electrical potential was applied.

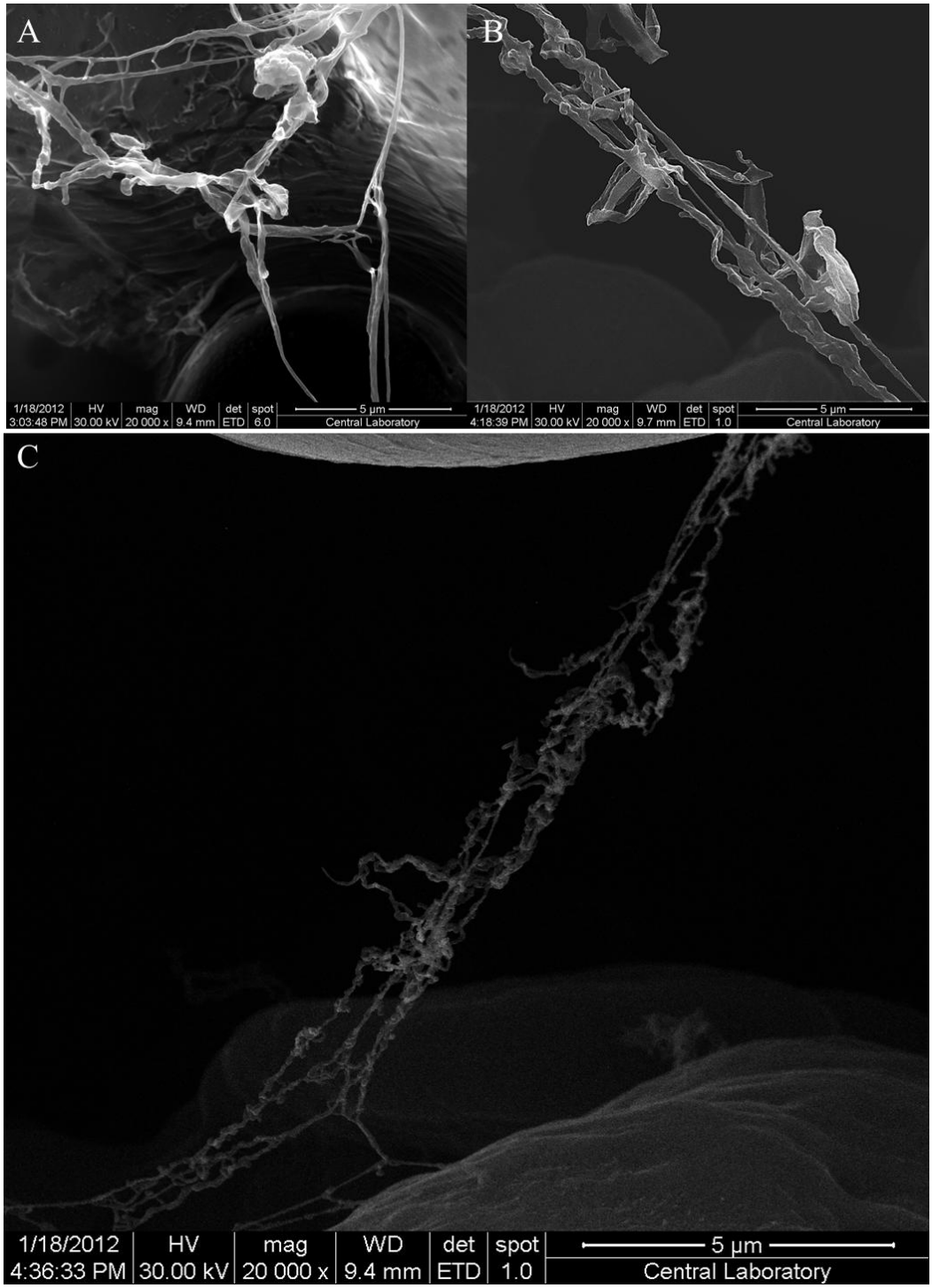

Figure 32. SEM micrographs of culture of neuroblastoma cells on 3% mwCNT-pHEMA membranes with 2 V potential application. A) 3 h, B) 12 h, C) 24 h. The membranes were removed from the incubator for 10 min at every hour and 2 V of electrical potential was applied.

3.3.2.2. Fluorescence Microscopy

The fluorescence micrographs of cell seeded membranes are seen in the Figure 33. The cells were stained with DAPI for the nuclei (blue). Upon 2 V electrical application, no cells were observed on pHEMA surfaces (Figure 33C) while they were viable on the samples with 1 V and no electrical application (Figures 33A and B). The cells on the membranes with 3% mwCNT were viable without electrical potential and after 1 and 2 V application (Figures 33C, D and E).

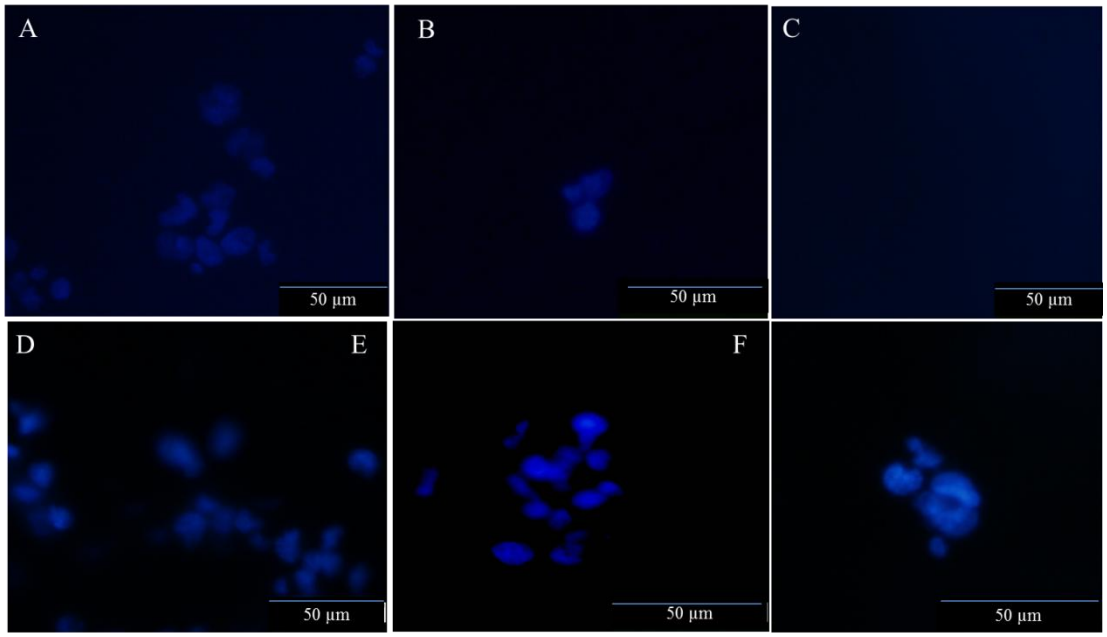

Figure 33. Fluorescence micrographs of 3 h culture of neuroblastoma cells on the membranes. A) pHEMA membrane , B) pHEMA membrane with 1 V electrical potential, C) pHEMA membrane with 2 V electrical application, D) mwCNT-pHEMA membrane, E) mwCNT-pHEMA membrane with 1 V of electrical potential, F) mwCNT-pHEMA membrane with 2 V of electrical potential. The membranes in A and D were removed from the incubator for 10 min at every hour but no potential was applied. DAPI (blue) staining for nucleus.

3.3.2.3.MTT Viability Assay

To assess the effect of the electrical potential on the attachment and viability of neuroblastoma cells on the membranes, MTT viability assay was performed (Calibration curve in Appendix C) (Figure 34). $2x10^5$ cells were seeded to obtain 10^4 cells/cm^2. Three controls were used; cells on TCPS, cells on the membranes incubated (control) and cells on the membranes that were removed from the incubator for 10 min at every hour like the test samples with no electrical potential (no stimulation). Cells on both the membranes were viable after 24 h, showing that the short treatments out of the incubator did not affect the viability of the cells. In the application of 1V electrical potential, the cells attached and were viable for 72 h on the composite membrane. On the pHEMA membrane, however, most of the cells were dead after 3 h. Remaining cells did survive and proliferated. Upon 2V application, however, the cells were not able to attach the pHEMA surface. The results for composite membranes showed that the application of potential did not affect the cell viability on the mwCNT-pHEMA composites. For the 3 controls, there was no change in the first 24 h (Statistically insignificant small differences were found). The cell number increases for all the samples after 24 h were statistically significant and very similar to each other.

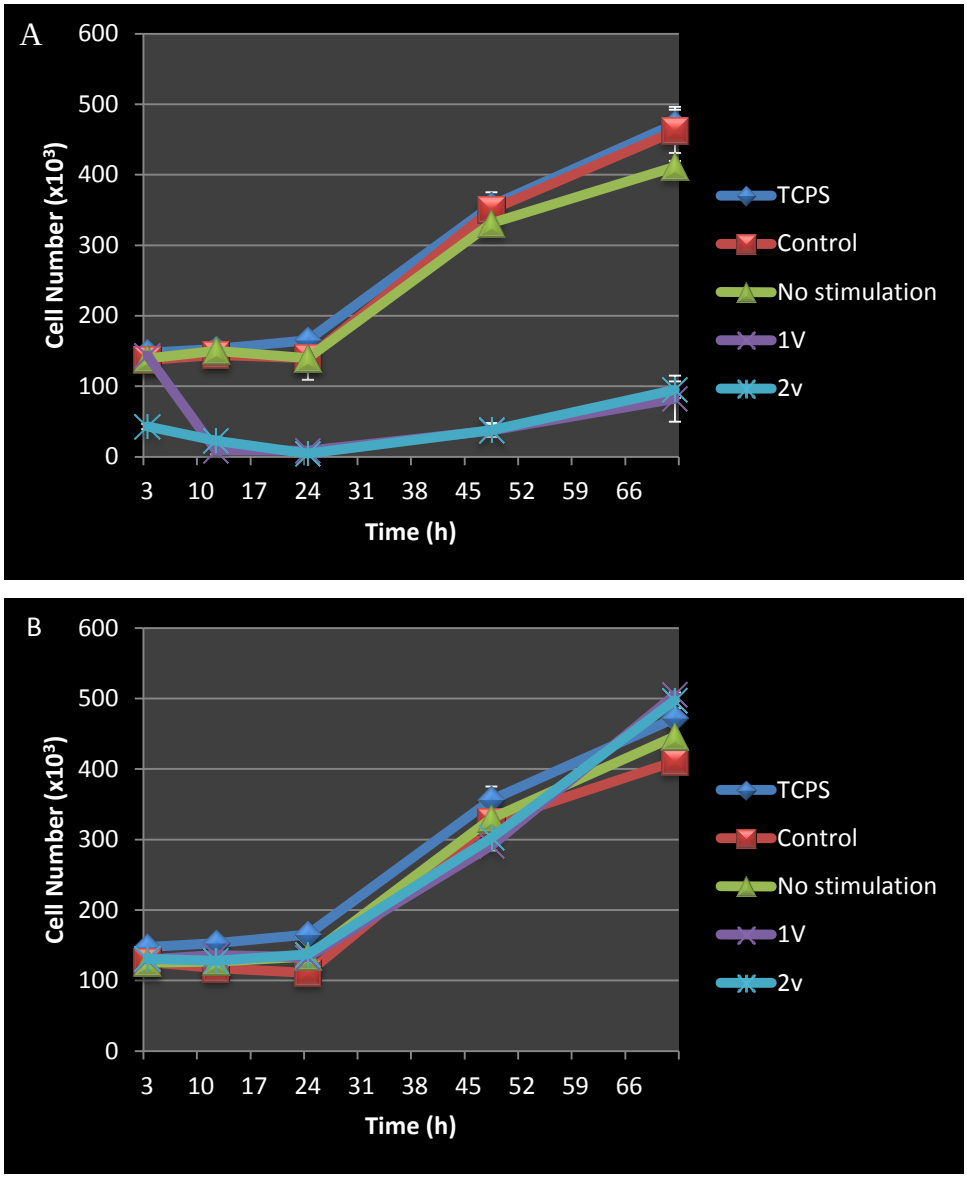

Figure 34. The effect of electrical potential on SHSY5Y neuroblastoma cells seeded on viability of membranes, MTT viability assay. A) pHEMA membrane, B) 3% mwCNT-pHEMA membrane. (10^4 cells/cm^2, n=3).

CHAPTER 4

CONCLUSION AND FUTURE STUDIES

This study presents a nerve conduit consisting of pHEMA and mwCNT. The hydrogel structure of the pHEMA and the conductive nature of mwCNT were thought to be suitable for axon regeneration, and the construct was designed and characterized.

The hollow structure of the pHEMA conduit was obtained in cylindrical mold and optimized for the water absorption. Its swelling ability led to a viscoelastic structure similar to that observed in soft tissues. The mwCNT-pHEMA composite membranes were characterized for their contact angles and conductivities. An increase in the amount of the mwCNT made the membranes more hydrophobic which is needed for cell adhesion in general and more conductive which was considered as useful in a nerve guide. The tensile tests of the membranes showed that the composites could withstand the muscular contraction, and that the elastic modulus of the composites was similar to that of the nerve fibers.

Microscopical examination of the membranes revealed that the mwCNTs were embedded in the pHEMA structure and the structure was porous.

Cell viability studies and microscopical examination of the cell seeded membranes showed that the neuroblastoma cells are able to attach and proliferate on both

pHEMA and mwCNT surface. Upon electrical potential application, the cells on pHEMA surfaces could not survive, but the presence of mwCNT protected the cells and there was no loss of cell activity.

The nerve guides constructed and characterized as explained above revealed that the presence of carbon nanotubes improved cell adhesion on flexible, porous and hydrated nerve guides. The presence of mwCNT also prevented any adverse effects of application of electrical potential. Anyhow, no distinct advantage of potential application could be observed either in cell alignment or proliferation. There might be several routes for improving the results. The first one is the alignment of the mwCNT on the pHEMA surface. This could be obtained by contact printing on the membrane form. Other parameters to change would be the potential and its application regime. In addition, Schwann cells may be seeded on pHEMA surface, while neurons are seeded on mwCNT surface. This type of cultivation could lead to the transfer of the neurotrophic factors secreted by the Schwann cells across the walls of the conduit and reach to the regenerating axon. Finally, growth factors and neurotrophic factors could be used to improve the proliferative process.

REFERENCES

Allen NJ, Barres BA. Neuroscience: Glia, more than just brain glue. Nature 2009; 457; 675–7.

Augistin JG, Purves D, Fitzpatrick D, Hall WC, Lamantia AS, McNamara JO, Williams AM, eds. Neuroscience. 3rd edition. Sinauer Associates, Inc.; 2004; 31-198.

Bajada S, Mazakova BA, Richardson JB, Shammakhi N. Stem cells in regenerative medicine. In: Ashammakhi, N., Reis, R., Chiellini, F, eds. Topics in tissue engineering, Vol.4. Expertissues; 2008; Chp 13.

Bernadic M. Pathophysiology of the nervous system. In: Kvasnicka V, Benuskova L, Farkas I, Pospichal J, Tino P, Kral A, eds. Introduction to the Theory of Neuronal Networks. Bratislava, SAP; 1997; Chp 6.

Bian YZ. Wang Y. Aibaidoula G. Chen GQ. Wu Q. Evaluation of poly(3-hydroxybutyrate-co-3-hydrox- yhexanoate) conduits for peripheral nerve regeneration. Biomaterials 2009; 30:2; 217-225.

Borschel GH, Kia KF, Kuzon WM, Dennis RG. Mechanical Properties of Acellular Peripheral Nerve. Journal of Surgical Research 2003; 114; 133–139.

Burnett MG, Zager EL. Pathophysiology of peripheral nerve injury: a brief review. Neurosurg Focus 2004; 16; 1–7.

Cai L. Wang S. Poly(ε-caprolactone) acrylates syn- thesized using a facile method for fabricating networks to achieve controllable physicochemical properties and tunable cell responses. Polymer 2010; 51:1; 164-177.

Cheng M, Deng J. Study on physical properties and nerve cell affinity of composite films from chitosan and gelatin solutions. Biomaterials 2003; 24; 2871-2880.

Chiu DT. Special article: the development of autogenous venous nerve conduit as a clinical entity. In PandS Medical Review, New York: Columbia- Presbyterian Med Cent; 1995; 3(1).

Chirila TV, Chen YC, Griffin BJ, Constable IJ. Hydrophilic sponges based on 2-hydroxyethyl methacrylate. I. Effect of monomer mixture composition on the pore size. 1993; 32:3; 221-232.

Comet JJ, Revillard JP. Peripheral nerve allografts. Transplantation 1978; 28; 103.

Cui T. Yan Y. Zhang R. Liu L. Xu W. Wang X. Rapid prototyping of a double-layer polyurethane-collagen conduit for peripheral nerve regeneration. Tissue Engineering 2009; 15:1; 1-9.

Dahlin LB. Nerve injury and repair: from molecule to man. In: Slutsky, D.J., Hentz, V.R, eds. Peripheral nerve surgery: practical applications in the upper extremity. Philadelphia: Churchill Livingstone, Elsevier; 2006; 1–22.

Dahlin L, Lundborg G. The use of silicone tubing in the late repair of the median and ulnar nerves in the forearm. J Hand Surg [Br.] 2001; 26; 393–394.

Dalton PD. Hlynn L. Shoichet MS. Manufacture of poly(2-hydroxyethyl methacrylate-co-methyl methacrylate) hydrogel tubes for use as nerve guidance channels. Biomaterials 2002; 23:18; 3848-3851.

Darling AL, Sun W. 3D microtomographic characterization of precision extruded poly-e-capro-lactone scaffolds. J Biomed Mater Res B Appl Biomater 2004; 70B:2; 311–317.

Davis JB, Stroobant P. Platelet-derived growth factors and fibroblast growth factors are mitogens for rat Schwann cells. J Cell Biol 1990; 110; 1353–1360.

Delcomyn F. (Ed.) Foundations of Neurobiology, W.H. Freeman, New York; 1997; Chp 7.

Dodla MC. Bellamkonda RV. Differences between the effect of anisotropic and isotropic laminin and nerve growth factor presenting scaffolds on nerve regeneration across long peripheral nerve gaps. Biomaterials 2008; 29:1; 33-46.

Dumitru D, Zwarts MJ, Amato AA. Peripheral nervous system's reaction to injury. In: Dumitru, D, Amato, AA, Zwarts, M, ed. Electrodiagnostic medicine. 2nd ed. Philadelphia: Hanley and Belfus; 2001; 115–156.

Fansa H, Keilhoff G, Plogmeier K, Frerichs O, Wolf G, Schneider W. Successful implantation of Schwann cells in acellular muscles. J Reconstr Microsurg 1999; 15; 61-65.

Fansa H, Keilhoff G, Wolf G, Schneider W. Tissue engineering of peripheral nerves: A comparison of venous and acellular muscle grafts with cultured Schwann cells. Plast Reconstr Surg 2001; 107; 485-494.

Forehand CJ. Integrative functions of the nervous system. In: Rhoades, RA, Bell, DR, eds. Medical Physiology: Principles for Clinical Medicine, 3rd Edition. Lippincott Williams and Wilkins, a Wolters Kluwer business; 2009; 119-136.

Fu SY, Gordon T. The cellular and molecular basis of peripheral nerve regeneration. Mol Neurobiol 1997; 14; 67–116.

Funakoshi H, Frisen J, Barbany G, Timmusk T, Zachrisson O, Verge VM, Persson H. Differential expression of mRNAs for neurotrophins and their receptors after axotomy of the sciatic nerve. J Cell Biol 1993; 123; 455–465.

Gamez E. Goto Y. Nagata K. Iwaki T. Sasaki T. Matsuda T. Photofabricated gelatin-based nerve conduits: nerve tissue regeneration potentials. Cell Transplantation 2004; 13:5; 549-564.

George PM, Saigal R, Lawlor MW, Lavan DA, Marini RP, Selig M, Makhni M, Burdick JA, Langer R, Kohane DS. Three dimensional conductive constructs for nerve regeneration. Journal of biomedical materials research part A 2009; 91: 2; 519-527.

Gray KJ, Shenaq SM, Engelmann UH, Fishman IJ, Jeraj K, Spira M. Use of human amnion for microvascular inter-positional grafts. Plast Reconstr Surg 1987; 79; 778–785.

Griffith LG. Emerging design principles in biomaterials and scaffolds for tissue engineering. Ann NY Acad Sci USA 2002; 961; 83-95.

Guyton AC, Hall JH, eds. Textbook of Medical Physiology. Elsevier Sounders. 11th Edition 2006; 554-700.

Hall RH. Structure of the Nervous System. Lecture notes 1998; Retrieved from http://web.mst.edu/~rhall/neuroscience (Last accessed date; 01.11.2012).

Hall S. Mechanisms of repair after traumatic injury. In: Dyck PJ, Thomas PK, eds. Peripheral neuropathy. Philadelphia: Elsevier, Saunders 2005; 1403–1433.

Heimer L. The human brain and spinal cord: Functional neuro-anatomy and dissection guide. New York: Springer; 1983; 149-165.

Hsiang SW, Tsai CC, Tsai FJ, Ho TY, Yao CH, Sheng Y. Novel use of biodegredable casein conduits for guided peripheral nerve regeneration. J R Soc Interface 2011; 8; 1622-1634.

Hu H, Ni Y, Montana V, Haddon RC, Parpura V. Chemically Functionalized Carbon Nanotubes as Substrates for Neuronal Growth. Nano Lett 2004; 4; 507-511.

Hudson TW, Evans GR, Schmidt CE. Engineering strategies for peripheral nerve repair. Clin Plast Surg 1999; 26: 617–628.

Israelachvili J. Intermolecular Surface Forces (2nd edition). Academic Press, New York, NY; 1997; 439-467.

Jeng CB. Coggeshall RE. Nerve regeneration through holey silicone tubes. Brain Research 1985; 361:1-2; 233-241.

Kalantarian B, Rice DC, Tiangco DA, Terzis JK. Gains and losses of the XII-VII component of the "baby-sitter" procedure: a morphometric analysis. J Reconstr Microsurg 1998; 14; 459-471.

Kalbermatten DF. Kingham PJ. Mahay D. Mantovani C. Pettersson J. Raffoul W. Balcin H. Pierer G. Terenghi G. Fibrin matrix for suspension of regenerative cells in an artificial nerve conduit. Plastic, Reconstructive and Aesthetic Surgery 2008; 61:6; 669-675.

Kalbermatten DF, Pettersson J, Kingham PJ, Pierer G, Wiberg M, Terenghi G. New fibrin conduit for peripheral nerve repair. J Reconstr Microsurg 2009; 25; 27-33.

Kamp T, Svendsen C. What is regenerative medicine? Stem Cell and Regenerative Medicine Center, University of Wisconsin-Madison 2008.

Retrieved from http://www.stemcellresources.org (Last accessed date; 01.11.2011)

Kandel ER, Schwartz JH, Jessel TM, eds. Nerve cells and behavior. Principles of Neural Science. McGraw-Hill Professional; 2000; Chp 2.

Keilhoff G, Stang F, Wolf G, Fansa H. Biocompatibility of type I/III collagen matrix for peripheral nerve reconstruction. Biomaterials 2003; 24: 2779-2787.

Kincaid JC. The autonomic nervous system. In: Rhoades, R.A., Bell, D.R, eds. Medical Physiology: Principles for Clinical Medicine, 3rd Edition. Lippincott Williams and Wilkins, a Wolters Kluwer business; 2009; 108-118.

Kokai LE. Ghaznavi AM. Marra KG. Incorporation of double-walledmicrospheres into polymer nerve guides for the sustained delivery of glial cell line-derived neurotrophic factor. Biomaterials 2010; 31:8; 2313-2322.

Kumar NA, Ganapathy HS, Kim JS, Jeong YS, Jeong YT. Preparation of poly 2-hydroxyethyl methacrylate functionalized carbon nanotubes as novel biomaterial nanocomposites. European Polymer Journal 2008; 44; 579-586.

Laanger R, Vacanti JP. Tissue engineering. Science 1993; 260; 920-926.

Lanza RP, Langer RS, Vacanti J. Principles of tissue engineering. Academic Press, San Diego 2000; 1 – 73.

Li GN, Livi LL, Gourda CM, Deweerd ES, Hoffman-Kim D. Genomic and morphological changes of neuroblastoma cells in response to three-dimensional matrices. Tissue Engineering 2007; 13:5; 1035-1047.

Lietz M. Ullrich A. Schulte-Eversum C. Oberhoffner S. Fricke C. Müller HW. Schlosshauer B. Physical and biological performance of a novel block copolymer nerve guide. Biotechnology and Bioengineering 2006; 93:1; 99-109.

Liuzzi FJ. Tedeschi B. Peripheral nerve regeneration. Neurosurg Clin N Am 1991; 2; 31–42.

Lovat V, Pantarotto D, Lagostena L, Cacciari B, Grandolfo M, Righi M, Spalluto G, Prato M, Ballerini L. Carbon nanotube substrates boost neuronal electrical signaling. Nano Letters 2005; 5:6; 1107-1110.

Lundborg G. A 25-year perspective of peripheral nerve surgery: evolving neuroscientific concepts and clinical significance. J Hand Surg. [Am.] 2000; 25; 391–414.

Lundborg G. Vascular systems. In: Lundborg G, ed. Nerve Injury and Repair. New York: Longman Group UK; 1988; 32-63.

Macdonald AR, Christopher MV, Kariolis M, Stegemann JP. Carbon nanotubes increase the electrical conductivity of fibroblast seeded collagen hydrogels. Acta Biomaterialia 2008; 4; 1583–1592.

Mackinnon SE, Dellon AL. Clinical nerve reconstruction with a bioabsorbable polyglycolic acid tube. Plast Reconstr Surg 1990; 85; 419-424.

Malarkey EB, Parpura V. Applications of carbon nanotubes in neurobiology. Neurodegenerative Dis 2007; 4; 292-299.

Maricevic A, Erceg M. War injuries to the extremities. Mil Med 1997; 162; 808–811.

Martini F. M, ed. Fundamentals of Anatomy and Physiology, Seventh Edition. Pearson, Benjamin Cummings; 2006; 379-416.

Martini R. Expression and functional roles of neural cell surface molecules and extracellular matrix components during development and regeneration of peripheral nerves. J Neurocytol 1994; 23; 1–28.

Mattson MP, Haddon RC, Rao AMJ. Molecular functionalization of carbon nanotubes and use as substrates for neuronal growth. Mol Neurosci 2000; 14; 175-182.

Meek MF, Bertleff MJ, Ritt MJ, Robinson PH, Nicolai JP. A degradable artificial nerve guide to bridge peripheral nerve defects. Ned Tijdschr Geneeskd 2003; 147; 717-721.

Meiss RA. Sensory physiology. In Rhoades, R.A., Bell, D.R, eds. Medical Physiology: Principles for Clinical Medicine, Third Edition. Lippincott Williams and Wilkins, a Wolters Kluwer business, 2009; 62:89.

Menzies KL, Jones L. The impact of contact angle on the biocompatibility of biomaterials. Optometry and Vision Science 2010; 87:6; 387–399.

Midha R. Munro CA. Dalton PD. Tator CH. Shoichet Ms. Growth factor enhancement of peripheral nerve regeneration through a novel synthetic hydrogel tube. Journal of Neurosurgery 2003; 99:3; 555-565.

Millesi H, Ganglberger J, Berger A. Erfahrungen mitder Mikrochirurgie peripherer. Nerven Chir Plast 1967; 3; 47.

Mohammad J, Shenaq J, Rabinovsky E, Shenaq S. Modulation of peripheral nerve regeneration: a tissue-engineering approach. The role of amnion tube nerve conduit across a 1-centimeter nerve gap. Plast Reconstr Surg 2000; 105; 660–666.

Moore MJ, Jabbari E, Ritman EL, Lu L, Currier BL, Windebank AJ, Yaszemski MJ. Quantitative analysis of interconnectivity of porous biodegradable scaffolds with micro-computed tomography. J Biomed Mater Res A 2004; 71:2; 258–267.

Nakayama K. Takakuda K. Koyama Y. Itoh S. Wang W. Mukai T. Shirahama N. Enhancement of peripheral nerve regeneration using bioabsorbable poly-mer tubes packed with fibrin gel. Artificial Organs 2007; 31.7; 500-508.

Neubauer CM, Jennings HM. The role of the environmental scanning electron microscope in the investigation of cement-based materials. Scanning 1996; 18:7; 515–21.

O'Brien FJ, Harley BA, Waller MA, Yannas IV, Gibson LJ, Prendergast PJ. The effect of pore size on permeability and cell attachment in collagen scaffolds for tissue engineering. Technol Health Care 2007; 15; 3-17.

Peppas NA. Hydrogels- Classes of materials used in medicine. In Ratner BD, ed. Biomaterials Science, An Introduction to Materials in Medicine. Elsevier Academic Press; 2004; 100-107.

Pfister LA. Papalo M. Merkle HP. Gander B. Hydrogel nerve conduits produced from alginate/chitosan complexes. Biomedical Materials Research 2007; 80:4; 932-937.

Pollock M. Nerve regeneration. Curr Opin Neurol 1995; 8; 354–358.

Radulescu D. Dhar S. Young CM. Taylor DW. Trost HJ. Hayes DJ. Evans GR. Tissue engineering scaffolds for nerve regeneration manufactured by ink-jet technology. Materials Science and Engineering 2007; 27:3; 534-539.

Reichert F, Saada A, Rotshenker S. Peripheral nerve injury induces Schwann cells to express two macrophage phenotypes: phagocytosis and the galactose-specific lectin MAC-2. J Neurosci 1994; 14; 3231-3245.

Riazi AM, Kwon SY, Stanford WL. Stem cell sources for regenerative medicine. Methods in Molecular Biology 2009; 482; 55–90.

Richardson PM, Lu X. Inflammation and axonal regeneration. J Neurol 1994; 242; 57–60.

Robinson LR. Traumatic injury to peripheral nerves. Muscle Nerve 2000; 23; 863–873.

Robinson LR. Traumatic injury to peripheral nerves. Suppl Clin Neurophysiol 2004; 57; 173–186.

Rosen JM, Hentz VR, Kaplan EN. Fascicular tubulization: A cellular approach to peripheral nerve repair. Ann Plast Surg 1983; 11; 397-411.

Rotshenker S. Wallerian degeneration: the Innate Immune Response to Traumatic Nerve Injury. Neuroinflammation Reviews 2011; 8; 109.

Rydevik B, Lundborg G. Permeability of intraneural microvessels and perineurium following acute, graded experimental nerve compression. Scand J Plast Reconstr Surg 1977; 11; 179–187.

Sakai Y. Matsuyama Y. Takahashi K. Sato T. Hattori T. Nakashima S. Ishiquro N. New artificial nerve conduitsmade with photo-crosslinked hyaluronic acid for peripheral nerve regeneration. Bio-MedicalMaterials and Engineering 2007; 17:3; 191-197.

Seckel BR. Enhancement of peripheral nerve regeneration. Muscle Nerve 1990; 13; 785–800.

Seckel BR: Jones D. Hekimian KJ. Wang KK. Chakalis DP. Costas PD. Hyaluronic acid through a new injectable nerve guide delivery system enhances peripheral nerve regeneration in the rat. Neuroscience Research 1995; 40:3; 318-324.

Seddon H. Three types of nerve injury. Brain 1943; 66; 237–288.

Schmidt CE, Leach JB. Neural tissue engineering repairing strategies. Annu Rev Biomedical Engineering 2003; 5; 293-347.

Schmidt CE, Shaastri VR, Vacanti JP, Langer R. Stimulation of neurite outgrowth using an electrically conducting polymer. Proc Natl Acad Sci USA 1997; 94: 17; 8948-8953.

Shi Q, Jackowski G. One-dimensional polyacrylamide gel electrophoresis. In: Hames BD, ed. Gel Electrophoresis of Proteins: A Practical Approach, 3rd edn, Oxford University Press, Oxford; 1998; 1-52.

Sisken BF, Kanje M, Lundborg G, Herbst E, Kurtz W. Stimulation of rat sciatic nerve regeneration with pulsed electromagnetic fields. Brain Res 1989; 485; 309–316.

Stanec S, Tonkovic I, Stanec Z, Tonkovic D, Dzepina I. Treatment of upper limb nerve war injuries associated with vascular trauma. Injury 1997; 28; 463–468.

Stang F, Keilhoff G, Hansa H. Biocompatibility of different nerve tubes. Materials 2009; 2; 1480-1507

Stoll G, Muller HW. Nerve injury, axonal degeneration and neural regeneration: basic insights. Brain Pathol 1999; 9; 313–325.

Studenovska H, Slouf M, Rypacek F. Poly(HEMA) hydrogels with controlled pore architecture for tissue regeneration applications. J Mater Sci: Mater Med 2008; 19; 615-621.

Sundback CA. Shyu JY. Wang Y. Faguin WC. Langer Rs. Vacanti JP. Hadlock TA. Biocompatibility analysis of poly(glycerol sebacate) as a nerve guidematerial. Biomaterials 2005; 26:27; 5454-5464.

Sunderland S. Nerves and nerve injuries. 2nd ed. Edinburgh: Churchill Livingstone; 1978; 780-795.

Sunderland S. The anatomy and physiology of nerve injury. Muscle Nerve 1990; 13:771–784.

Takezawa T. A strategy for the development of tissue engineering scaffolds that regulate cell behavior. Biomaterials 2003; 24; 2267 – 2275.

Thiele CJ. Neuroblatoma cell lines. In (Ed.) Masters, J. Human Cell Culture. Lancaster, UK: Kluwer Academic Publishers 1998; 1; 21-53.

Thomas PK. Invited review: focal nerve injury: guidance factors during axonal regeneration. Muscle Nerve 1989; 12; 796–802.

Veetil JV, Ye K. Tailored carbon nanotubes for tissue engineering applications. Biotechnology Progress 2009; 10; 165.

Verreck G. Chun I. Li Y. Kataria R. Zhang Q. Rosenblatt J. Decorte A. Heymans K. Adriaensen J. Bruining M. Van Remoortere M. Borghys H. Meert T. Peeters J. Brewster ME. Preparation and physic- ochemical characterization of biodegradable nerve guides containing the nerve growth agent sabeluzole. Biomaterials 2005; 26:11; 1307-1315.

Voytik-Harbin SL, Brightman AO, Kraine MR, Waisner B, Badylak SF. Identification of extractable growth factors from small intestinal submucosa. J Cell Biochem 1997; 67; 478–91.

Waller A. Experiments on the section of the glossopharyngeal and hypoglossal nerves of the frog, observations of the alterations produced thereby in the structure of their primitive fibers. Phil Transact Royal Soc London 1850; 140; 423-429.

Wang F, Shor L, Darling A, Khalil S, Sun W, Guceri S, Lau A. Precision extruding deposition and characterization of cellular poly-e-caprolactone tissue scaffolds. Rapid Prototyp J 2004; 210:1; 42–49.

Wang JS. Basic fibroblast growth factor for stimulation of bone formation in osteoinductive or conductive implants, Acta Orthop Scand Suppl 1996; 269; 1–33.

Wang S. Wan ACA. Xu X. Gao S. Mao HQ. Leong KW. Yu H. A new nerve guide conduit material composed of a biodegradable poly(phosphoester). Biomaterials 2001; 22:10; 1157-1169.

Wang S. Yaszemski MJ. Gruetzmacher JA. Lu L. Photo-crosslinked poly(ε-caprolactone fumarate) networks: roles of crystallinity and crosslinking density in determining mechanical properties. Polymer 2008; 49:26; 5692-5699.

Wang W. Itoh S. Matsuda A. Aizawa T. Demura M. Ichinose S. Enhanced nerve regeneration through a bilayered chitosan tube: the effect of introduction of glycine spacer into the CYIGSR sequence. Journal of BiomedicalMaterials Research 2008; 85:4; 919-928.

Wen X. Tresco PA. Effect of filament diameter and extracellular matrix molecule precoating on neurite outgrowth and Schwann cell behavior on multifilament entubulation bridging device in vitro Biomedical Materials Research 2006; 76:3; 626-637.

Widmer MS. Gupta PK. Lu L. Meszlenvi RK. Evans GR. Brandt K. Savel T. Gurlek A. Patrick CW. Mikos AG. Manufacture of porous biodegradable polymer conduits by an extrusion process for guided tissue regeneration. Biomaterials 1998; 19:21; 1945-1955.

Wilbourn AJ. Peripheral neuropathies associated with vascular diseases and the vasculitides. In: Brown, WF, Bolton, CF, Aminoff, MJ, eds. Neuromuscular function and disease. Philadelphia: Saunders 2002; 1229–1262.

Wrede L. Ueberbrueckung eines Nervendefektes mittels Seidennaht und lebendem Venenstueckes. Dtsch Med Wochenschr 1909; 35; 1125-1230.

Yang Y. Ding F. Wu J. Hu W. Liu W. Gu X. Development and evaluation of silk fibroin-based nerve grafts used for peripheral nerve regeneration. Biomaterials 2007; 28:36; 5526-5535.

Yoshitani M. Fukuda S. Itoi SI. Morino S. Tao H. Nakada A. Inada Y. Endo K. Nakamura T. Experimental repair of phrenic nerve using a polyglycolic acid and collagen tube. Journal of Thoracic and Cardiovascular Surgery 2007; 133:3; 726-e3.

Yu W, Zhao W, Zhu C, Zhang X, Ye D, Zhan W, Zhou Y, Jiang X, Zhang Z. Sciatic nerve regeneration in rats by a promising electrospun collagen/poly(ε caprolactone) nerve conduit with tailored degradation rate. BMC Neuroscience 2011; 12; 68.

Yucel D, Kenar H, Ndreu A, Endoğan T, Hasirci N, Hasırcı N. Nanotechnlogy in biomaterials: Nanofibers in tissue engineering. In: Reisner, DE. ed. Biotechnology Global Prospects II. CRC Press Taaylor and Francis Group; 2012; 227-246.

Yucel D, Kose GT, Hasirci V. Polyester based nerve guidance conduit design, Biomaterials 2010; 31:7; 1596-1603.

Zhu H, Ji J, Shen J. Biomacromolecules electrostatic self-assembly on 3-dimensional tissue engineering scaffold, Biomacromolecules 2004; 5; 1933–1939.

APPENDIX A

STRESS-STRAIN CURVE FOR A VISCOELASTIC MATERIAL

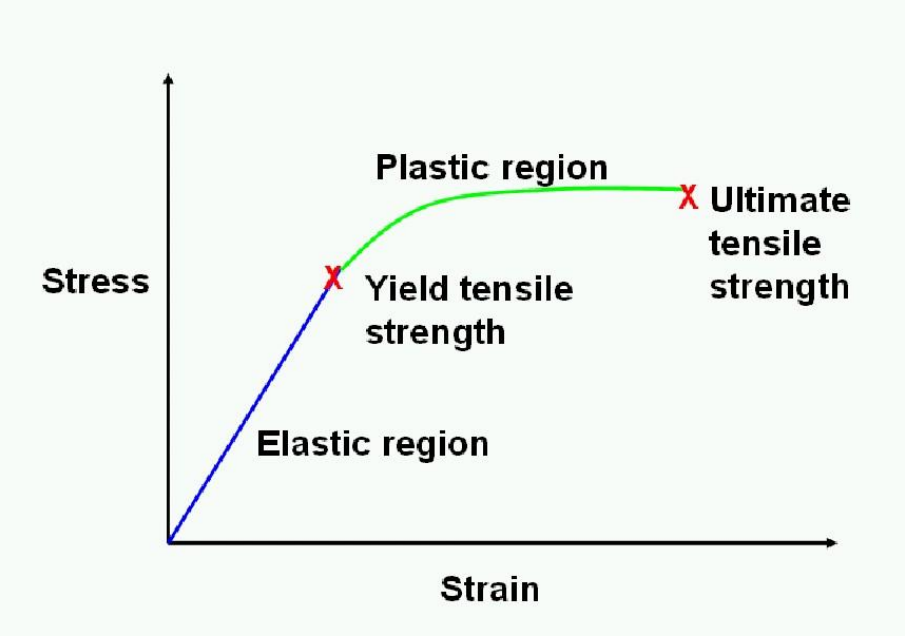

Figure 35. An example stress train cur for viscoelastic materials. Slope of the elastic region gives the Elastic Modulus (E).

APPENDIX B

TENSILE TEST RESULTS

Sample Dimensions: 3 cm x 1 cm x 0.4 mm

Device: Lloyd LRX5K Mechanical Tester (UK)

Strain rate: 2 mm/min

(Raw data)

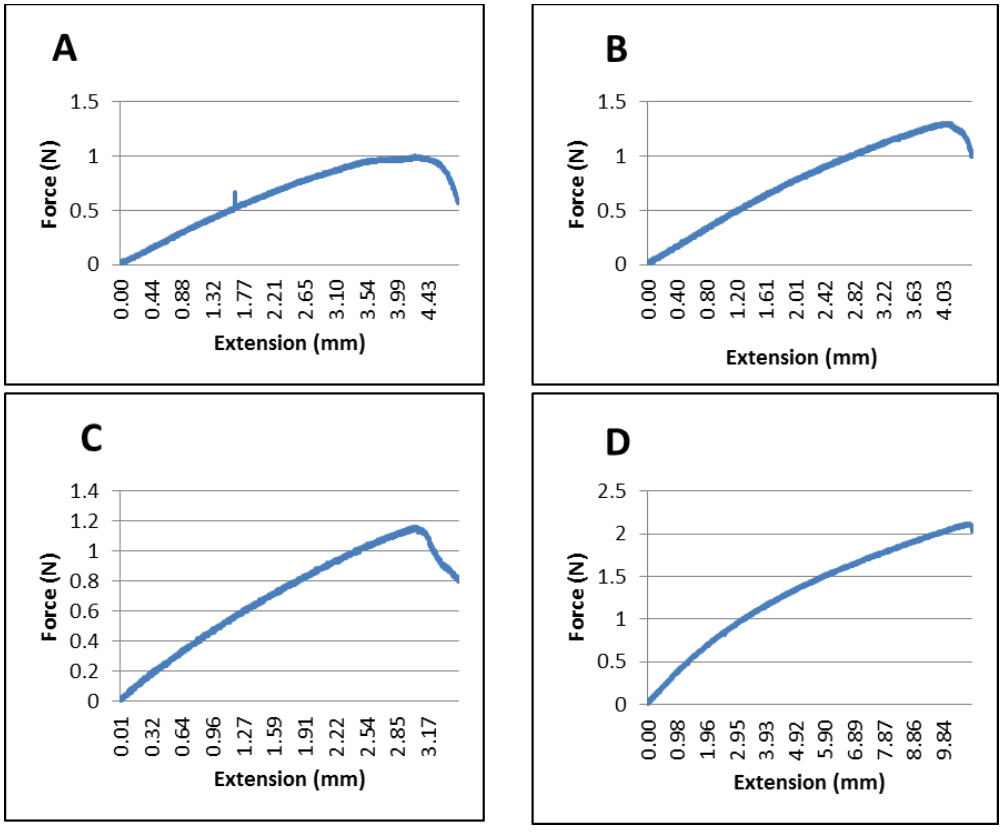

Figure 36. Tensile test results of pHEMA membranes with mwCNT. A) 0%, B) 1%, C) 3%, D) 6%.

APPENDIX C

MTT CALIBRATION CURVE

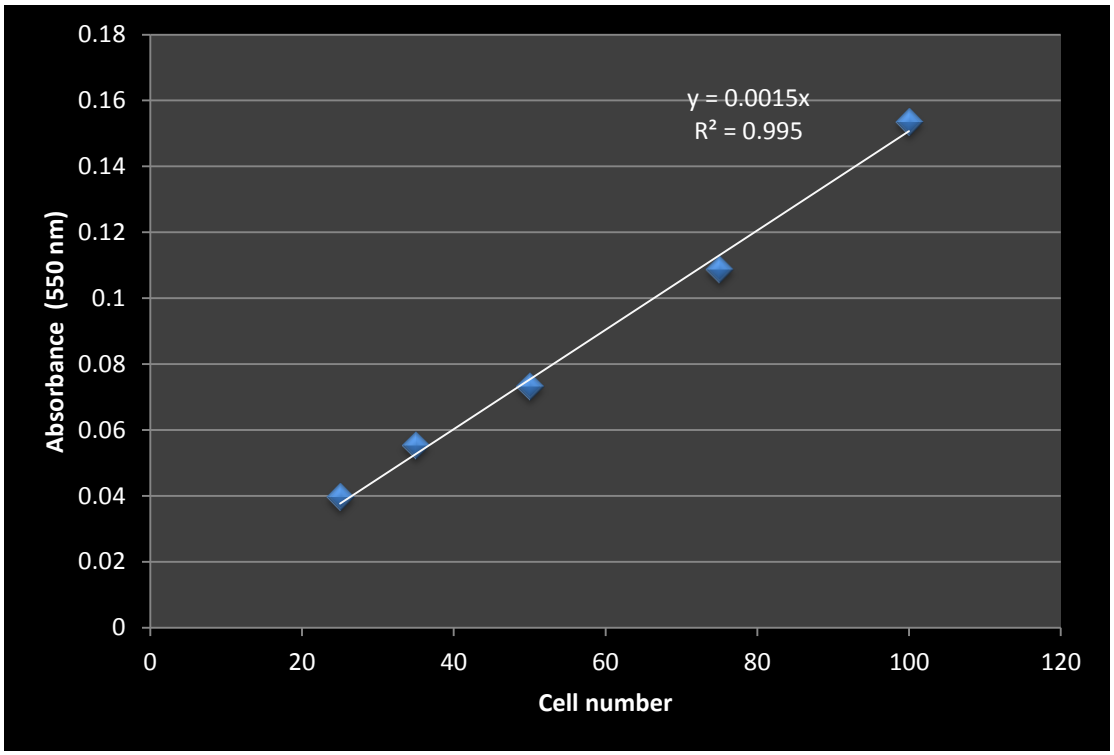

Figure 37. MTT calibration curve of SHSY5Y neuroblastoma cell line.